First Preliminary Report of African Studies

March 1975

Association for African Studies, Nagoya University
c/o Department of Earth Sciences, Faculty of Science,
Nagoya University, Chikusa, Nagoya 464, JAPAN

First Preliminary Report

Editor: Kanenori Suwa March 1975

Association for African Studies, Nagoya University
c/o Department of Earth Sciences
Faculty of Science
Nagoya University

The Preliminary Reports of African Studies are printed and distributed privately by the Association for African Studies, Nagoya University.
The papers printed in the Preliminary Reports are generally résumés, while the publication of the full texts is left to the respective authors' choice.
Any reference to this report in a formal list should read:
1 st Prelim. Rep. Afr. Studies., Nagoya Univ.

Contents

Introduction

This report covers work done in Africa from the Association for African Studies, Nagoya University and some related work done from the Department of Earth Sciences, Nagoya University during the periods 1973 and 1974.

In 1962, Nagoya University dispatched the Eastern Africa Scientific Investigation Commission to four countries of northeastern Africa, namely Egypt, Sudan, Ethiopia and French Somaliland(Afars and Issas), for field investigations of geology and medical plants, and gained many valuable results. In the same year the Association for African Studies, Nagoya University made a start.

Since then, some geologists, geochemists, geochronologists, geophysicists and archaeologists of Nagoya University have performed continuously their field surveys in several countries as follows.

1968--- I.Matsuzawa, I.Shiida, K.Suwa, K.Miyakawa, S.Mizutani, K.Yairi, H.Aoki, G.Ohmi, H.Kurimoto (Tanzania and Kenya)

1969·1970--- K.Suwa, (Kenya, Uganda, Rwanda, Burundi, South Africa)

1971--- I.Matsuzawa, Y.Kato, K.Suwa, H.Shiozaki, K.Yairi(Kenya and Uganda)

1972·1973--- F.Yamazaki (Kenya and Tanzania)

1973--- I.Matsuzawa, K.Suwa, K.Miyakawa, K.Shibata, K.Yairi, H.Kagami, M.Adachi(Kenya and South Africa)

1973·1974--- K.Biyajima (Kenya and Tanzania)

In this report, Mr.Adachi performed a sedimentological study on the late Precambrian Bukoban orthoquartzite, Mr.Biyajima performed structural and petrological studies on mantled gneiss dome around Machakos area and Dr.Kagami reported petrographical characters of Precambrian granites in western Kenya. Mr.Adachi found sole markings from Upper Triassic near Mombasa and carbonatitic clasts in Miocene sediments near Mt.Tinderet. Mr.Yairi discussed geometry and mechanics of East African Rift System and Kavirondo Rift Valley. Prof.Kato made a summit level in western Uganda.

Prof.Miyakawa found black staurolite crystals in Kioo pegmatite. Dr.Suwa described petrographical features of plagioclases in three groups of anorthosite, and he discussed reverse pleochroism of phlogopites occurring characteristically in kimberlites and their related rocks with Prof.Aoki. Dr.Suwa described and discussed peridotite nodules from central Kenya with EPMA analysis by Mr.Yusa. Mr.Shiozaki reported fuchsite from southern Kenya.
Dr.Shibata performed Rb-Sr isochron dating on the Mozambiquian metamorphic rocks. Prof. Ueda made K-Ar dating on Tanzanian rocks. Dr. Suwa discussed the carbonatite problem with isotope analysis by Prof. Oana and his co-workers.

These works were supported mainly by the grant-in-aid for Scientific Research of the Ministry of Education of Japanese Government and by the Japan Society for Promotion of Science, for which I would like to record my sincere thanks.

The present report has been edited by Dr.Kanenori Suwa.

ISAO MATSUZAWA

Director

February, 1975

Sedimentological Notes on the Bukoban Orthoquartzite (Late Precambrain) around Kisii, Kenya

Mamoru ADACHI and Kenji YAIRI

Department of Earth Sciences, Faculty of Science, Nagoya University

Introduction

A volcano-sedimentary formation with NNE trend around Kisii, southwest Kenya, is regarded as one of the isolated massifs of the late Precambrian Bukoban system. It consists mainly of porphyritic and non-porphyritic basalts, orthoquartzite, chert, andesitic lava and tuff, and rhyolite resting unconformably on the basement granitic rocks and on the Nyanzian and Kavirondian systems (Schoeman, 1949; Huddleston, 1951; Saggerson, 1952; Binge, 1962). Unlike the Bukoban system in Tanzania and Uganda, it is almost entirely devoid of argillaceous sandstone, shale, and dolomite.

While staying in Kisii, we carried out a field investigation to know the sedimentation environment of the Bukoban orthoquartzite. It was found that current ripple marks and cross-bedding are well developed in the orthoquartzite. These sedimentary structures yielded us a basic information as to the direction of sediment transport.

The Bukoban orthoquartzite

As the general description of the Bukoban orthoquartzite has been given by Huddleston (1951) and others, the details need no repetition here. Important features of the orthoquartzite worthy to note are as follows: (1) generally it has a gentle dip, and is underlain by basalt and in turn capped by andesite; (2) chert is developed, though locally, above the orthoquartzite; (3) it is about 75 m in thickness with a maximum of 120 m, thinning out to the north; (4) oscillation ripple marks are commonly seen, and cross-bedding is rare; (5) it is composed almost entirely of well-rounded grains of quartz with trace quantities of heavy minerals; no feldspar grains have been detected.

Cross-bedding and ripple marks

Cross-bedding found in the Bukoban orthoquartzite is invariably tabular(Fig. 1), and trough-shaped bedding has not been found.

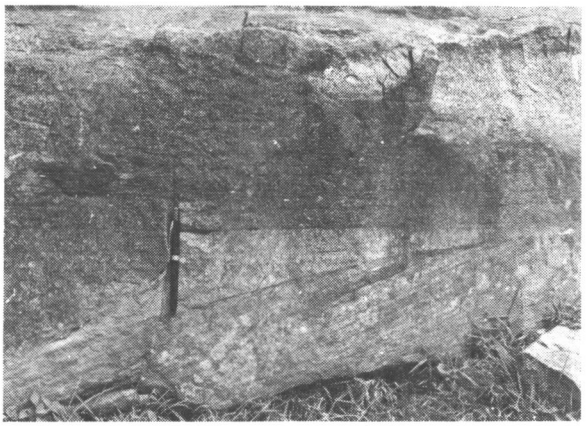

Fig. 1 Tabular cross-bedding in the Bukoban orthoquartzite (late Precambrian). Current from right to left. Manga Ridge about 10 km northeast of Kisii, Kenya (Photo by M.A.).

The sedimentation units range from 15 to 60 cm in thickness and most of the units are about 30 cm thick. In some coarse-grained parts, the cross-bedding is sometimes graded, with the larger-sized grains toward the bottom of each cross-bed. Occasionally, load-cast-like structure was observed on the base of cross-bedded orthoquartzite layer.

Two types of ripple mark, current ripple mark(Fig. 3) and oscillation ripple mark, are seen on the orthoquartzite of the Manga

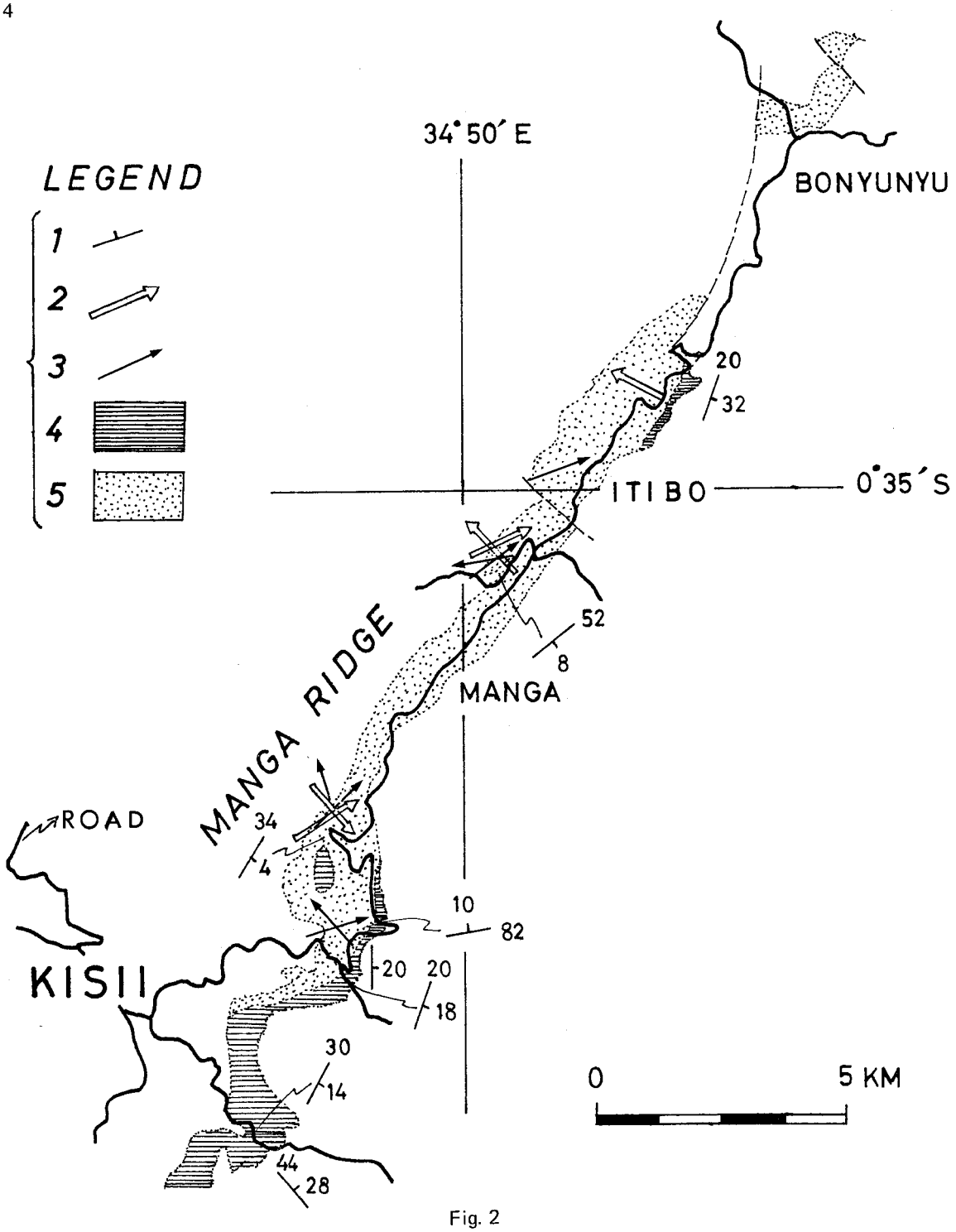

Fig. 2

Paleocurrent map of the Manga Ridge, northeast of Kisii based on the orientation of current ripple marks and cross-bedding. 1, strike and dip of beds; 2, ripple mark direction; 3, cross-bedding direction; 4, chert; 5, orthoquartzite.

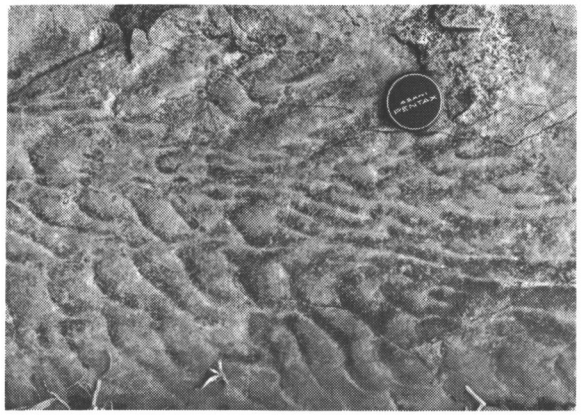

Fig. 3 Current ripple marks on the Bukoban orthoquartzite (late Precambrian). Current from left to right. Manga Ridge about 10 km northeast of Kisii, Kenya (Photo by M.A.).

Ridge(Fig.2), and the former predominates over the latter. According to Allen's classification(Allen, 1969), the current ripples commonly found are small-scale sinuous ripples. The wave length of current ripple marks ranges from 2.5 to 8.5 cm with an average length of 4.5 cm, the amplitude of which ranges from 3 to 7 mm, mostly less than 5 mm. It is noted that two sets of ripples(Pettijohn et al., 1972), though rare, have been found; large main ripples have an average wave length of 8 cm, and the smaller ripples perpendicular to main ones about 2.5 cm.

Direction of sediment transport

Paleocurrent directions inferred from cross-bedding(48 readings) and current ripple marks(27 readings) are shown in Fig.2. The variation in direction of cross-bedding and ripple marks is commonly recognized. In addition, the cross-bedding direction often has deviation of more than 90° from the ripple mark direction. It is interesting that the strike of ripple mark is, in many cases, subparallel to that of bedding of the orthoquartzite. However, the existence of two sets of ripple marks and the variable nature in orientation of ripples in one outcrop suggest a complicated current flow during and after the sedimentation.

Although a few measurements in a restricted area cloud a precise discussion, the paleocurrent data favour the interpretation that the sediments were derived largely from the southwest and southeast. A northeasterly paleocurrent is also indicated by current ripple marks on the orthoquartzite in Itumbi about 15 km southwest of Kisii. A northerly sediment transport seems to be in harmony with the evidence that the orthoquartzite thins out toward the north. Judging from the paleocurrent data as well as the petrological characteristics of the orthoquartzite. the source area for the Bukoban orthoquartzite would exist to the south rather far from Kisii, where basement granitic and metamorphic rocks were extensively exposed during the late Precambrian time.

Further work is needed to throw more light on it.

Acknowledgements—Special thanks go to Dr.S.Mizutani of Nagoya University for his advice and for reading the manuscript.

References

ALLEN, J.R.L. (1969): *Current ripples.* North Holland Publ. Co., 433pp.
BINGE, F.N. (1962): Geology of the Kericho area. *Rept. Geol. Surv. Kenya,* **50,** 67pp.
HUDDLESTON, A. (1951): Geology of the Kisii district. *Rept. Geol. Surv. Kenya,* **18,** 64pp.
PETTIJOHN, F.J., POTTER, P.E., and SIEVER, R. (1972): *Sand and sandstone.* Springer-Verlag, 618pp.
SCHOEMAN, J.J. (1949): Geology of the Sotik district. *Rept. Geol. Surv. Kenya,* **16.***
SAGGERSON, E.P. (1952): Geology of the Kisumu district. *Rept. Geol. Surv. Kenya,* **21,** 86pp.

* Not consulted in original

Mantled Gneiss Dome in the Mozambique Belt around the Machakos Area, Kenya

Katsumi BIYAJIMA*, Kanenori SUWA* and Kunihiko MIYAKAWA**

* Department of Earth Sciences, Faculty of Science, Nagoya University
** Department of Earth Science, Nagoya Institute of Technology.

Introduction

The Machakos area is situated about 70 km south-east of Nairobi in central Kenya and the main investigated area is bounded by the latitudes 1°30'S and 1°42'S and by the longitudes 37°20'E and 37°28'E as shown in Figs. 1 and 3.

The Machakos area is occupied mainly by Precambrian metamorphic rocks constituting part of the Mozambique belt of Kenya, mostly belonging to the amphibolite facies of metamorphism. The metamorphic rocks consist mainly of pelitic and psammitic gneiss and schist with subordinate basic and calcareous rocks(hereafter these rocks are called Mozambique metamorphic rocks). Granitoid gneiss also occurs, especially in the core part of the dome structure.

Structural and petrological studies of these gneisses have been performed. Attention is also paid to garnet zoning of Mn, Fe and Mg using microprobe analysis. Finally these problems concerned are discussed.

The previous studies of the Machakos area are the field-geological works by Baker(1954) and by Fairburn(1963) of Kenya Mines and Geological Department.

Structure

As shown in Fig.1, several domes can be recognized in the Machakos area. These domes show elongated forms with concordant to the general trend of the Mozambique belt and the domes are about 5-20 km in diameter. General structural trend of the Mozambique metamorphic rocks is between north–south and north-west–south-east except for the nearby area around the domes, where the trend changes into concentric arrangements as clearly seen around Opete and Mbooni domes. Around the domes, anticlinal and synclinal structures with vertical dips of foliation are sometimes found. Lineation directions, however, are approximately parallel to the general structural trend of the Mozambique metamorphic rocks in most cases and are plunging to north or north-west at low angles as shown in Fig.2. Stereographic plots of the lineation reveal a prefered maximum X_I plunging at 28° in a direction of 338° in the southern Machakos area and at 17° in a direction of 326° in the northern Machakos area.

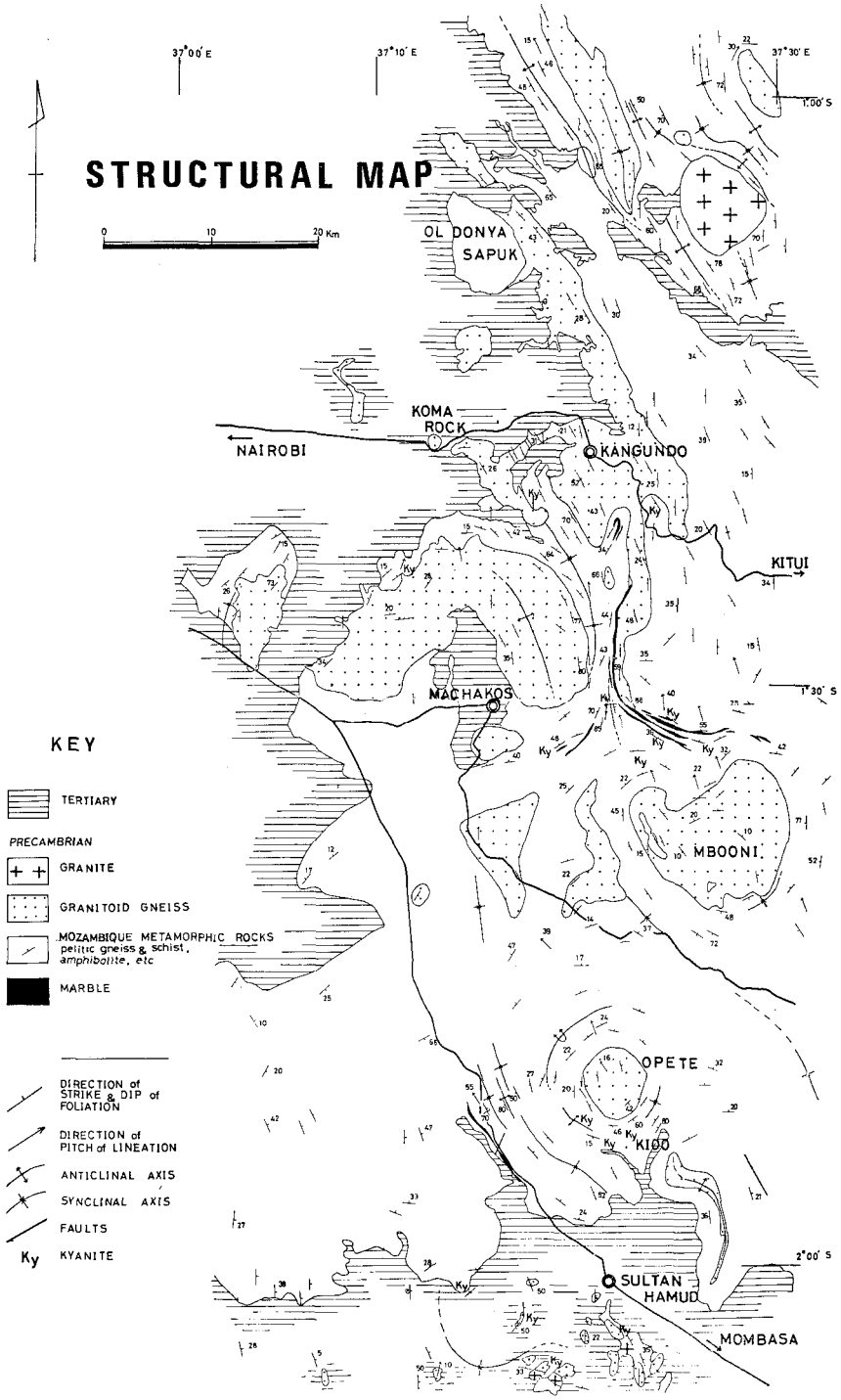

Fig. 1

Structural Map of the Machakos area.

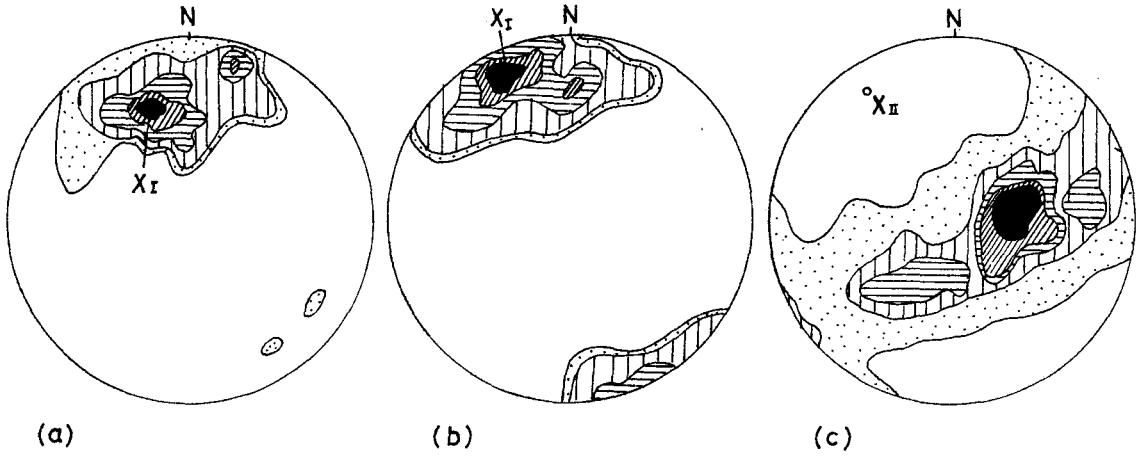

Fig. 2

Orientation diagrams of lineation and foliation in the Machakos area.

(a) . . . Orientation diagram of lineation in the southern Machakos area, in latitudes 1°30′-1°42′S and longitudes 37°20′-37°30′E. (100 readings)

(b) . . . Orientation diagram of lineation in the north Machakos-Thika area, in latitudes 1°00′-1°30′S and longitudes 37°00′-37°30′E. (100 readings)

(c) . . . Orientation diagram of foliation poles in the north Machakos-Thika area. (700 readings)

XI is the lineation maximum. XII is the statistical fold axis. Contours at 1, 2, 4, 5-10 and 10 per cent per one per cent area in each diagram. (b) and (c) are after Fairburn(1963).

Geology

The domes consist of granitic gneiss or dioritic gneiss and sometimes of granite. Granitoid gneiss is usually homogeneous and consists of quartz, plagioclase, microcline and biotite. Microscopically the granitoid gneiss shows xenomorphic and replacement textures in marginal parts of domes. Muscovite is sometimes present in small amount, and sphene, apatite and iron-ores occur as accessories.

The main part except for the domes is occupied by the Mozambique metamorphic rocks, which is considered to represent an original sedimentary series of shale, sandstone and limestone, into which basic igneous rocks have been intruded. Because much of the banding in the metamorphic rocks is so continuous over several hundreds meters that it is concluded that the banding exhibits original differences in the ocmposition of sedimentary series.

Porphyroblastic almandine - kyanite - staurolite gneiss is commonly found. Muscovite-biotite gneiss, almandine-bearing biotite gneiss and muscovite gneiss are also found to occur frequently. Almandine-epidote amphibolite and epidote amphibolite are subordinate. Crystalline limestone with or without quartz, tremolite and wollastonite are found as thin bands or lenses, varying from a few inches to two or three hundreds feet in thickness, in pelitic and psammitic gneisses.

In some places between the domes and the Mozambique metamorphic rocks, intermediate rocks are found; which are shown as migmatitic gneiss in Fig. 3. The boundaries between the migmatitic gneisses and the other rocks are not so clear.

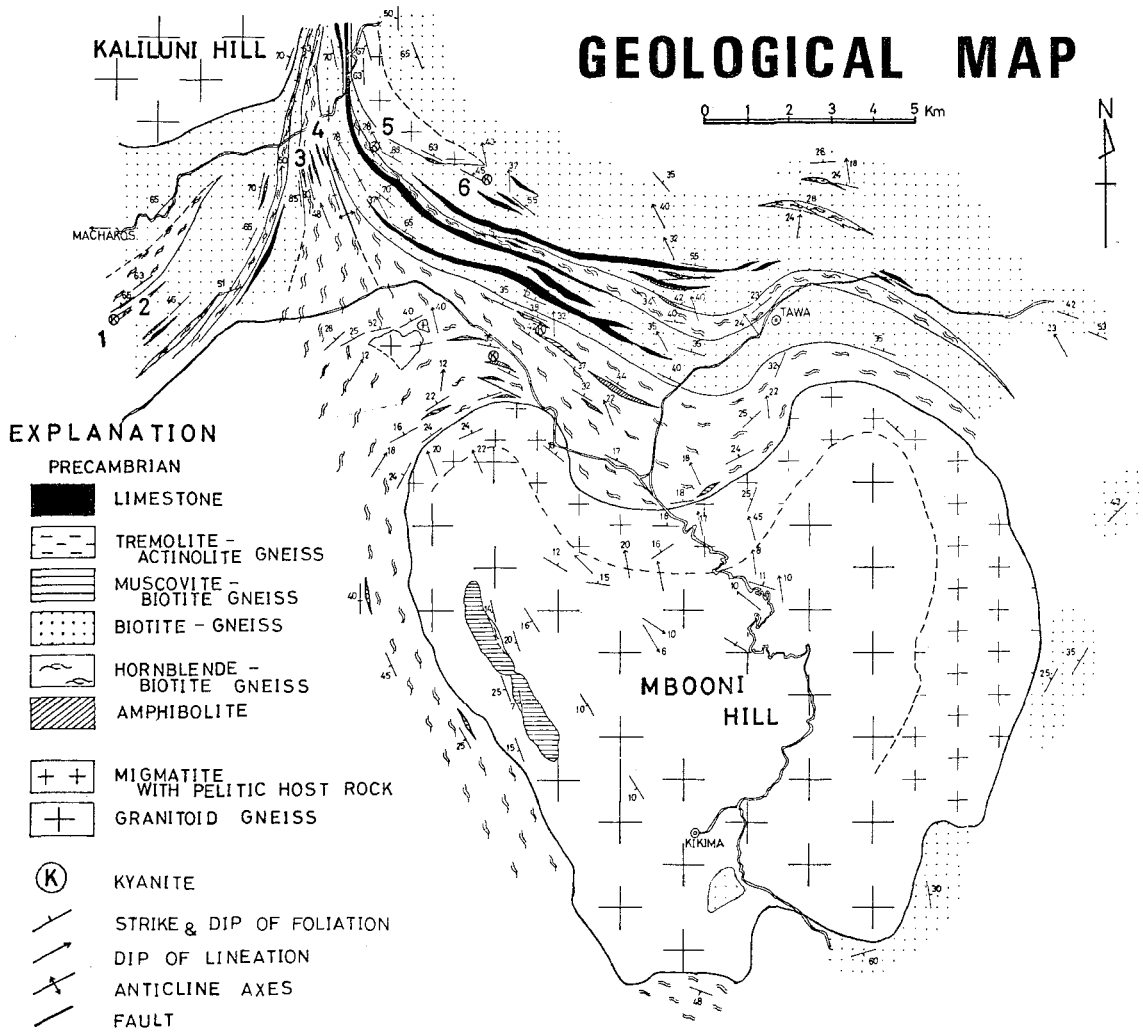

Fig. 3

Geological Map of Mbooni Hill, southern Machakos area.

Garnet zoning of Mn, Fe and Mg

From the investigated area, six garnet-bearing rocks have been selected to study the compositional zoning of garnet and total twelve garnet grains have been analysed by EPMA and the results are shown in Table1, Figs. 4 and 5.

These garnets are actually almandine and no garnet having higher spessartine and lower pyrope compositions occur. This vacant compositional area corresponds to that of garnet in greenschist facies rocks(Miyashiro, 1953).

Two patterns of garnet zoning in Mn are recognized; one shows a general decrease of Mn content along traverse from the centre of the grain to the margin(normal zoning) as seen in Fig. 4(1-1 and 6-1) and the other has an inverted zoning pattern which increases Mn content from the centre to the margin of the grain(reverse zoning) as seen in Fig.4(4-1).

Table 1

Compositions of zoned garnets in the Mozambique metamorphic rocks of the Machakos area. These compositions are plotted in Fig. 5.

		Margin		Core	
No 1	Almandine–kyanite–staurolite–muscovite–biotite schist	(1–1)	(1–2)	(1–1)	(1–2)
	MnO	0.93	0.76	5.88	5.68
	FeO	32.96	32.22	28.32	26.70
	MgO	3.50	3.91	1.44	1.32
No 2	Epidote-bearing almandine amphibolite	Margin		Core	
		(2–1)	(2–2)	(2–1)	(2–2)
	MnO	4.53	4.58	4.19	4.00
	FeO	26.92	25.87	25.92	25.76
	MgO	3.84	3.29	3.68	4.12
No 3	Almandine-bearing hornblende–epidote–biotite gneiss	Margin		Core	
		(3–1)	(3–2)	(3–1)	(3–2)
	MnO	3.34	3.29	6.08	3.63
	FeO	29.07	29.00	25.73	29.00
	MgO	3.16	3.54	2.37	3.27
No 4	Almandine-bearing biotite gneiss	Margin		Core	
		(4–1)	(4–2)	(4–1)	(4–2)
	MnO	13.20	12.21	9.02	9.65
	FeO	25.01	25.72	24.31	26.03
	MgO	2.32	2.61	2.86	3.24
No 5	Almandine–kyanite–staurolite–muscovite–biotite gneiss	Margin		Core	
		(5–1)	(5–2)	(5–1)	(5–2)
	MnO	2.02	1.94	1.51	1.71
	FeO	29.66	33.81	28.13	31.79
	MgO	2.08	3.63	2.34	3.29
No 6	Almandine–kyanite–staurolite–muscovite–biotite gneiss	Margin		Core	
		(6–1)	(6–2)	(6–1)	(6–2)
	MnO	1.01	0.92	2.25	1.15
	FeO	31.80	30.70	32.17	33.55
	MgO	2.97	2.40	1.51	2.50

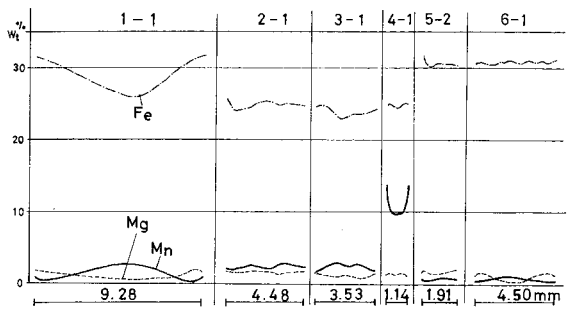

Fig. 4

Profiles of zoned garnets, occurring in the Machakos area, traversed across the diameter.

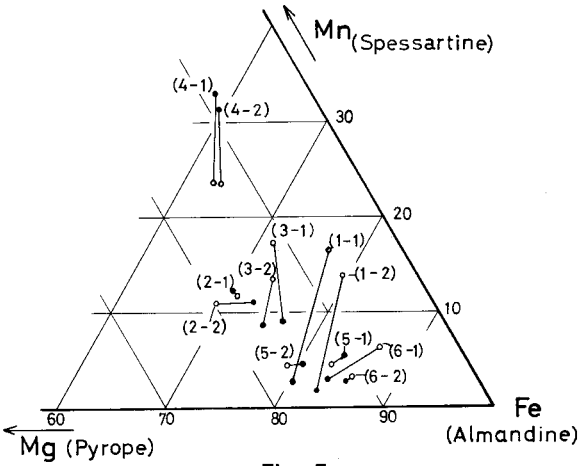

Fig. 5

Mn-Fe-Mg diagram of zoned garnets in the Mozambique metamorphic rocks of the Machakos area.
Solid circle shows the composition of margin and open circle that of centre.

Discussion

(a) Mantled gneiss dome

"Mantled gneiss dome" was first described by Eskola in 1948 as follows: in many orogenic zones there occur domes having a supercumbent mantle of sedimentary strata parallel to the dome contacts and the foliation of the gneiss. Many similar domes have been reported from the Mozambique belt: northern Rhodesia (Leyshon, 1973), northern Zambia(Garlick, 1973) and central Malawi (Bloomfield, 1970) and also reported from the other metamorphic areas, for examples Conneticut(Lundgren, 1962), South-Idaho(Armstrong, 1968), Australia(Pidgeon and Compston, 1965; White et al., 1967) and Scotland (Tobisch, 1966).

It should be noted that characteristic dome structure has been made in experiments by Ramberg in 1964. He took a model in which a single plane surface separates two substances of unlike viscosity and deformed this by a principal compressive strain parallel to the boundary surface, an instability was set up and surface became folded as like as the dome structure.

The metamorphic and structural development of the Mozambique belt around the Machakos area may be considered as follows; in the earlier orogenic period (late Archaean ?), basement rocks : granitic and metamorphic rocks were formed, and after that the area concerned uplifted and sedimentary rocks (early Proterozoic ?) covered unconformably on the basement rocks. In the later orogenic period(late Proterozoic), intense compression of east-west direction with rising temperature has resulted in these rocks being transformed into higher grade metamorphic rocks. During the compression and folding of basement rocks and their covering sedimentary rocks, the covering rocks have changed to metamorphic rocks and have been intruded by anatectic granitic rocks originated in preexisting basement rocks. The granitoid gneisses consisting the core part of the domes have originated from the basement rocks of late Archaean (?) and they have been mobilized by anatexis and intruded statically and concordantly to the overlying Mozambique sedimentary series(this is now Mozambique metamorphic rocks). Anatectic granitic rocks gave intense effect to the nearby Mozambique metamorphic rocks, namely the latter was partly granitized and migmatized.

(b) Metamorphic grade

Porphyroblastic almandine-kyanite-staurolite rocks are commonly found to occur in south-western Kenya and change into sillimanite-bearing rocks in eastern Kenya where the original sediments are considered to be sufficiently aluminous. The change from

kyanite to sillimanite suggests an increase in metamorphic grade from west to east in Kenyan portion of the Mozambique belt (Sanders, 1954).

The metamorphic rocks of this area are the product of kyanite-sillimanite type metamorphism(Miyashiro, 1961), namely medium-pressure metamorphism.

(c) Garnet zoning of Mn, Fe and Mg

Up to now several works have dealt with the relation among the zoning pattern, chemical composition of garnet and metamorphic grade.

The changing of chemical composition of garnet can be used as an indicator of temperature in metamorphic rocks, i.e., it changes from spessartine through almandine to pyrope with rising temperature and pressure(Miyashiro, 1953; Sturt, 1962).

It has been reported that reverse zoning of Mn is seen in retrogressive poly-metamorphosed area and normal zoning in lower grade area(Birk, 1973; Kano and Kuroda, 1973).

In this area, typical normal zoning of Mn is observed in Nos. 1 and 6, and reverse zoning in No.4(see Fig.4). Their chemical compositions are actually almandine and the garnets showing reverse zoning are slightly richer in spessartine molecule than the garnet showing normal zoning. Complex pattern are also seen as shown in Nos. 2,3 and 5 in Fig. 5.

The causes of these phenomena have been explained by several interpretations: difference of bulk compositions of host rocks (Kano and Kuroda, 1973), oxygen fugacity(Müller and Schneider, 1971), a restriction on diffusion in chlorite and/or biotite during the reaction(Kretz, 1973) and poly-metamorphism(Birk, 1973; Kano and Kuroda, 1973). These problems remain to be solved through future investigations.

Acknowledgements—Many facilities for field work were made available by Dr.John Walsh and Mr.S.Dodhia of Kenya Mines and Geological Department, to whom the authors express their deep gratitude. The senior author is indebted to Professor I.S. Loupekine of Nairobi University for his advice and encouragement.

References

ARMSTRONG, R.L. (1968): Mantled gneiss dome in the Albion Range, Southern Idaho. *Geol. Soc. Am. Bull.* **79,** 1295-1314.

BAKER, B.H. (1954): Geology of the Southern Machakos District. *Report No.27, Geol. Surv. Kenya.*

BIRK, D. (1973): Chemical zoning in garnet of the Kashabowie group, Shebandowan, Ontario. *Canad. Mineral.* **12,** 124-128.

BLOOMFIELD, K. (1970): Orogenic and post-orogenic plutonism in Malawi. *"African Magmatism and Tectonics"* ed. by Clifford, T.N. and Gass, I.G., 119-155. Oliver and Boyd.

ESKOLA, P.E. (1948): The problem of mantled gneiss domes. *Quart. J. Geol. Soc. Lond.* **104,** 461-476.

FAIRBURN, W.A. (1963): Geology of the Northern Machakos-Thika area. *Report No.59, Geol. Surv. Kenya.*

GARLICK, W.G. (1973): The Nchanga granite. *Spec. Publ. Geol. Soc. S. Afr.* **3,** 455-474.

KANO, H. and KURODA, Y. (1973): On the chemistry of coexisting garnet and biotite in pelitic-psammitic metamorphic rocks, central Abukuma, Japan. *J. Geol. Soc. Japan,* **79,** 621-641.

KRETZ, R. (1973): Kinetic of the crystallization of garnet at two localities near Yellowknife. *Canad. Mineral.* **12,** 1-20.

LEYSHON, P.R. (1973): Two granite-gneiss domes in the Copper Queen area, Rhodesia. *Spec. Publ. Geol. Soc. S. Afr.* **3,** 97-109.

LUNDGREN, L. (1962): Deep river area, Conneticut; stratigraphy and structure. *Amer. J. Sci.* **260,** 1-23.

MIYASHIRO, A. (1953): Calcium-poor garnet in relation to metamorphism. *Geochim. Cosmochim. Acta.* **4,** 179-208.

MIYASHIRO, A. (1961): Evolution of metamorphic belts. *J. Petrol.* **2,** 277-311.

MÜLLER, G. and SCHNEIDER, A. (1971): Chemistry and genesis of garnet in metamorphic rocks. *Contr. Mineral. and Petrol.* **31,** 178-200.

PIDGEON, R.T. and COMPTSON, W. (1965): The age and origin of the Cooma granite and its associated metamorphic zones. *J. Petrol.* **6,** 193-222.

RAMBERG, H. (1964): Selective bukling of composite layers with contrasted rheological properties; theory for simultaneous formation of several orders of folds. *Tectonophys.* **1,** 307-341.

SANDERS, L.D. (1954): The status of sillimanite as an index of metamorphic grade in the Kenya Basement System. *Geol. Mag.* **91,** 144-152.

STURT, B.A. (1962): The composition of garnets from pelitic schist in relation to the grade of regional metamorphism. *J. Petrol.* **3,** 181-191.

TOBISCH, O.T. (1966): A large scale basin and dome pattern resulting from the interference of major folds. *Geol. Soc. Am. Bull.* **77,** 393-408.

WHITE, J.R., COMPTON, W. and KLEEMAN, A.W. (1967): The Palmer granite— a study within a regional metamorphic environment. *J. Petrol.* **8,** 29-50.

Maragori Granite in Tanganyika Craton

Hiroo KAGAMI

Geological and Mineralogical Institute, Faculty of Science, Tokyo University of Education

There are two main granite batholiths in the northeast area of the Tanganyika craton: the Maragori granite in the vicinity of the Kavirondo rift; and the Kitoshi granite to the south of Mt.Elgon(Fig. 1). Small batholiths

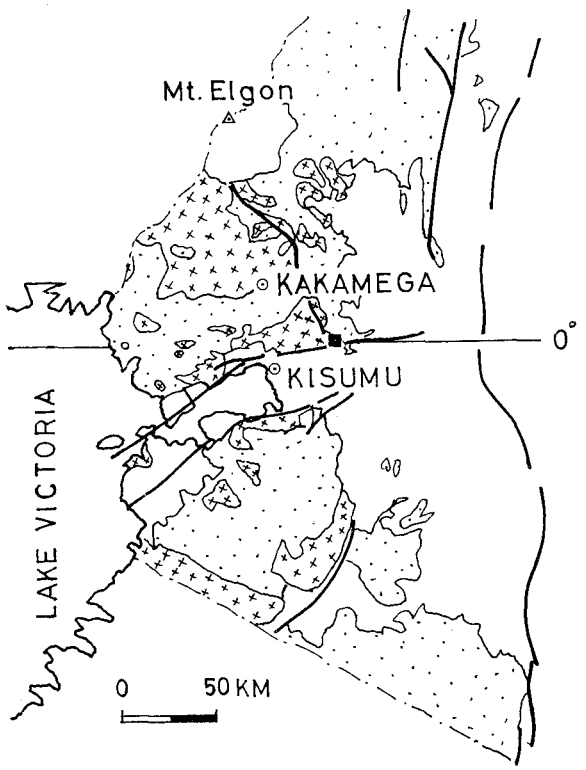

Fig. 1 Index map of the area northeast of Kisumu.

are also found in the Nyanzian and Kavirondian systems between these two batholiths. The Rb-Sr whole-rock isochron age for these granites has not been measured as yet. However, that of the Buteba granite in Uganda, western extension of the Kitoshi granite, is 2570 m.y.(Old and Rex, 1971).

In this paper, the writer describes briefly the rock facies and occurrence of the Maragori granite. Based on the rock facies, this granite is classified into the following eight types(A-type~H-type).

A-type: This is a porphyritic, heterogeneous, schistose granite characterized by conspicuous pinkish phenocrysts of K-feldspar(1-2 cm across). The groundmass is fine-grained. No xenolith and aplite are found in this type.

B-type: This is a medium-grained, leucocratic biotite granite slightly tinged with pink, and has some phenocrysts of K-feldspar.

C-type: This is a weakly schistose, medium-grained, pink granite with conspicuous crystals of long prismatic euhedral hornblende.

D-type: This is a medium-grained, schistose granite. Many mafic inclusions, aplite, and pegmatite are discernible.

E-type: This is a medium-grained biotite granite. No phenocrysts of K-feldspar and xenoliths are present.

F-type: This is a coarse-grained, leucocratic biotite granite. Schistose structure is slightly observed.

G-type: This is a coarse-grained quartz diorite characterized by the massive rock facies and the faint schistose structure.

H-type: This is a massive, homogeneous, fine-grained biotite granite. The phenocrysts of K-feldspar is not observed.

These eight types are the main rock facies of the Maragori granite, but their mutual relationship is not clear. A-type seems to change gradually into B- and C-types; the in-

1st Prelim. Rep. Afr. Studies., Nagoya Univ. 14-16, 1975.

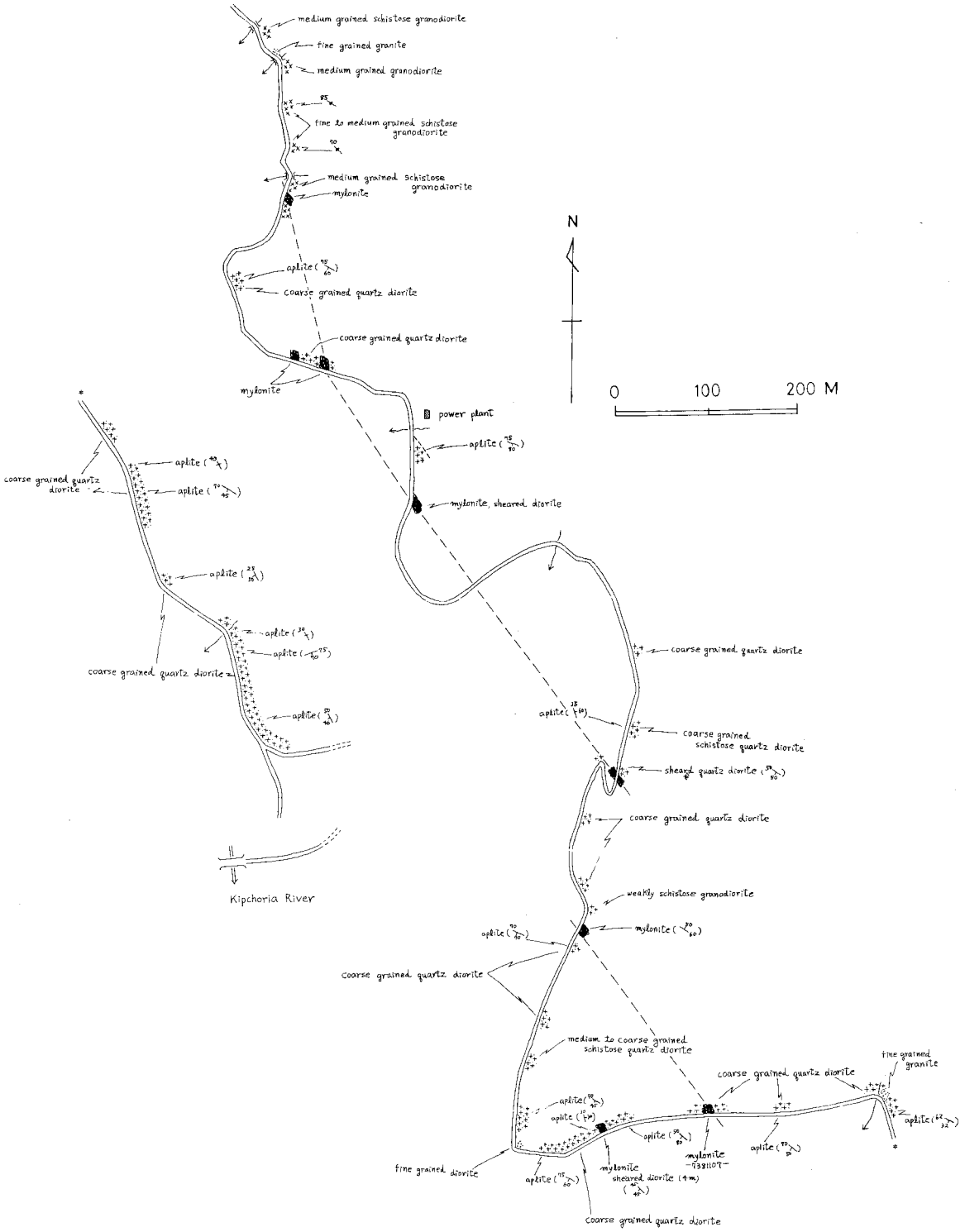

Fig. 2 Route map along the Kipchoria River.

termediate rock type is sometimes observed. A-type found near the Nandi fault has suffered mylonitization and recrystallization. In such a granite, biotites show the glomeroporphyritic aggregate. D-type is distributed in the area near the Nandi fault. Both E- and F-types are found near the Kavirondo rift, and their distribution is very limited. Similar fact is recognized in G-type, which is found only in a valley "Kipchoria River" in the north of Miwani. In this type, the mylonite zone is observed along the Nandi fault(Fig. 2). The relation between the coarse-grained quartz diorite and mylonite is shown in Fig. 3. H-type also occurs in a narrow extent.

The trends of quartz veins and aplites in the Maragori granite adjacent to the Kavirondo rift are parallel to the rift trend. Whether these trends are essentially parallel to the rift trend or accidentally so is unknown.

The relationship among the Nyanzian system, the Kavirondian system, and the Maragori granite, is not clear in this area. However, the xenoliths which seem to be derived from the Nyanzian system are sometimes found in the Maragori granite, suggesting that the granite is younger than the Nyanzian system. Thermal effect of the granite on the xenoliths is not so strong.

Acknowledgements—The writer would like to thank Dr.K.Suwa of Nagoya University for his fruitful advice on this report.

Reference

OLD, R.A. and REX, D.C. (1971): Rubidium and strontium age determinations of some Pre-Cambrian granitic rocks, S.E.Uganda. *Geol. Mag.*, **108**, 353-360.

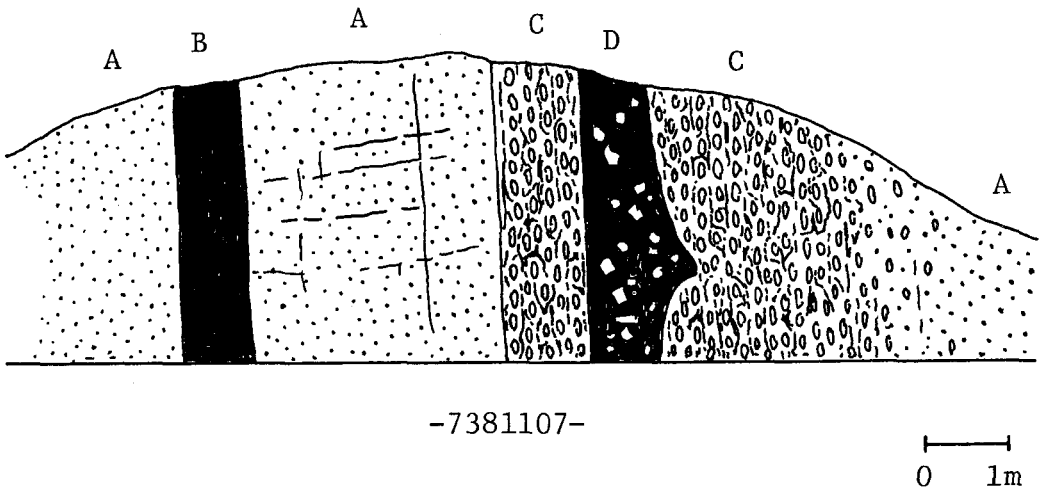

Fig. 3

The relation between coarse-grained quartz diorite and mylonite. A: coarse-grained quartz diorite(G-type), B: fault clay, C: mylonite, D: fault clay and fault breccia.

The Rocks Constituting the Mozambique Belt in the Northeast District of Lake Victoria

Hiroo KAGAMI*, Mamoru ADACHI**, Kenji YAIRI** and Isao MATSUZAWA***

* Geological and Mineralogical Institute, Faculty of Science, Tokyo University of Education
** Department of Earth Sciences, Faculty of Science, Nagoya University
*** Emeritus Professor of Nagoya University

The writers carried out a geological survey of the Mozambique belt in the northeast district of Lake Victoria, about 50 km northeast of Kisumu(Fig. 1). This district is situated in the north of the Kavirondo rift (Shackleton, 1951) and in the east of the Nandi fault(Jennings, 1964). In this district, banded gneiss, amphibolite, granite, aplite and so on are well exposed along the Nandi Hills Road. The route map along the road is shown in Figs. 2-A and 2-B.

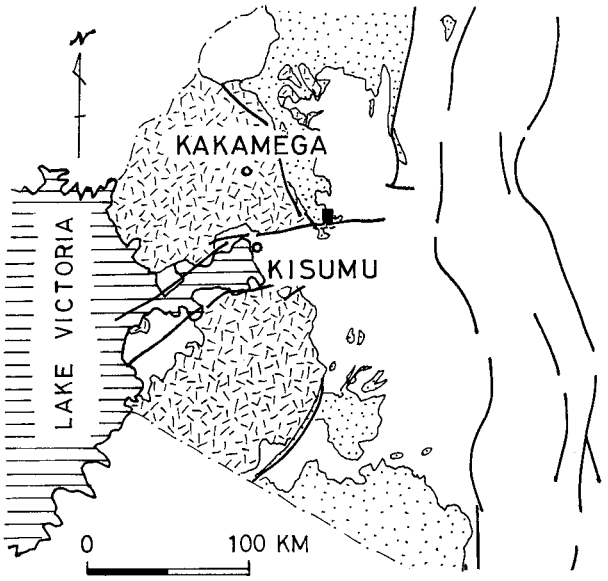

Fig. 1 Index map of the area northeast of Lake Victoria.

The problem on the parent rocks as well as the geologic history of the Mozambique belt has not been solved as yet. The writers intend to clarify this problem on the basis of the Rb-Sr absolute age method. As a first step, the writers report here some field evidences on the relationship between the metamorphic rocks and the igneous rocks in this district.

1: The relation between banded gneiss and amphibolite

The trend of amphibolite is slightly discordant to the banded structure of the gneiss. But "schistose structure" of amphibolite is concordant to that of the banded gneiss. This fact suggests that the metamorphism took place after the emplacement of the basic rocks.

2: The relation between banded gneiss-amphibolite and aplite(including pegmatite)

Broadly speaking, there are two cases for the relation between them: (1) the aplite approximately concordantly intrudes into the gneiss, but slightly intersects the banded structure. Interior structure of aplite, however, is concordant to the gneissose structure of the host gneiss; (2) the aplite derived from the granite injects into the gneiss or amphibolite as network or lit-par-lit veins(Figs. 3 and 4). In addition, some contaminated rocks are formed at the contact of the amphibolite with the aplite. In some cases, aplite gradually changes into the granite.

3: The relation between banded gneiss-amphibolite and granite

The granite in this district is bluish gray, fine-grained, massive, and equigranular. The foliation of the granite is found only at the contact of granite with gneiss or amphibolite. Such foliation is concordant to the boundary with host rocks. The granite intrudes into the gneiss and amphibolite and carries some xenoliths of the gneiss and

1st Prelim. Rep. Afr. Studies., Nagoya Univ. 17-20, 1975.

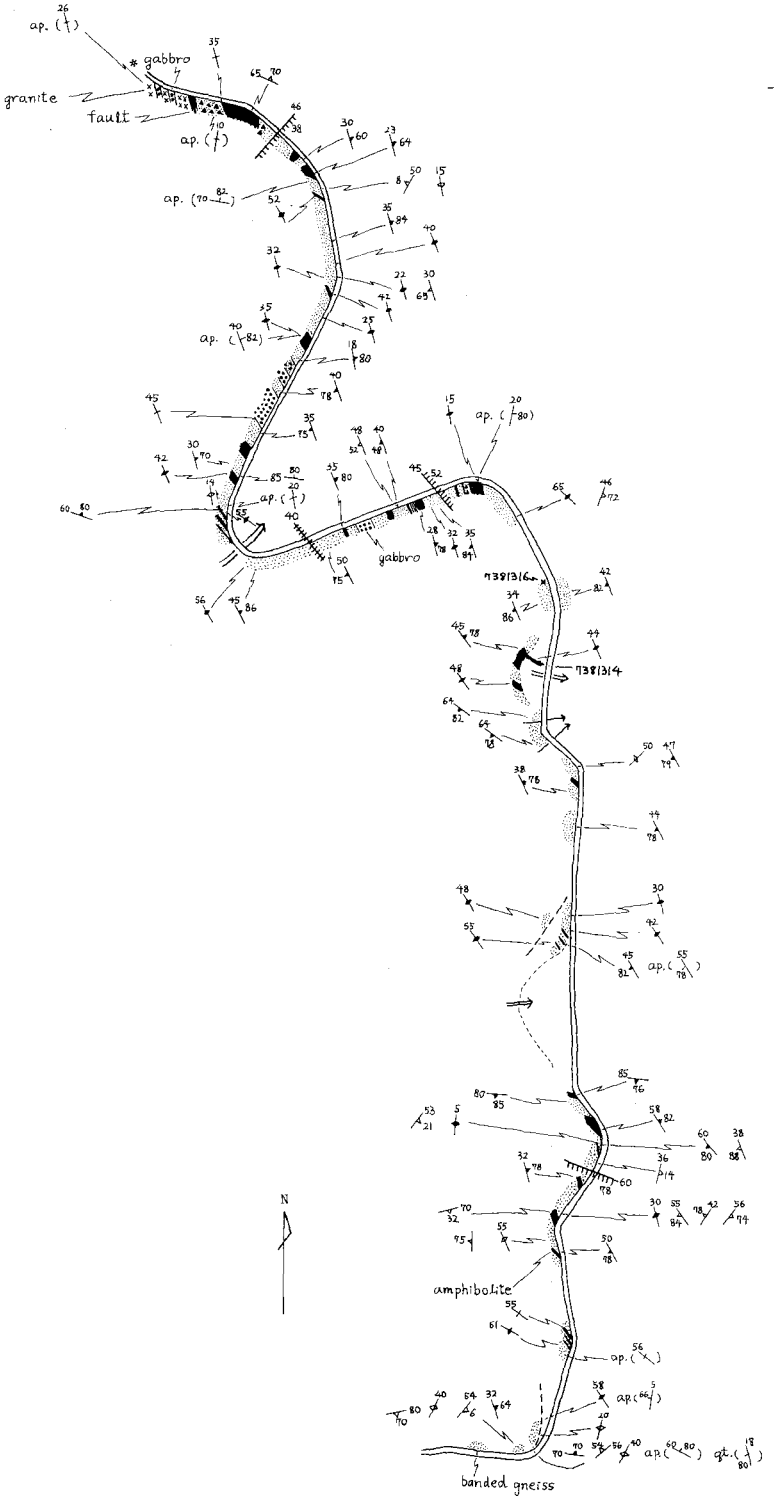

Fig. 2(2-A, 2-B) Route map along the Nandi Hills Road.

2-B

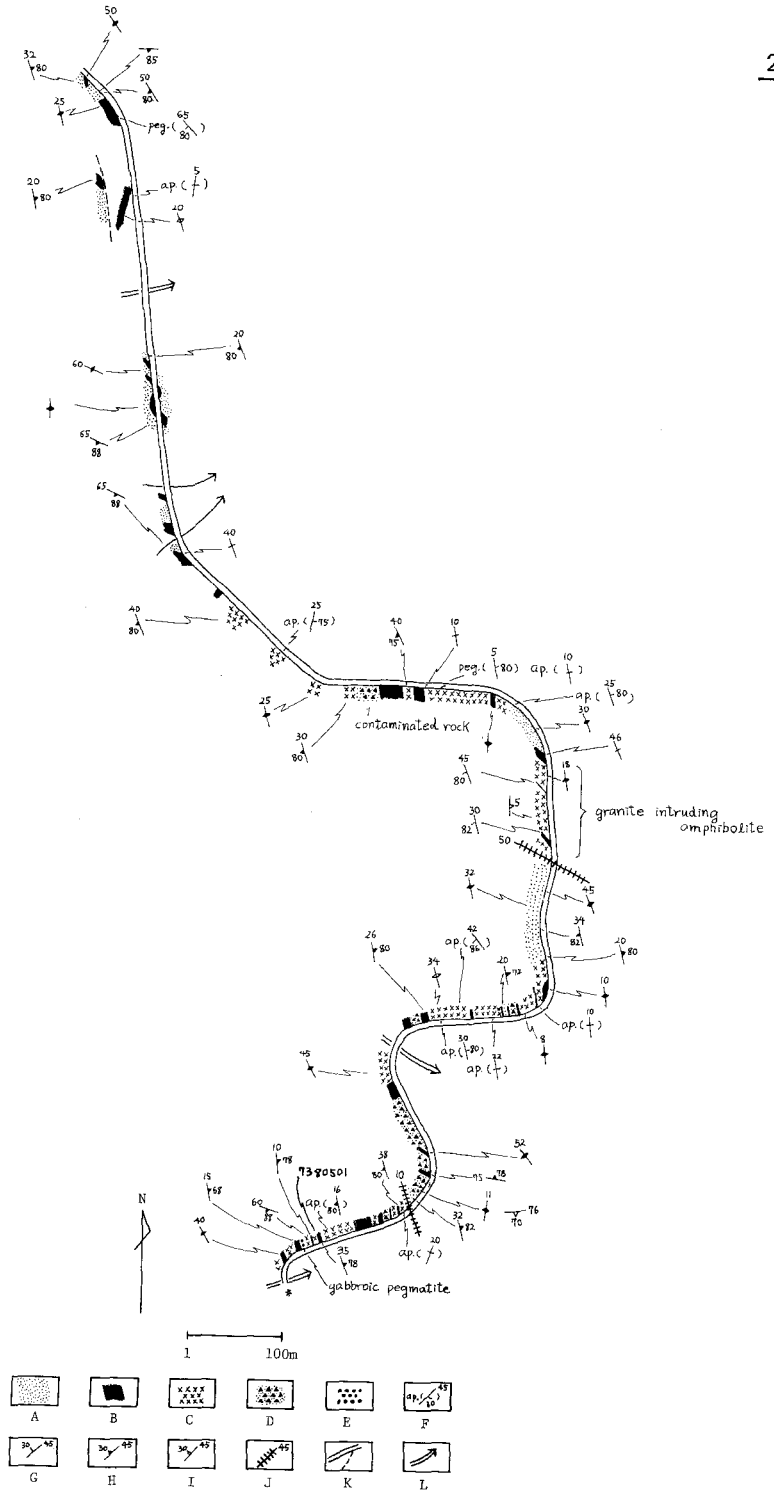

A : banded gneiss
B : amphibolite
C : granite
D : contaminated rock
E : dolerite, gabbro
F : direction of aplite
G : boundary direction between two rocks
H : gneissose structure
I : joint
J : fault
K : road
L : valley

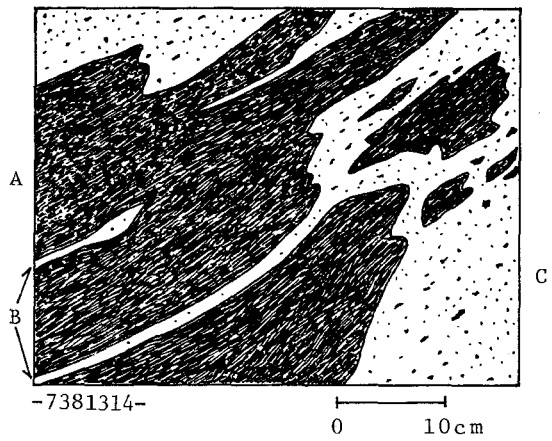

Fig. 3 Relation between amphibolite(A) and aplite (B) derived from granite(C).

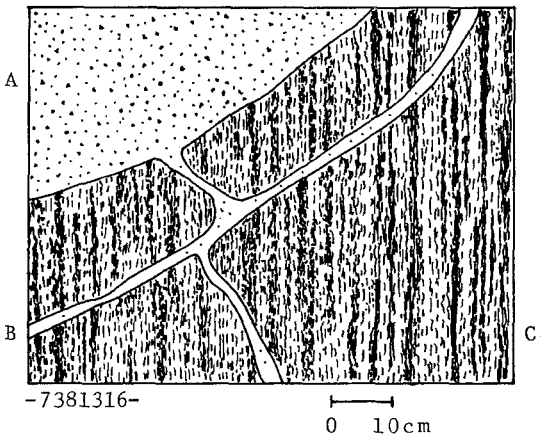

Fig. 4 Relation between banded gneiss(C) and aplite(B) derived from granite(C).

amphibolite(Fig. 5). The aplite derived from the granite injects into the gneiss and amphibolite as network or lit-par-lit veins.

4: The relation between basic dykes and other rocks

Some dykes of massive, fine-to coarse-grained dolerite and gabbro cut clean the gneiss, amphibolite, and granite. The grain size of the marginal part of some dolerite is finer than that of the central part, being interpreted as chilled margin.

From the evidences described above, the writers consider the mode of emplacement of these rocks as follows;
(1) The previously existed rocks were intruded by basic rocks. Some aplites and pegmatites might have intruded in this stage. (2) These rocks were metamorphosed and converted to banded gneiss and amphibolite. (3) The granite and its associated aplite intruded into these metamorphosed rocks. (4) In the last stage the basic rocks, dolerite and gabbro, intruded into these rocks.

Rb-Sr analysis for these rocks under study will be reported in a separate paper.

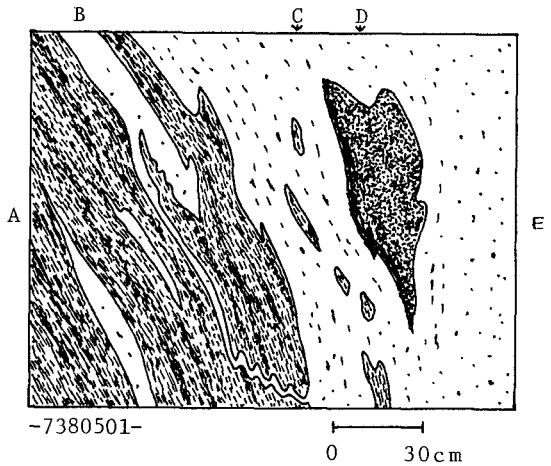

Fig. 5 Relation between banded gneiss–amphibolite and granite.
A: banded gneiss, B: aplite, C: xenoliths of banded gneiss, D: xenolith of amphibolite, E: granite

References

JENNINGS, D.J. (1964): Geology of the Kapsabet-Plateau area. *Rept. Geol. Surv. Kenya*, **63**, 43pp.

SHACKLETON, R.M. (1951): A contribution to the geology of the Kavirondo Rift Valley. *Q. J. Geol. Soc. London*, **106**, 345-392.

Sole Markings from the Mazeras Sandstones (Upper Triassic), Northwest of Mombasa, Kenya

Mamoru ADACHI

Department of Earth Sciences, Faculty of Science, Nagoya University

Introduction

On the coastal region of Kenya, upper Paleozoic to Mesozoic rocks correlative to the Karroo system in South Africa occur widely under the Tertiary to Quaternary sediments (Miller, 1952; Caswell, 1953; 1956; Tompson, 1956), and the rocks dip gently towards the coast. The stratigraphy of the Karroo system northwest of Mombasa is summarized in Table 1.

As a result of field investigation of 1973, a swarm of sole markings have been found from the rhythmically bedded sandstone and shale (Fig. 1) along the Mombasa-Nairobi road near Mazeras about 20 km northwest of

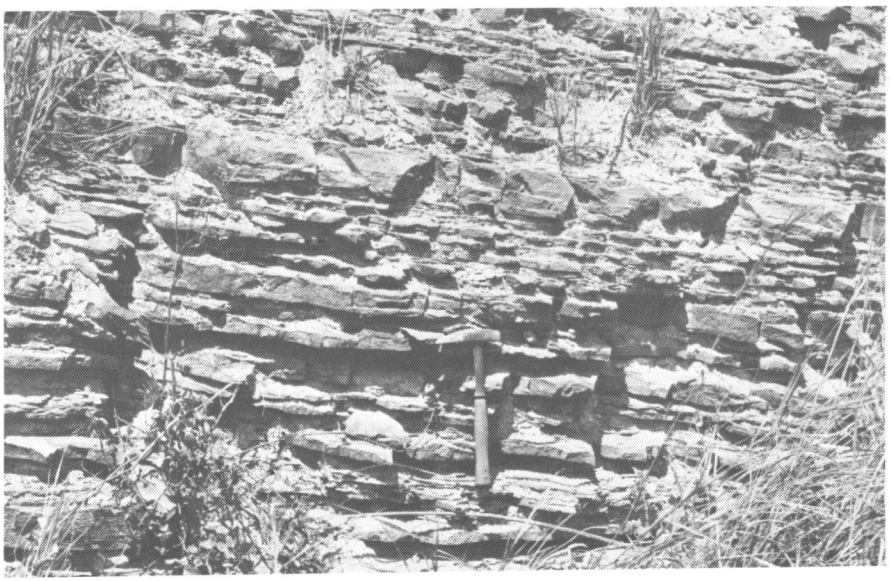

Fig. 1

Rhythmically bedded sandstone (feldspathic orthoquartzite) and shale of the Mazeras sandstones (upper Triassic). About 20 km northwest of Mombasa, Kenya (Photo by M.A.).

1st Prelim. Rep. Afr. Studies., Nagoya Univ. 21-25 , 1975.

Table 1 Stratigraphy of the Karroo system northwest of Mombasa (after Miller, 1952; Caswell, 1956)

Period	*Rock units*	*Lithology*	*Thickness*	*Depositional environment*	*Sedimentary structures*
Jurassic		limestone, shale, conglomerate	1500 m	mostly marine	cross-bedding ripple marks
		unconformity			
Upper Triassic	Mazeras sandstones	sandstone, shale, alternation of sandstone and shale	300 m	non-marine (partly marine)	cross-bedding slump structure
		unconformity?			
Lower Triassic	Mariakani sandstones	arkosic sandstone, quartzose sandstone, siltstone, shale	750 m	non-marine	cross-bedding ripple marks
Lower Triassic	Maji ya chumvi beds	sandstone, siltstone, shale, conglomerate, limestone	600 m	non-marine (partly marine)	cross-bedding ripple marks slump structure mud crack
Permian	Taru grits	arkose, conglomerate, shale, limestone	?	mostly non-marine	cross-bedding

Mombasa (Adachi, 1974). Unlike cross-bedding and ripple marks frequently found from the Karroo sandstones of Kenya, any occurrence of sole markings has not been reported from this area up to this time. A series of flysch-type sequence, thinly bedded sandstone (8-30 cm in thickness) and shale (3-10 cm) dipping gently northeastwards, is faced with yellowish gray shale by a fault which dips 50° to the southeast; fault clays and breccias about 1 m thick are seen along the fault plane. According to Caswell (1956), this alternation of sandstone and shale belongs to the Mazeras sandstones of upper Triassic age. As fossil evidence from the alternation is scanty, this has neither been confirmed nor refuted by the present work, and here I provisionally follow the Caswell's opinion.

Sole markings

Sole markings closely spaced and slightly deformed are well preserved on the base of sandstone exhibiting a purplish drab color due to iron-staining. They are flute casts (predominant), furrow casts, load casts, and small groove casts. The common types of flute casts (Fig. 2) range from a few centimeters to 10 cm long and 1 to 3.5 cm wide, the relief of which is mostly less than 1 cm. From the texture and mineralogical composition, the sandstone is classified as a medium-grained feldspathic orthoquartzite. It is composed chiefly of well-rounded to sub-angular grains of quartz, microcline, plagioclase, and white mica with accessories of sphene, zircon, tourmaline, epidote, allanite, and opaques cemented by carbonate and iron oxide of secondary products. Carbonate

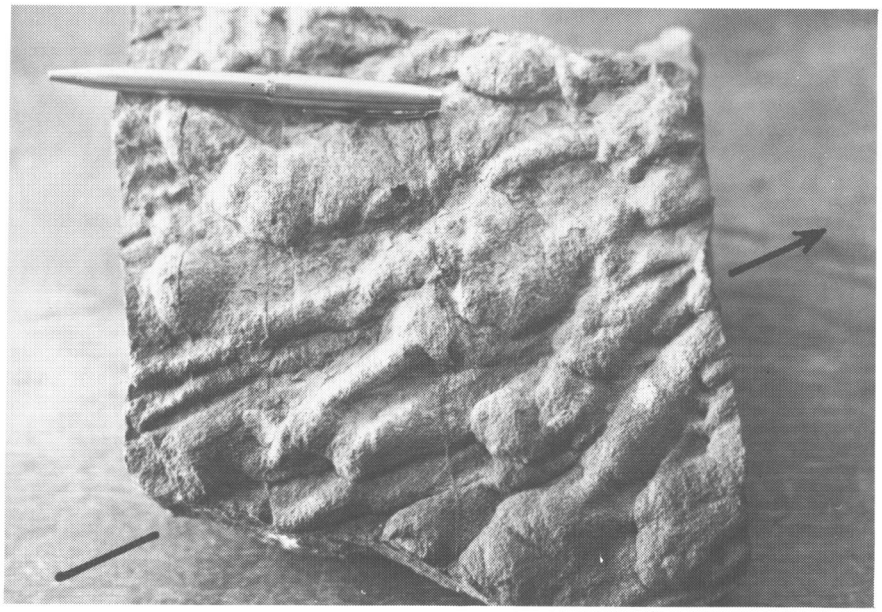

Fig. 2

Flute casts on sole of feldspathic orthoquartzite in the Mazeras sandstones. Arrow indicates the current direction (Photo by M.A.).

cement in places has eaten into and replaced the detrital grains, especially feldspars. Some of the grains are coated with iron oxide. Subangular quartz grains have, though rarely, tiny inclusions of zircon and tourmaline. It is noteworthy that the sandstone commonly carries detrital grains of quartz with overgrowth (Fig. 3); they are invariably large and rounded. Undoubtedly they are orthoquartzite fragments. Well-rounded grains of plagioclase and microcline are also occasionally discernible.

It was difficult to observe and record the attitude of sole markings in these subhorizontal beds, and only 32 measurements were taken in the outcrop. The paleocurrent inferred from flute casts clearly demonstrates that the clastic material making up the feldspathic orthoquartzite came from the northwest (Fig. 4).

Discussion

The paleocurrent towards the southeast and the mineralogical composition of the sandstone suggest much of the clastics were derived from the metamorphic terrain of the Mozambique belt. Then a question arises where the orthoquartzite fragments came from. The present exposure of orthoquartzite in Kenya is restricted in the late Precambrian Bukoban system around Kisii some 600 km northwest from Mombasa; it seems rather far distant for the direct provenance of the fragments. Caswell (1956) also noted the quartz grains with marginal growths from the Mazeras sandstones and the Mariakani sandstones about 50 km northwards from here, suggesting that the influx of orthoquartzite fragments took place during the period of middle to upper Triassic. As for the provenance of the orthoquartzite fragments, broadly speaking, there are two possibilities:

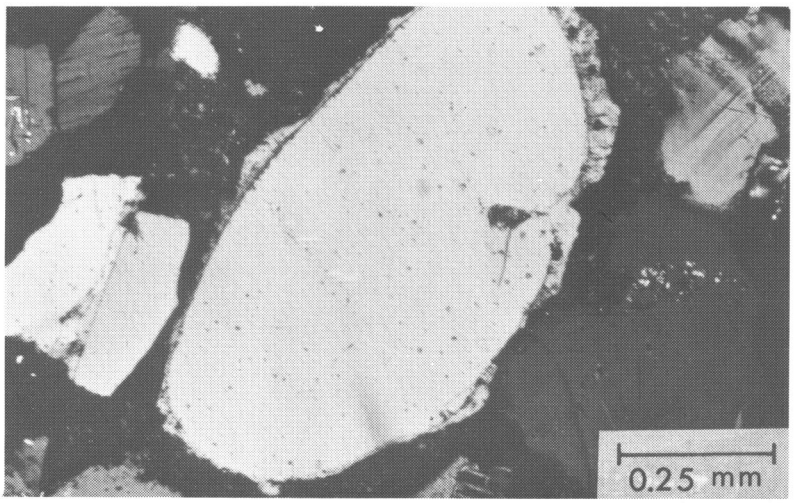

Fig. 3

Photomicrograph of feldspathic orthoquartzite of the Mazeras sandstones. Note a large well-rounded orthoquartzite fragment with overgrowth. Also visible are detrital grains of microcline, quartz, and plagioclase (Photo by M.A.). Crossed nicols.

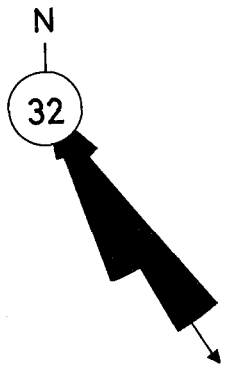

Fig. 4 Rose diagram showing the paleocurrent direction from the sandstone-shale alternation of the Mazeras sandstones. The number of readings is shown in the circle.

(1)the Bukoban orthoquartzite or its equivalents were exposed northwest of the basin not so far from Mombasa at Triassic time; (2) as the older Karroo sandstones are predominantly non-marine arkose in nature, orthoquartzitic sandstones were locally formed, and the fragments were derived therefrom. I prefer the latter possibility.

According to Caswell (1956), the lowermost Mazeras sandstones are subaquous, the uppermost continental, and between the two are deltaic in origin. Lithology and sedimentary structures such as cross-bedding and ripple marks, as a whole, seem to confirm this (Table 1). However, the existence of sole markings in a flysch sequence of the Mazeras sandstones strongly attests that the sequence has been deposited from turbidity currents. Presumably turbidity currents related to the submarine collapse were triggered by some earth movements during the upper Triassic time, transporting sediments into the N-S elongated basin. As has been discussed by many authors, the earth movement may be interpreted as a result of faultings in the basement ascribed to the rifting of the Gondwanaland.

Anyway the occurrence of sole markings will give us a sharper view on the sedimentation and paleogeography of the Mesozoic rocks of Coastal Kenya.

Acknowledgements—I wish to express my sincere thanks to Dr. S. Mizutani of Nagoya University for his fruitful advice on the sandstone and for reading the manuscript.

References

ADACHI, M. (1974): The Mesozoic group near Mombasa, Kenya. *J. Afri. Studies,* **14,** 14-20(in Japanease with English abstract).
CASWELL, P.V. (1953): Geology of the Mombasa-Kwale area. *Rept. Geol. Surv. Kenya,* **24***
CASWELL, P.V. (1956): Geology of the Kilifi-Mazeras area. *Rept. Geol. Surv. Kenya,* **34,** 54pp.
MILLER, J.M. (1952): Geology of the Mariakani-Mackinnon road area. *Rept. Geol. Surv. Kenya,* **20,** 32pp.
TOMPSON, A.O. (1956): Geology of the Malindi area. *Rept. Geol. Surv. Kenya.* **36,** 63pp.

* Not consulted in original.

Preliminary Report on the Carbonatitic Clasts in Tertiary Sediments from the Eastern Kavirondo Rift Valley, Kenya

Mamoru ADACHI and Kenji YAIRI

Department of Earth Sciences, Faculty of Science, Nagoya University

Introduction and general geology

Mt.Tinderet stands approximately in the eastern end of the Kavirondo Rift Valley (Fig. 1). Tertiary sediments composed chiefly

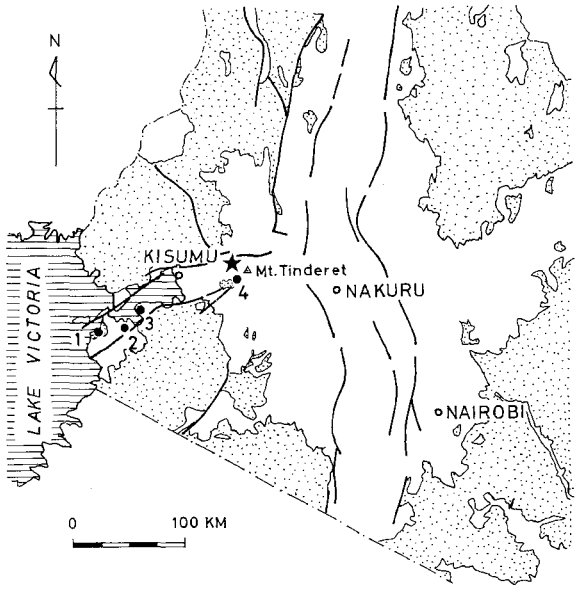

Fig. 1

Map showing the rift system in central Kenya and locations of carbonatitic clasts (black star) and Tertiary carbonatite centers (solid circle) in the Kavirondo Rift Valley. 1, Kisingiri; 2, Ruri; 3, Homa; 4, Legetet. Dotted area indicates pre-Tertiary basements. Bold lines represent major faults.

of limestone, marl, silt, sand, and tuff sporadically occur under the main volcanic succession of Tinderet, and they are considered to be of Miocene age(Shackleton, 1951; Binge, 1962; Jennings, 1964). While our stay in Kisumu in the summer of 1973, we carried out a field investigation in the eastern Kavirondo Rift Valley and its environs and found carbonatitic clasts in the Tertiary sediments near the Nyando fault scarp about 18 km northwest of Mt.Tinderet(location: Fig. 1, black star). The outcrop lies on the central southernmost part of the geological map of the Kapsabet-Plateau area(Jennings.1964), where Miocene limestone, tuff, and ash and Tertiary agglomerate rest on the basement Mozambique gneisses.

As shown on the route map(Fig. 2), sand, silt, mud, tuff, and agglomerate occur on both sides of impure limestone mass of Ngeron, but their mutual relationship is not clear owing to the poor exposure and the rapid change of lithofacies. It is noted that tuffaceous silt north of Ngeron yields some fossils(location: Fig. 2, solid circle). They are mainly gastropod fauna, the systematic description of which will be reported in a separate paper. This gastropod-bearing tuffaceous silt gradually passes upwards into tuff with white pumice and is in turn underlain by tuffaceous sand with cross-bedding.

Occurrence of carbonatitic clasts

In coarse-grained tuffaceous dirty-yellow sand are contained rounded to subrounded cobbles and boulders(5-30 cm in size) of carbonatitic rocks, together with other subangular volcanic clasts(location: Fig. 2, black star). There is found at least one traceable horizon rich in carbonatitic boulders, and the gravelly layer about 50 cm in thickness gradually changes vertically into coarse-grained sand, in which small volcanic clasts are sparsely scattered. Detrital grains of magnetite are often contained in a tuffaceous part of the sand, which further to the east passes into agglomerate and tuff. It is notable

1st Prelim. Rep. Afr. Studies., Nagoya Univ. 26-28, 1975.

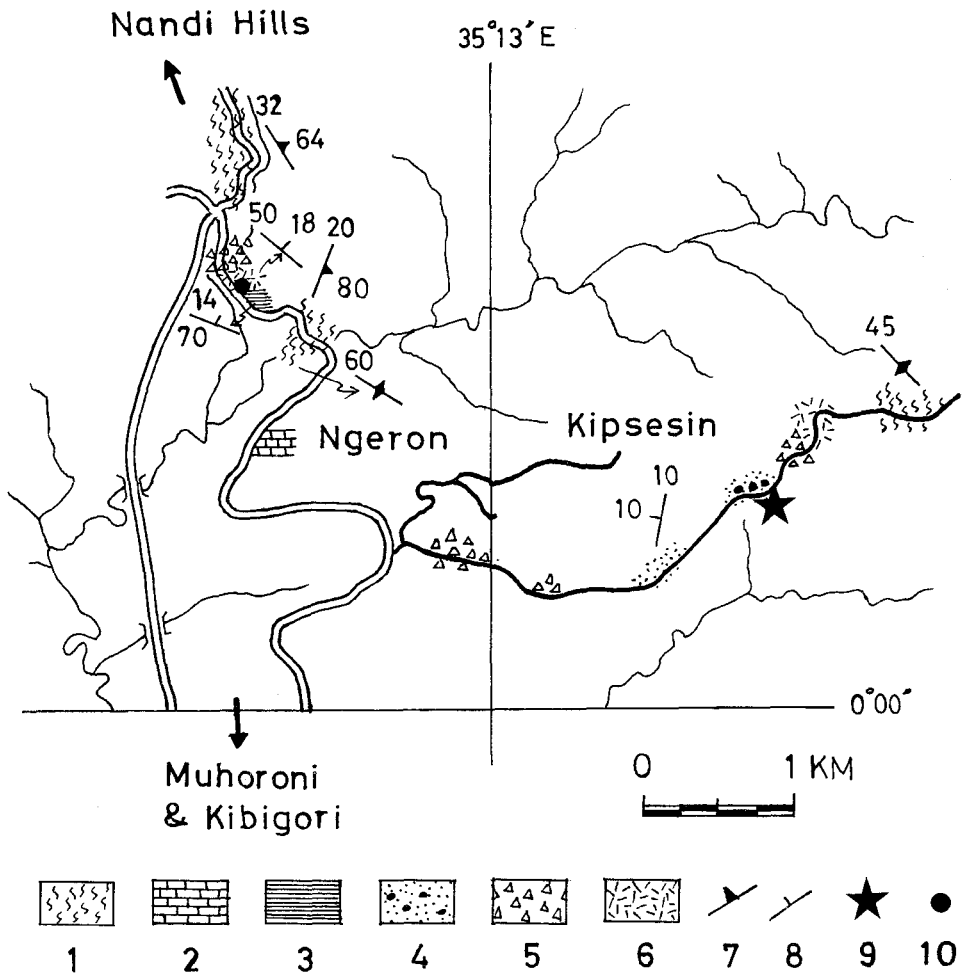

Fig. 2

Route map in the vicinity of Ngeron about 18 km northwest of Mt.Tinderet in the eastern Kavirondo Rift Valley. 1, basement gneisses of the Mozambique belt; 2–6, Tertiary sediments, 2, impure limestone; 3, tuffaceous and calcareous mud, 4, silt and sand with or without pumice and exotic clasts; 5, agglomerate; 6, tuff, 7, strike and dip of foliation; 8, strike and dip of beds; 9, location of carbonatitic clasts; 10, location of fossils.

that larger carbonatitic clasts show an imbricate structure, and the longest axes of the clasts dip to the east.

Macroscopically the carbonatitic clasts are divided into two types: (1) medium-grained carbonatite showing banding of white-colored and dark gray-colored parts, with abundant euhedral magnetite in the white-colored part; (2) fine-grained, heterogeneous, pinkish carbonatite with flow(?) structure. Both types of carbonatitic rocks have suffered a mild alteration, and are made up essentially of calcite with accessory magnetite and apatite, rarely with altered mica. Some calcite grains are coated with iron oxide. Apatite occurs as tiny needles or stumpy rhombs throughout in the calcite matrix. Magnetite often forms a

large crystal up to 3 mm across. Judging from the constituent minerals, these rocks may be classified as sövite(Tuttle and Gittins, 1966).

Discussion

Tertiary carbonatite centers so far recognized in the Kavirondo Rift Valley are: (1) Kisingiri; (2) Ruri; (3) Homa; (4) Legetet(Fig. 1). The Legetet carbonatite(Le Bas and Dixson, 1965) occurs at the southwestern foot of Mt.Tinderet and is located about 18 km south of the present area. This was previously thought to be a Miocene limestone. As for the provenance of carbonatitic clasts now under discussion, the Legetet carbonatite is a possible source area, but at present there is no direct evidence to confirm this. It is also possible to assume some carbonatite centers now eroded away or concealed under the Tinderet volcanics. We incline to favour the latter possibility, though this is a problem remained in the future.

According to King et al.(1972), the carbonatite activities in the Kavirondo Rift Valley are confined to the period from middle Miocene to Pliocene. However, our finding of carbonatitic clasts clearly demonstrates some carbonatite activity prior to the sedimentation of Miocene deposits in or around the Kavirondo trough. This evidence does throw some light on the carbonatite activity related to the birth or early development of the Kavirondo Rift Valley.

Detailed petrology and chemistry of the carbonatitic clasts will be given in the near future, together with paleontological data.

Acknowledgements—We thank Mr.S.Araki of Kenya Fishnet Industries who gave us facilities during our stay in Kisumu. Thanks are also extended to Drs.K.Suwa and S.Mizutani of Nagoya University for their keen interest and encouragement.

References

BINGE, F.N. (1962): Geology of the Kericho area. *Rept. Geol. Surv.Kenya,* **50,** 67pp.

JENNINGS, D.J. (1964): Geology of the Kapsabet-Plateau area. *Rept. Geol. Surv. Kenya,* **33,** 43pp.

KING, B.C., LE BAS, M.J., and SUTHERLAND, D.C. (1972): The history of the alkaline volcanoes and intrusive complexes of eastern Uganda and western Kenya. *J. Geol. Soc.,* **128,** 173 - 205.

LE BAS, M.J. and DIXON, J.A. (1965): A new carbonatite in the Legetet Hills, Kenya. *Nature,* **207,** 68.

SHACKLETON, R.M. (1951): A contribution to the geology of the Kavirondo Rift Valley. *Q. J. Geol. Soc. London,* **106,** 345-392.

TUTTLE, O.F. and GITTINS, J. (1966): *Carbonatites.* Wiley and Sons, New York, 591pp.

Geometry and Mechanics of En Echelon Faulting with Applications to the East African Rift System

Kenji YAIRI

Department of Earth Sciences, Faculty of Science, Nagoya University

Introduction

The East African Rift System is a complex zone of graben faults, broad elongated uplifts, and extensive volcanics since the Tertiary time (Baker, Mohr and Williams, 1972). The Afro-Arabian rift system is now known to be an extension of the global mid-oceanic ridge system (Heezen and Ewing, 1963). Recently, this recognition has led to interpretation in terms of plate tectonics (LePichon and Heirtzler, 1968; Gass and Gibson, 1969; Roberts, 1969; Baker, 1970; McKenzie and others, 1970; Baker and Wohlenberg, 1971; Mohr, 1972). Geological evidences such as normal faulting and fissure eruption roughly parallel to the general trend of the rift valley suggest that the rifting might have occurred under the horizontal tensional stress field. Earthquake mechanism studies show the active rifting in East Africa to be related to a tensional stress field in an east-southeast direction (Fairhead and Girdler, 1972). It is of much interest for us to get the information of the earlier stress field from the geological features.

The rift system consists of some graben structures arranged en echelon, and each graben also consists of en echelon normal faults(King, 1970; Walthall and Walper, 1967; Yairi, 1974). McConnell(1972) stressed that the Cenozoic rift faults followed mobile belts moulded upon ancient shields originating in the Precambrian time. We can consider the belt as a mechanically weak zone to be deformed and fractured between two relatively rigid plates. The stress state having occurred in the belt can be regarded as the second order's one caused and reorientated by the relative movement of the two plates under the regional stress field. We can easily imagine that en echelon faulting may occur when the direction of extension is rather oblique than normal to the trend of the weak zone; the orientation of faults arranged en echelon must reflect the stress state of second order. The object of this paper is to obtain the past regional stress field around the rift valley area on a basis of the geometry and mechanics of en echelon faulting.

Geometry and mechanics

En Echelon Pattern

In this paper, the following terminology is used for en echelon pattern. The term row expresses the orientation of the belt which comprises en echelon structures (Shainin, 1950); and the individual structural units are termed elements (Tokuda, 1926-27). Two patterns illustrated in Figs. 1-a and 1-b are clearly distinguished by using terms "italic m" type and "backhand writing m" type, respectively(Tokuda, 1926-27; Mizutani, 1964). From the point of view of pattern discrimination, these terms are more proper than the genetical nomenclature such as left-hand and

1st Prelim. Rep. Afr. Studies., Nagoya Univ. 29-38, 1975.

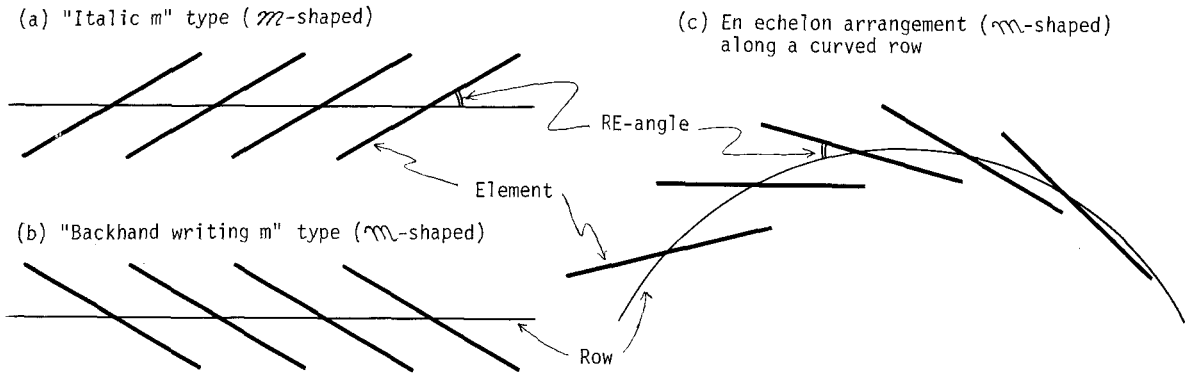

Fig. 1 En echelon pattern.

right-hand(Campbell, 1958). This terminology is applied to the case where the row curves and elements is not necessarily parallel to each other (Fig. 1-c).

Second Order Strain State

Some authors have mentioned that en echelon fractures occur under the tensional stress field (Cloos, 1968; Lajtai, 1969; Nakamura, 1970; Wendell and Nakamura, 1973), though most of studies of en echelon patterns have been based on the simple shear mechanisms (e.g. Riedel, 1929). En echelon extension fractures and normal faults are treated to be related to the strain state of the second order reorientated within a mechanically weak zone under the regional horizontal extension. En echelon fracturing is expected when the trend of the weak zone is oblique to the direction of extension. The following discussion is developed on the assumption that failures occur in compliance with the maximum principal strain theory.

Above-mentioned deformation is simplified as illustrated in Fig. 2; that is, an original parallelogram, ABCD, in an unstrained state is deformed into the parallelogram, A′B′C′D′. We can set up an oblique coordinate $\overline{X}O\overline{Y}$ ($\angle\overline{X}O\overline{Y} = \phi$) with the origin, O, at the center of the parallelogram, the axes $O\overline{X}$ and $O\overline{Y}$ chosen in the direction of the horizontal extension and in the trend of the deformed zone, respectively (Fig. 3). In the oblique coordinate $\overline{X}O\overline{Y}$, suppose that point P which is at $(\bar{x}, \bar{y})$ before straining is at P′ $(\bar{x} + \bar{u}, \bar{y} + \bar{v})$ after straining, $(\bar{u}, \bar{v})$ being the components of the displacement from point P to point P′. If the extension to the directions of $O\overline{X}$ and $O\overline{Y}$ are given by e_x and e_y, respectively, we get

$$\bar{u} = e_{\overline{x}}\,\bar{x},\ \bar{v} = e_{\overline{y}}\,\bar{y},\ (e_{\overline{x}} \leqq 0,\ e_{\overline{y}} \leqq 0) \quad (1)$$

Using the rectangular coordinate XOY ($O\overline{X} = OX$), the coordinates of the points P and P′ are expressed by (x, y) and (x + u, y + v), respectively; then the components of the displacement (u, v) are given by

$$u = \bar{u} + \bar{v}\cos\phi,\ v = \bar{v}\sin\phi \quad (2)$$

The coordinate (x, y) is related to the coordinate $(\bar{x}, \bar{y})$ by the following equation,

$$x = \bar{x} + \bar{y}\cos\phi,\ y = \bar{y}\sin\phi \quad (3)$$

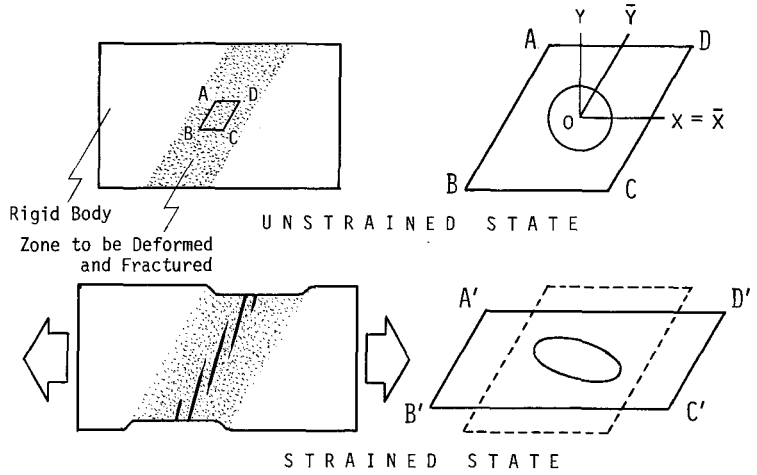

Fig. 2 Strain state of second order in a deformed zone.

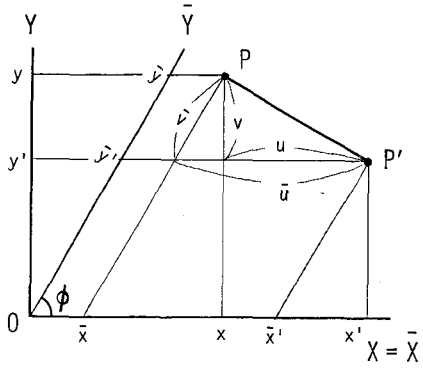

Fig. 3 Strain translation.

From (1), (2), and (3), we get

$$u = e_{\bar{x}}\, x - (e_{\bar{x}} - e_{\bar{y}})y \cot \phi, \quad v = e_{\bar{y}}\, y \quad (4)$$

The coordinates (x′, y′) after deformation are

$$x' = (1 + e_{\bar{x}})x - (e_{\bar{x}} - e_{\bar{y}})y \cot \phi, \qquad y' = (1 + e_{\bar{y}})y \quad (5)$$

The most general strain displacement, where the coordinates (x, y) of any points before deformation are displaced to position (x′, y′), is given by

$$x' = ax + by, \quad y' = cx + dy, \quad (a>0,\ d>0) \quad (6)$$

The simplest way of considering finite homogeneous two dimensional strain state is to study the deformation of a circle of a unit radius in unstrained state. By (6), the circle $x^2 + y^2 = 1$ becomes the ellipse

$$(c^2 + d^2)x'^2 - 2(ac + bd)x'y' + (a^2 + b^2)y'^2 = (ad - bc)^2 \quad (7)$$

This is called the strain ellipse (Jaeger, 1962).

Angle θ between coordinate OX and the major or minor axis of the ellipse is given by

$$\tan 2\theta = 2(ac+bd) / (a^2+b^2-c^2-d^2) \quad (8)$$

In the case of the strain state of (5), substituting $a = (1 + e_{\bar{x}})$, $b = -(e_{\bar{x}} - e_{\bar{y}})\cot\phi$, $c = 0$, and $d = (1 + e_{\bar{y}})$ into (8), we get

$$\tan 2\theta = -2(1 + e_{\bar{y}})\cot\phi \,/\, [(e_{\bar{x}} + e_{\bar{y}})(\cot^2 \phi + 1) + 2] \quad (9)$$

When angle ϕ is not so small and extensions $e_{\bar{x}}$ and $e_{\bar{y}}$ is negligibly small,

$$\tan 2\theta \fallingdotseq -\cot\phi, \quad \theta \fallingdotseq \phi/2 \pm 45^\circ \quad (10)$$

When the strain are very small, the theory of infinitestimal strain may be developed. Then two dimensional strain state in a body can be expressed in terms of two normal strains ε_x and ε_y, and shear strain γ_{xy}. They are also expressed in terms of displacements with reference only to two directions x and y as $\varepsilon_x = \partial u/\partial x$, $\varepsilon_y = \partial v/\partial y$, and $\gamma_{xy} = \partial v/\partial x + \partial u/\partial y$. From (5),

$$\varepsilon_x = e_{\bar{x}},\ \varepsilon_y = e_{\bar{y}},$$
$$\gamma_{xy} = -(e_{\bar{x}} - e_{\bar{y}}) \cot \phi \qquad (11)$$

This relationship shows the superposition of the strain in the extension on the simple shear. Lajtai (1969) got the general solution on the origin of en echelon fractures occurring under the similar stress state. According to the theory of infinitestimal strain, the directions of the principal axes of strain are given by $\tan 2\theta = \gamma_{xy}/(\varepsilon_x - \varepsilon_y)$, where the maximum or minimum principal axis is inclined to the x-axis at an angle of θ. From (11),

$$\tan 2\theta = -\cot\phi,\ \theta = \phi/2 \pm 45° \qquad (12)$$

Thus we get the same results as induced from the geometrical consideration of strain ellipse.

Estimation of Regional Horizontal Extension

Equations (10) and (12) show that the direction of the principal strain axes in the deformed zone is related to the direction of the regional horizontal extension. Under the assumption of the maximum principal strain theory of failure, we can estimate the direction of extension from the geometrical interrelationship among the directions of row and elements and their pattern. As is evident from Fig. 4, angle θ between x-axis and the minor axis of the ellipse is given by $\theta = \phi/2 + 45°$, and RE-angle α is related to ϕ and θ by $\alpha = \theta - \phi$. Thus the angle between the direction of the row and that of the horizontal extension, ϕ, is given by

$$\phi = 90° - 2\alpha \qquad (13)$$

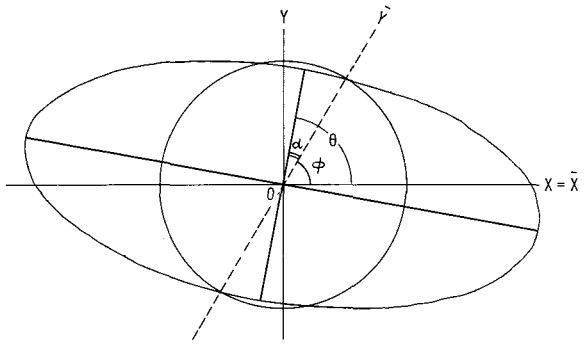

Fig. 4 Strain ellipse and RE-angle

Angle ϕ is measured clockwise from the direction of the row when en echelon pattern is "italic m" type, and anticlockwise in the case of "backhand writing m" type.

As far as we deal with fracture patterns on a plane view, the result described above can be applied whether they are extension fractures or normal faults in origin. The strain state in a deformed zone is determined by the relative movement of two rigid plates, between which the zone is sandwiched. If the movement is attributed to the rotation around a point, RE-angle varies continuously along the row. By using the geometrical analysis of en echelon faults, therefore, we can find the pole of rotation between two plates or the variation of the direction of the horizontal extension along the rifting area.

Order of En Echelon Structure

In the East African Rift System, there can be found en echelon patterns of various scales ranging from some centimeters to some thousands of kilometers in dimension of their elements as shown in Table 1 (Yairi, 1974).

Table 1 Dimension of elements arranged en echelon in East African Rift System

order	dimension of elements		examples
	width	length	
1	150 km	2500 km	Western and Eastern Rifts
2	40 km	100 – 400 km	Lake Albert Rift
3	2 km	40 – 80 km	normal faults along the rift shoulder
4	200 – 500 m	10 – 20 km	
5	10 – 50 m	200 – 800 m	photogeologic lineaments
6	2 – 4 m	20 – 60 m	
7	1 – 3 mm	2 – 8 cm	field observation (Yairi and Mizutani, 1969)

Let us suppose as shown in Fig. 5-a that a weak zone with a trend represented by double lines is affected by a horizontal extension whose direction is indicated by open arrows. The first order arrangement of fractures, as shown by dotted lines, occurs first in the zone in compliance with equation (12). As the element of the first order is also considered to be a kind of weak zone, in the next stage, en echelon arrangement of fractures of the second order may occur along the element, where the first order's element itself represents a row for the arrangement of the second order. Thus, the patterns of the lower order will be formed successively. The value of RE-angle decreases with progress of fracturing, and we can get the same result of horizontal extension no matter what order of en echelon patterns is. Yairi (1974) also pointed out that a row forming a circular arc is always associated with elements forming a circular arc, and the curvature of the latter is smaller than that of the former, and the curvatures of the row and elements decrease with lowering of the order of en echelon structure (Fig. 5-b).

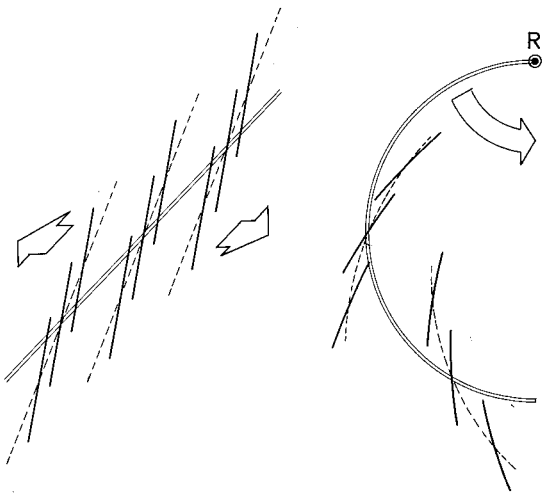

Fig. 5 Order of en echelon arrangement, R denoting a pole of rotation.

Applications to the East African Rift System

An Example: The Lake Albert Rift

The Lake Albert Rift consists of two parts of different graben structures: in the northern part Albert Nile region is characterized by en echelon arrangements of faults, and in the southern part Lake Albert to the Lower Semliki region by rather simple rectilinear fault lines. The arrangement of faults developed on the rift shoulder in the former shows

a typical en echelon pattern of "backhand writing m" type, though the outline of trough itself forms a roughly circular arc, whose radius of curvature is about 100 km (Fig. 6). The trend of the fault line varies continuously from N45° E in the north and to N20° E in the south. We can recognize two curved rows arranged en echelon on the eastern shoulder and western one, respectively; these rows also form en echelon pattern of "backhand writing m" type.

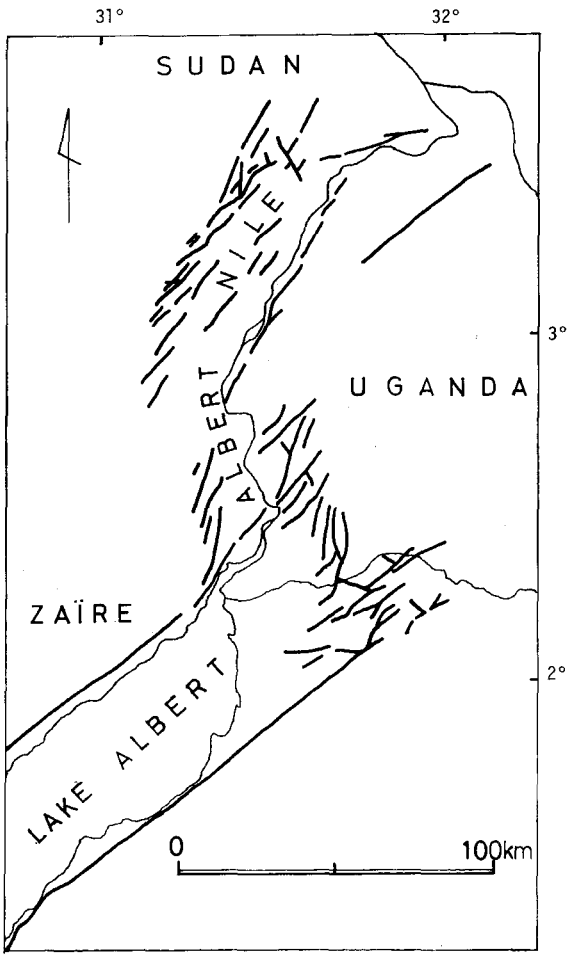

Fig. 6 Lake Albert Rift.

Using en echelon patterns of the two different orders, we get the values of N40° – 45° W of the direction of horizontal extension. This result is favourable to interpret the rectilinear figure of faults trending N45° E along Lake Albert to the Semliki area. This trend is also in accordance with that of the Aswa Fault (Almond, 1962; MacDonald, 1969; Hepworth, 1967). The author is in an opinion that the Aswa-Nandi line, which is a part of the Pangani-Aswa Lineament by McConnell (1974), play an important role as a transform fault connecting the Western Rift and the Eastern one; the detailed discussion will be given in a separate paper. The direction of the horizontal extension obtained above may be attributed to the regional stress field resulted in rift faulting at least in the northernmost part of the Western Rift.

The Eastern and Western Rifts

The same procedure as mentioned above was applied to many different segments of the East African Rift System, and the result was summarized in Fig. 7 (Yairi, 1974). In the Red Sea and Gulf of Aden Rifts, lineaments found in the central trough or ridge axis are regarded as elements of en echelon arrangement, and the results obtained agree well with the spreading direction of plates given by McKenzie and others (1970) and Laughton (1966). This suggests that the method proposed in this paper is applicable to the zigzag or en echelon pattern found in the mid-oceanic ridge system, and we can estimate the spreading direction only from geometry of ridge arrangement without knowledge of the transform fault direction. The present results obtained in the Gregory Rift also agree well with the results from earthquake mechanisms(Fairhead and Girdler,

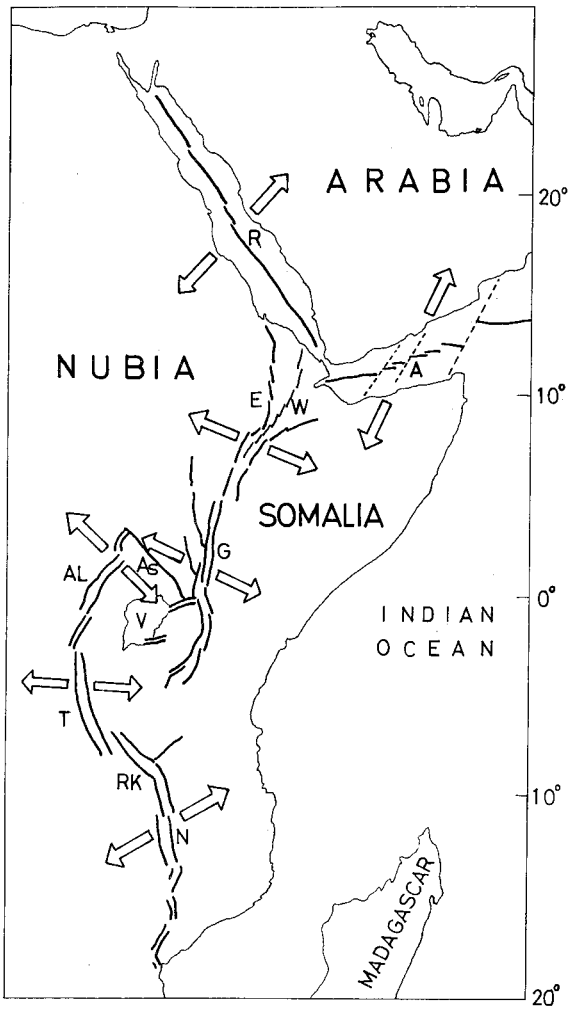

Fig. 7 Crustal extension along East African Rift System.

1972) and from gravity anomalies (Searle, 1970).

The Western Rift, at least from Lake Albert to Lake Rukwa rift, consists of five graben structures arranged en echelon along the row forming a roughly circular arc with a radius of curvature of 870 km, their pattern being "backhand writing m" type. As shown in Fig. 7, the direction of the extension changes continuously along the row. The explanation of this arrangement lies in an interpretation that the amount of the extension increases gradually southwards (Yairi, 1974). In other words, a pole of rotation for two plates, between which the rifting zone is found, is supposed to be situated far north.

As well known, the relative movement of two rigid plates on a spherical surface is given by a rotation with a constant angular velocity around a pole. However, for the interpretation of the extension variation along the Western Rift, it is necessary to take account of the angular velocity not being uniform but variable along the plate boundary. This argument contradicts the assumption that the plate is a rigid body. Although it is the subject for a future study to clarify whether the contradiction suggests the deformation of the continental crust itself or only suggests a lack of uniformity of the strain orientation in the deformed zone, the following consideration is presented provisionally. By regarding the Western and the Eastern Rifts as two elements of en echelon arrangement involved in a much wider zone, it is suggested that a small amount of extension in the northern part of the Western Rift is compensated by a large amount of extension of the Eastern Rift around the central Kenya, where enormous volume of volcanics is found. On the other hand, it is also suggested that a large amount of extension in the southern part of the Western Rift is compensated by a small amount of extension around the northern Tanzania in the southern extremity of the Gregory Rift, where the typical rift faulting and volcanism become indistinct.

The First Order Structure of the East African Continent

We can consider the Western Rift and the Eastern one as two elements of en echelon arrangement of "italic m" type. A third element following them corresponds to the uplifted area from Rhodesia to South Africa, where no evidence of the remarkable rift faulting and volcanism is found so far. The row in which these three elements are comprised may represent the first order structural unit in Africa, it trending approximately NNE, gently curving convexly to the west, and its dimension amounting to 7000 km in length and 1500 km in width. The concept of the perenial deep lineament by McConnell (1972) can be accepted for understanding the geological meaning of the first order's row. It is supposed that such deep lineament in the lower part of the lithosphere might have controlled the trend and space of the large-scale structural pattern.

As already mentioned by Degens and others (1971), the evolution of an oceanic rift is preceded by three development stages: uplift; block faulting; and volcanic and hydrothermal activity. In East Africa, the evolutionary stages can be followed from south to north in this order. Fiarhead and Girdler (1972) suggested a pole of rotation for Nubia-Somalia somewhere southwest of Africa. It is now supposed that en echelon arrangement of the elemental rift structures as described above might occur under the first order regional tensional stress field, which affected the huge-scale weak zone formed along the subcrustal deep lineament.

Summary and conclusions

1. The East African Rfit System is divisible into the Eastern and Western Rifts. The arrangement of graben structures found in the Rifts is characterized by en echelon pattern on a plane view, and each graben consists also of en echelon normal faults.

2. Geological and geophysical phenomena in the rift valley area suggest that the fracturing of the African continent had occurred along the mechanically weak zone between two relatively rigid plates under the regional horizontal tension stress field.

3. En echelon faulting is related to the second order strain state reorientated in the weak zone, whose trend is oblique to the direction of the regional horizontal extension.

4. In terms of geometry and mechanics on the strain ellipse, we can find a formula, $\phi = 90^\circ - 2\alpha$, where ϕ is the angle between the trend of the weak zone and the direction of the horizontal extension, and α, defined as RE-angle, is the angle between an element of en echelon fractures and its row.

5. The method was applied to the determination of the direction of the horizontal extension along the East African Rift System (Fig. 7).

6. The Eastern Rift as well as the Western one can be considered as an element of en echelon structure. The belt which involves both Rifts is the first-order mobile zone manifested along a subcrustal deep lineament.

Aknowledgements – The author wishes to thank Dr. S. Mizutani of Nagoya University for helpful discussions and for critical reading of the manuscript.

References

ALMOND, D.C. (1962): Explanation of the geology of sheet 15(Kitugum). *Geol. Surv. Uganda, Rept.* **8,** 55pp.

BAKER, B.H. (1970): The structural pattern of the Afro-Arabian rift system in relation to plate tectonics. *Royal Soc. London Philos. Trans., Ser. A.,* **267,** 383-391.

BAKER, B.H. and WOHLENBERG, J. (1971): Structure and evolution of the Kenya rift valley. *Nature,* **229,** 538-542.

BAKER, B.H., MOHR, P.A. and WILLIAMS, L.A.J. (1972): Geology of the eastern rift system of Africa. *Geol. Soc. America, Spec. Paper 136,* 67pp.

CAMPBELL, J.D. (1958): En echelon folding. *Econ. Geol.,* **53,** 448-472.

CLOOS, E. (1968): Experimental analysis of Gulf Coast fracture patterns. *Am. Assoc. Petrol. Geol. Bull.,* **52,** 429-444.

DEGENS, E.T., VON HERZEN, R.P. and WONG, H.K. (1971): Lake Tanganyika: water chemistry, sediments, geological structure. *Naturwissenschaften,* **58,** 229-241.

FAIRHEAD, J.D. and GIRDLER, R.W. (1972): The seismicity of the east African rift system. *Tectonophysics,* **15** (1/2), 115-122.

GASS, I.G. and GIBSON, I.L. (1969): Structural evolution of the rift zones of the Middle East, *Nature,* **221,** 926-930.

HEEZEN, B.C. and EWING, M. (1963): The mid-oceanic ridge, *In: Hiel, M.N., ed., The Sea.* New York, Interscience Pub., **3,** 388-410.

HEPWORTH, J.V. (1967): The photogeological recognition of ancient orogenic belts in Africa. *Quart. J. Geol. Soc. Lond.,* **123,** 253-292.

JAEGER, J.C. (1962): *Elasticity, fracture and flow with engineering and geological applications.* London, Methuen, 212pp.

KING, B.C. (1970): Vulcanicity and rift tectonics in Africa. *In: T.N. Clifford and I.G. Gass, eds., African magmatism and tectonics.* Edinburgh, Oliver and Boyd, 263-283.

LAUGHTON, A.S. (1966): The Gulf of Aden, in relation to the Red Sea and the Afar depression of Ethiopia. *In: The world rift system— UMC symposium, Canada Geol. Surv. Paper 66-14,* 78-97.

LAJTAI, E.Z. (1969): Mechanics of second order faults and tension gashes. *Geol. Soc. Am. Bull.,* **80,** 2253-2272.

LEPICHON, X. and HEIRTZLER, J.R. (1968): Magnetic anomalies in the Indian Ocean and sea-floor spreading. *Jour. Geophys. Research,* **73,** 2101-2117.

MACDONALD, R. (1969): The Atlas of Uganda(2nd ed.), *Dept. of Lands and Surveys,* Entebe.

MCCONNELL, R.B. (1972): Geological development of the rift system of eastern Africa. *Geol. Soc. Am. Bull.,* **83,** 2549-2572.

MCCONNELL, R.B. (1974): Evolution of taphrogenic lineaments in continental platforms. *Geol. Rundsch.* **63,** 389-430.

MCKENZIE, D.P., DAVIES, D. and MOLNAR, P. (1970): Plate tectonics of the Red Sea and East Africa. *Nature,* **226,** 243-248.

MIZUTANI, S. (1964): Superficial folding of the Paleozoic system of central Japan. *J. Earth Sci., Nagoya Univ.,* **12,** 17-83.

MOHR, R.A. (1972): Surface structure and plate tectonics of Afar. *Tectonophysics,* **15,** (1/2), 3-18.

NAKAMURA, K. (1970): En echelon fractures of Icelandic ground fissures. *Acta Naturalia, Islandica,* **2,** 1-15.

RIEDEL, W. (1929): Zur Mechnik geologischer Brucherscheinungen(Ein Beitrag Zum Problem de Fiederspalten). *Centralblatt für Mineralogie, Geologie und Paläontologie, Abteilung B,* 354-368.

ROBERTS, D.G. (1969): Structural evolution of the rift zones in the Middle East. *Nature,* **223,** 55-57.

SEARLE, R.C. (1970): Evidence from garvity anomalies for thinning of the lithosphere benearh the rift valley in Kenya. *Geophys. J. R. Astr. Soc.,* **21,** 13-31.

SHAININ, V.E. (1950): Conjugate sets of en echelon tension fractures in the Athens limestone at Riverston, Virginia. *Geol. Soc. Am. Bull.,* **51,** 509-517.

TOKUDA, S. (1926-27): On the echelon structure of the Japanese Archipelagoes. *Jap. J. Geol. Geogr.,* **5**(41), 41-76.

WALTHALL, B.H. and WALPER, J.L. (1967): Peripheral Gulf Rifting in Northeast Texas. *Am. Assoc. Petrol. Geol. Bull.,* **51,** 102-110.

WENDELL, A.D. and NAKAMURA, K. (1973): A photogeologic method for determining the direction of horizontal dilation from patterns of en echelon fracturing. *Jour. Research U.S. Geol. Survey,* **1,** 283-287.

YAIRI, K. (1974): En echelon pattern of the East African Rift System. *Jour. Afr. Studies,* **14,** 21-46(in Japanese with English abstract).

Fault Pattern and Crustal Extension of the Kavirondo Rift Valley in Relation to a Bifurcating Rift Model

Kenji YAIRI

Department of Earth Sciences, Faculty of Science, Nagoya University

Introduction

The Kavirondo Rift Valley (Shackleton, 1951) branches from the Gregory rift at the center of the Kenya domal uplift (Baker and Wohlenberg, 1971), trending EW and ENE-WSW towards the Kavirondo Gulf of Lake Victoria. It is about 250 km in length and 25 to 30 km in width, forming a graben structure bounded apparently by normal faults (McCall, 1958; Saggerson, 1952; Jennings, 1964; Binge, 1962). The fault throws range up to 700 m in the central graben sector, but near the junction with the Gregory rift, the structure is obscured by Tertiary volcanoes. Unlike the Gregory rift there was no sign of Quaternary faulting and volcanism in the floor of the Kavirondo rift, it seems to have formed in the early Pliocene (Baker and others, 1972). McConnell (1974) stressed that the Kavirondo trend, including the Speke Gulf graben and Utimbara-Isuria fault zone (Shackleton, 1946; Williams, 1964), followed the Precambrian mobile belt between the Tanganyika and West Nile-Uganda shield. A gravity survey by Darracott and others (1972) suggested that the Speke graben was interpreted as a Precambrian rift and it was rejuvenated in Neogene rifting.

It is of much importance to clarify the mechanical origin of the bifurcation of rift faults. Based on the experiment of Cloos (1939), Holmes (1965) mentioned that the bifurcating or splaying-out pattern of the rift faults was developed towards the end of an elongated dome or upwarp. Burke and Whiteman (1973) proposed the conception of rrr (rift, rift, rift) triple junction in relation to plate tectonics; the Kavirondo rift, which intersects the northern and southern arms of the Gregory rift at Nakuru, was regarded as a rift arm which became inactive in Pliocene before reaching the spreading stage. In this paper I deal with en echelon fault pattern in the Kavirondo rift and estimate the direction of the crustal extension across the rift according to the method of Yairi (1974, 1975). Based on the results, a model is proposed to explain the formation of the bifurcating rift pattern.

Fault pattern and crustal extension

The outline of the Kavirondo depression forms a gentle curve convex to the northwest, trending EW in the east and ENE-WSW in the west. Although the escarpment bounding the depression represents a fault-line scarp rather than an actual fault line (McCall, 1958; Saggerson, 1952), we can know the fault pattern to some extent from its arrangement and lineaments developed along the escarpment. The fault pattern was studied mainly by aerial photographs and topographic maps, supplemented by field observations. Conclusively, the fault pattern shows en echelon arrangement of "italic m" type, RE-angle being 10° to 15° in the east and much smaller in the west (Fig. 1).

1st Prelim. Rep. Afr. Studies., Nagoya Univ. 39-43, 1975.

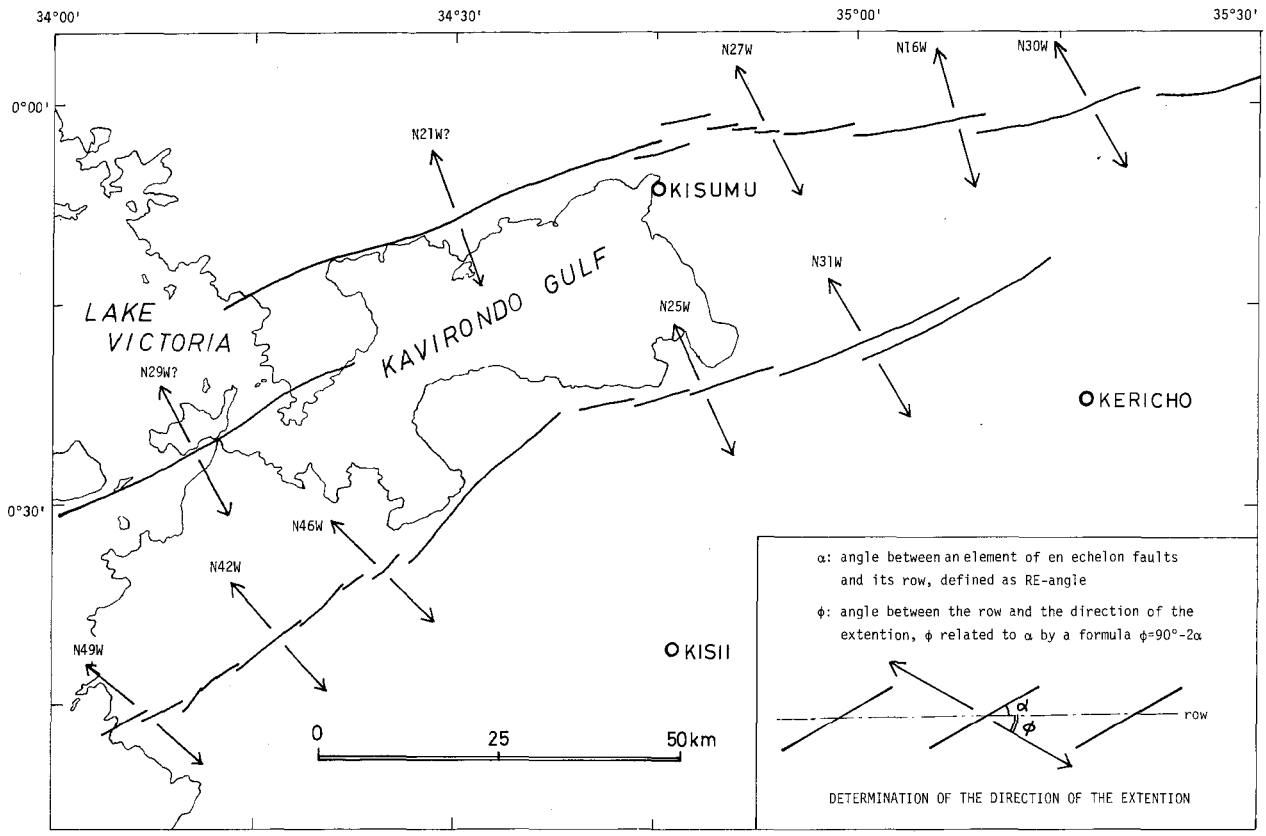

Fig. 1

Fault pattern of the Kavirondo rift. Arrows indicate the directions of the horizontal extension.

If the faults are attributed to the normal faulting in origin formed under the horizontal crustal extension, the method of Yairi (1974, 1975) is applicable to the determination of the direction of the extension. The results are summarized in Fig. 1: N16°—31°W in the east and N42°—49°W in the west. On the other hand, in the Gregory rift, a WNW-ESE extension was estimated from the pattern of faults formed during the Plio-Pleistocene (Fig. 2-b; Yairi, 1974); this direction is consistent with that of the plate motion inferred from earthquake mechanisms (Fairhead and Girdler, 1971, 1972) and gravity anomalies (Searle, 1970).

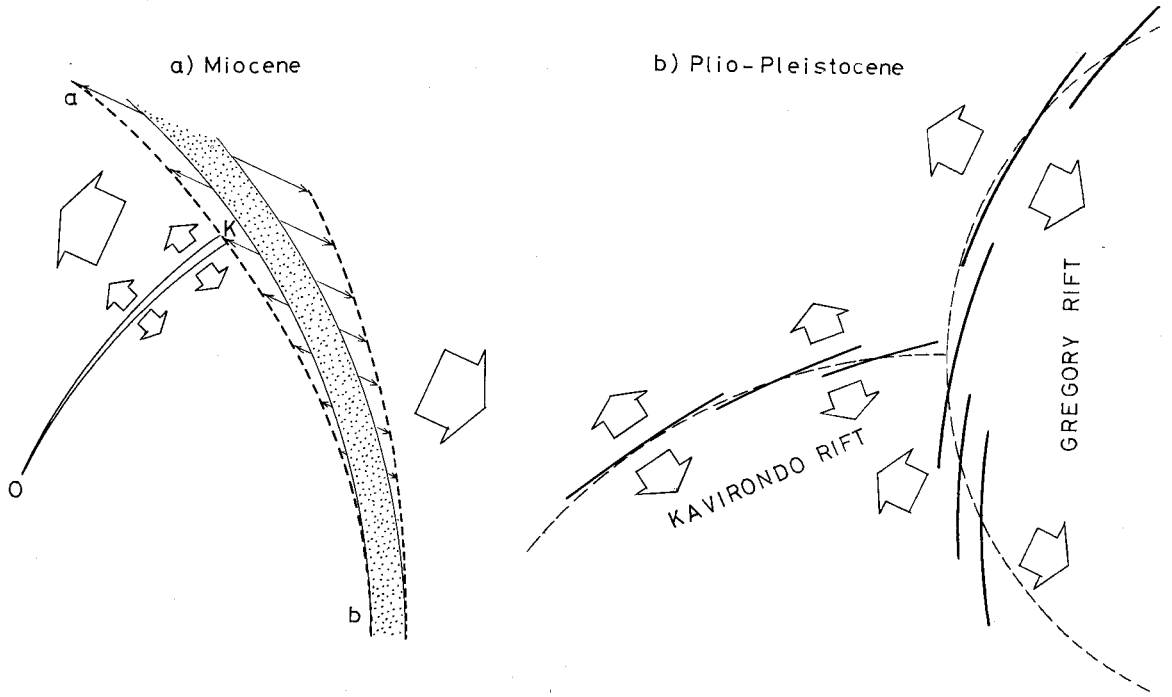

Fig. 2
Bifurcating rift model showing the formation of the Kavirondo rift.

Bifurcating rift model

The Plio-Pleistocene rift faulting in this region is preceded by the volcanic activity. Since fossil evidence from the sediments below or within the basal volcanics in the Kavirondo trough indicates an early Miocene age (King, 1970), the formation of the Kavirondo trend appears to have already originated in the Miocene time and to have been related to the formation of the linear arrangement of the Miocene volcanoes along the Kenya-Uganda border far west of the present Gregory rift. The volcanic zone forming a gentle curve convex to the east may be regarded as the most active zone of rifting during the Miocene.

Here a model is proposed to explain the origin and mechanism of the bifurcating rifts taking the relation between the Kavirondo and Gregory rifts as an example. In Fig. 2-a, a dotted strip forming a circular arc denotes the rifting zone of the Gregory trend in the Miocene, the zone regarded as a mechanically weak zone between two plates. It is now supposed that the crustal extension in WNW-ESE direction has a continuous variation in amount from the south to the north along the zone as shown by arrows in the figure. The deformation of the zone is apparently attributed to the rotation around a pole to the south of the zone, along which the angle velocity gradient is supposed. When the original strip is deformed into the zone bounded by broken lines, the eastern margin of the western plate is affected by a bending

moment and there occurs secondarily tension stresses along it. The Kavirondo trend, OK in Fig. 2-a, is considered to be originated under the tensional stress field, though it might have followed the Precambrian mobile belt.

The E-W variation in the extension across the Kavirondo rift can be interpreted by assuming a pole of rotation far southwest and the angle velocity of the rotation decreasing gradually westwards, because the straining is restricted around the pole. The disappearance or splaying-out of the rift faults as well as volcanics at the southern extension of the Gregory rift in northern Tanzania may be evidences in favor of interpreting the variation of the extension or angle velocity gradient assumed above. This suggests that the assumption of the plate being rigid may not hold true in dealing with the bifurcating rift pattern in the continental crust. The evolution of the Kavirondo rift involves two stages: (1) stage of the downwarping related to the formation of a shallow basin extending EW to ENE-WSW in the Miocene; (2) stage of the rift faulting in the Plio-Pleistocene. From the mechanical standpoint, the first stage may correspond to the stage of the crustal stretching and thinning, and the second to the stage of the crustal rupture and faulting under the tensional stress field.

Summary

Fault pattern of the Kavirondo rift was studied by aerial photographs and topographic maps. It shows en echelon arrangement of "italic m" type. According to the method of Yairi (1974, 1975), the direction of the horizontal extension across the Kavirondo rift was determined (Fig. 1): N16°—31°W in the east and N42°—49°W in the west. A possible model was proposed to explain the origin and mechanism of the bifurcating rift pattern taking the relation between the Kavirondo rift and the Gregory rift as an example (Fig. 2). The result seems to be incompatible with the former view; the assumption that the plate is rigid may not hold true in dealing with the rift fault pattern in the continental crust.

Acknowledgements—I wish to thank Mr.M. Adachi of Nagoya University for helpful discussions and for critical reading of the manuscript.

References

BAKER, B.H. and WOHLENBERG, J. (1971): Structure and evolution of the Kenya rift valley. *Nature,* **229,** 538-542.

BAKER, B.H., MOHR, P.A. and WILLIAMS, L.A.J. (1972): Geology of the eastern rift system of Africa. *Geol. Soc. Am., Spec. Pap.,* **136,** 67pp.

BINGE, F.W. (1962): Geology of the Kericho area. *Kenya Geol. Surv. Rept.,* **50,** 67pp.

BURKE, K. and WHITEMAN, A.J. (1973): Uplift, rifting and break-up of Africa. *In: "Implications of Continental Drift to the Earth Sciences",* D.H. Tarling and S.K. Runcorn, Eds., London(Academic Press), **2,** 735-755.

CLOOS, H. (1939): Hebung-Spaltung-Vulcanismus. *Geol. Rundsch.,* **30,** 405-527.

DARRACOTT, B.W., FAIRHEAD, J.D. and GIRDLER, R.W. (1972): Gravity and magnetic surveys in northern Tanzania and southern Kenya. *Tectonophysics,* **15,** 131-141.

FAIRHEAD, J.D. and GIRDLER, R.W. (1971): The seismicity of Africa. *Geophys. J. R. Astr. Soc.,* **24,** 271-301.

FAIRHEAD, J.D. and GIRDLER, R.W. (1972): The seismicity of the east African rift system. *Tectonophysics,* **15,** 115-122.

HOLMES, A. (1965): *Principles of physical geology(2nd ed.).* London, Thomas Nelson and Sons Ltd., 1288pp.

JENNINGS, D.J. (1964): Geology of the Kapsabet-plateau area. *Kenya Geol. Surv. Rept.* **63,** 43pp.

KING, B.C. (1970): Vulcanicity and rift tectonics in East Africa, *In: African magmatism and tectonics,* Clifford, T.N. and Gass, I.G., Eds., Edinburgh, Oliver and Boyd, 263-283. 283.

MCCALL, G.J.H. (1958): Geology of the Gwasi area. *Kenya Geol. Surv. Rept.,* **45,** 88pp.

MCCONNELL, R.B. (1974): Evolution of taphrogenic lineaments in continental platforms. *Geol. Rundsch.* **63,** 389-430.

SAGGERSON, E. (1952): Geology of the Kisumu district. *Kenya Geol. Surv. Rept.,* **21,** 86pp.

SHACKLETON, R.M. (1946): Geology of the country between Nanyuki and Maralal. *Kenya Geol. Surv. Rept.,* **11,** 54pp.

SHACKLETON, R.M. (1951): A contribution to the geology of the Kavirondo rift valley. *Quart. J. Geol. Soc. Lond.,* **106,** 345-392.

SEARLE, R.C. (1970): Lateral extension in the east African rift valleys. *Nature,* **227,** 267.

WILLIAMS, L.A.J. (1964): Geology of the Mara River-Sianna area. *Kenya Geol. Surv. Rept.,* **66,** 47pp.

YAIRI, K. (1974): En echelon pattern of the East African Rift System. *J. Afri. Studies,* **14,** 21-46(in Japanese with English abstract).

YAIRI, K. (1975): Geometry and mechanics of en echelon faulting with applications to the East African Rift System. *1st prelim. Rep. Afr. Studies. Nagoya Univ.,* 29-38.

Throw Variation of Normal Faults Arranged en Echelon

Kenji YAIRI* and Yoshijiro KATO**

* Department of Earth Sciences, Faculty of Science, Nagoya University
** Department of Geology, College of General Education, Nagoya University

The classic experiment of the graben formation of Hans Cloos (1936) was slightly modified in order to understand a fault system arranged en echelon on the rift shoulders (Yairi, 1974). In the latter experiment, a model layer made up of powdered sugar was set on two boards which could be pulled in opposite direction; the joining line of the two boards crosses obliquely the pull-direction as shown in Fig. 1. Then the layer was brought under tension, and it failed with the development of a graben structure parallel to the joining line; on either side of the graben there was formed a system of normal faults arranged en echelon on a plane view. Each fault trends obliquely not only to the pull-direction but also to the trend of the graben. The geometrical and mechanical bases of en echelon faulting are discussed in detail in a separate article of this volume (Yairi, 1975). We here deal with a problem of the throw variation of faults taking en echelon fault pattern found in the Lake Albert rift as an example.

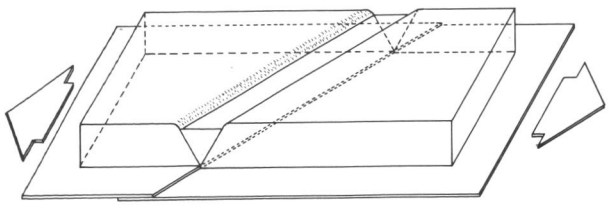

Fig. 1 Diagrammatic setup of graben experiment.

An example of the experimental results of en echelon faulting is shown in Fig. 2, where the fault throws diminish towards both ends of each fault. Since the strain

Fig. 2 Fault pattern on model surface illuminated at low angle from the left. Faults arranged en echelon are developed on either side of graben and fault throws diminish towards both ends of each fault.

1st Prelim. Rep. Afr. Studies., Nagoya Univ. 44-51, 1975.

concentrates in the deformed and failed zone which comprises faults arranged en echelon, the individual faults can not be developed beyond the zone. When the extension distribution is uniform along the zone, the fault throws are in proportion to the extension. If two faults are arranged en echelon and overlap each other, the amount of the extension is related to the total throws of the two faults. A schematic model is given to show the variation of fault throws diminishing towards both ends of the individual faults arranged en echelon (Fig. 3-a), and another model for en echelon arrangement of graben structures themselves is given in Fig. 3-b.

In the Albert Nile region, the northern end of the Western Rift, faults arranged en echelon are developed on either side of the graben (Fig. 4). As shown in a summit level map (Fig. 5), the zone which comprises en echelon faults is represented morphologically by a remarkable escarpment developed between the rift floor and the marginal plateau. From the mechanical standpoint, this zone can be regarded as a zone to be deformed and failed during the graben formation.

Fig. 6 shows a simplified topographic map of an area along the western walls of the Lake Albert rift; contour lines on the topographic map (scale; 1:50000) are modified and smoothed out by burying valleys more than 1 km in width. Two linear fault scarps arranged en echelon are recognized, and they overlap each other; the western fault diminishes southwards and the eastern one northwards. Although the fault throws, which are estimated from the topographic relief, have some

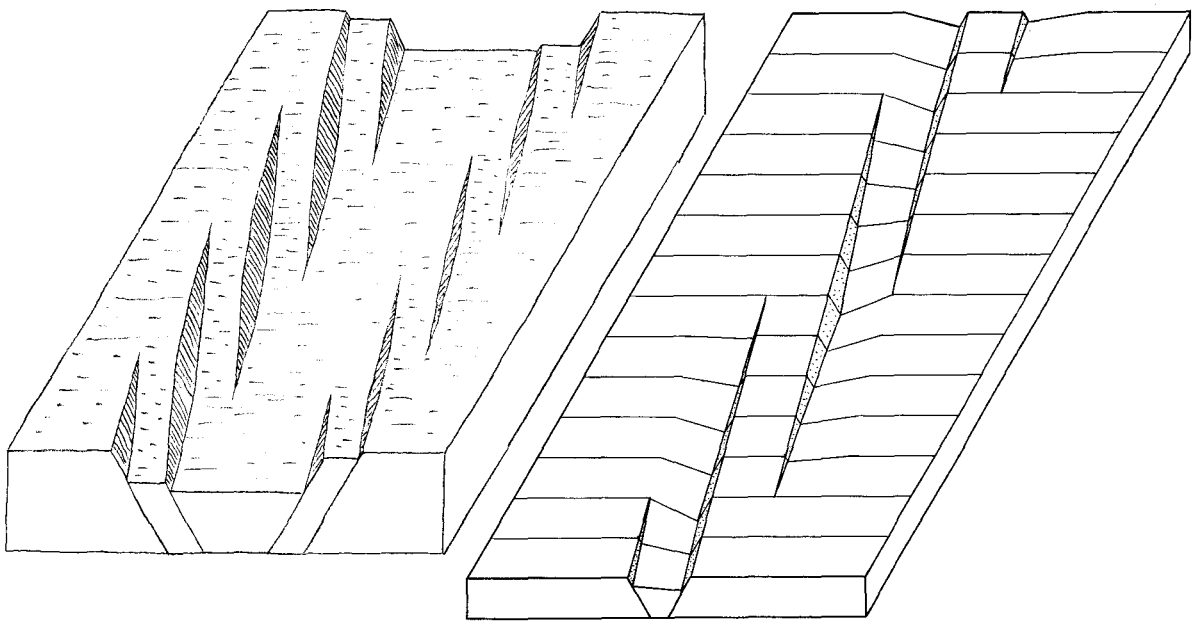

Fig. 3 Schematic model showing throw variation of normal faults arranged en echelon. a: en echelon faults developed on either side of graben. b: en echelon and overlapping graben structures.

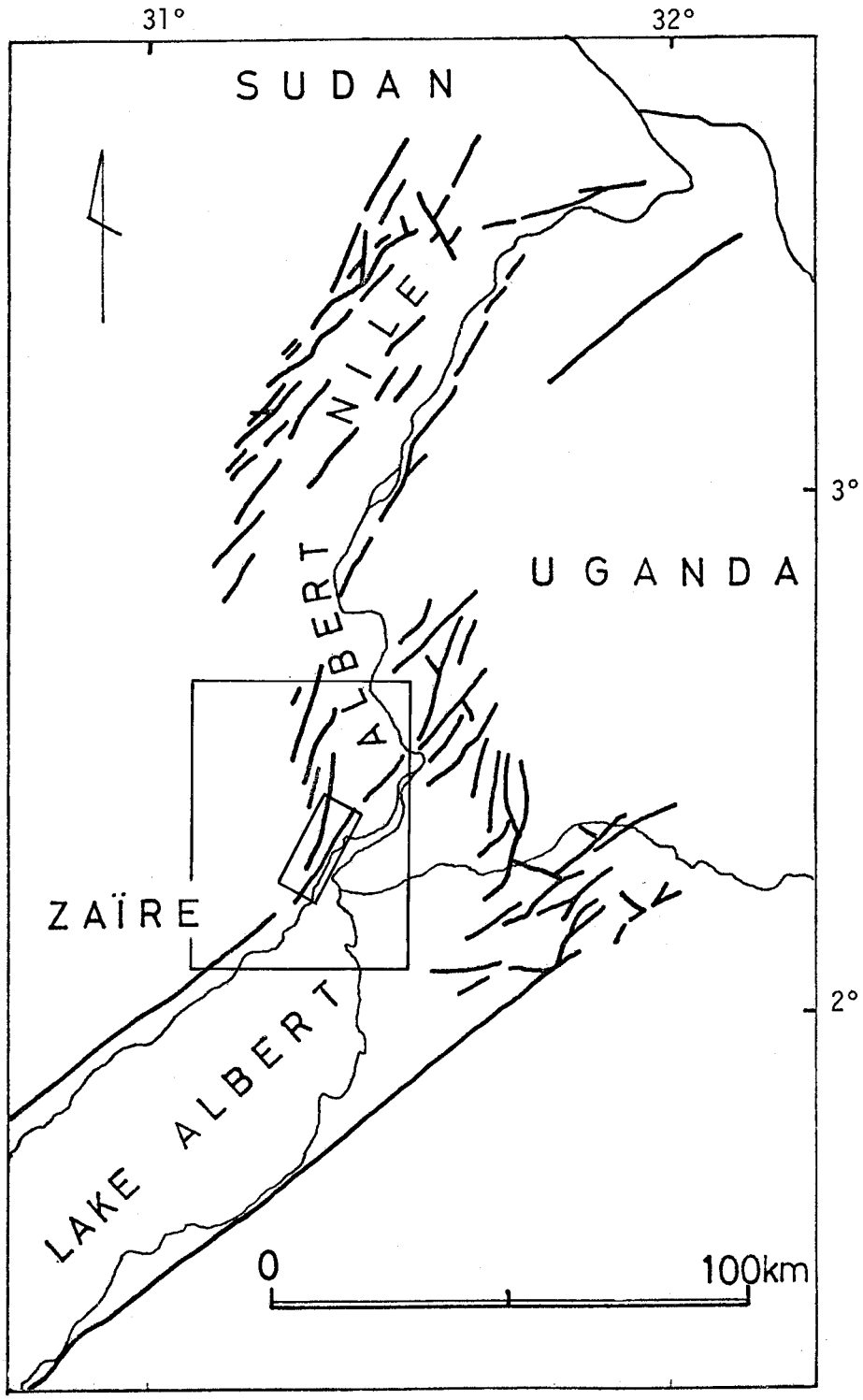

Fig. 4 Fault pattern in Albert Nile region. Faults are after MacDonald (1969) and the present work. Two squares in the map indicate localities of Fig. 5 and Fig. 6, respectively.

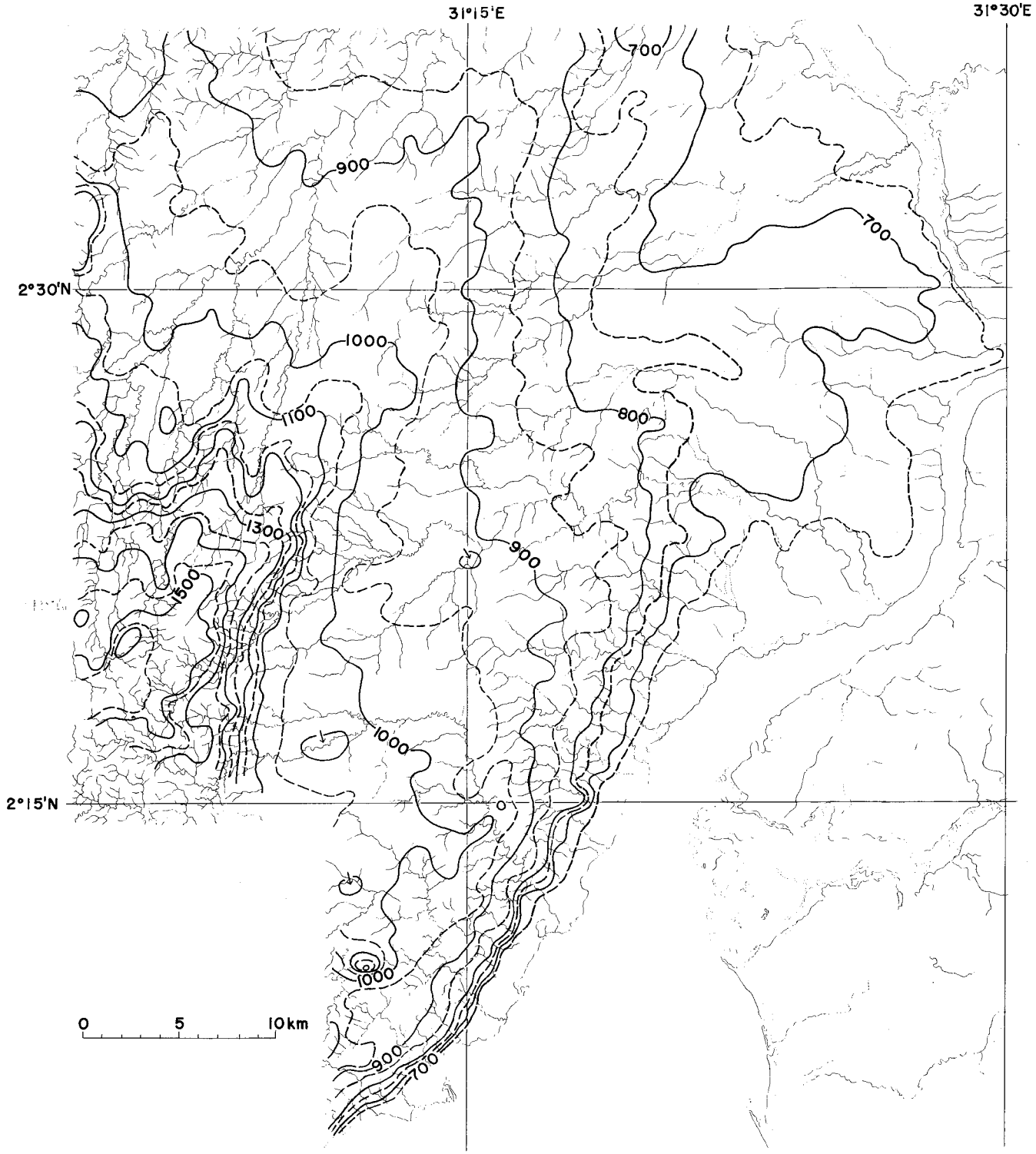

Fig. 5 Summit level map and drainage pattern in the southern part of Albert Nile region (contours: 50m intervals).

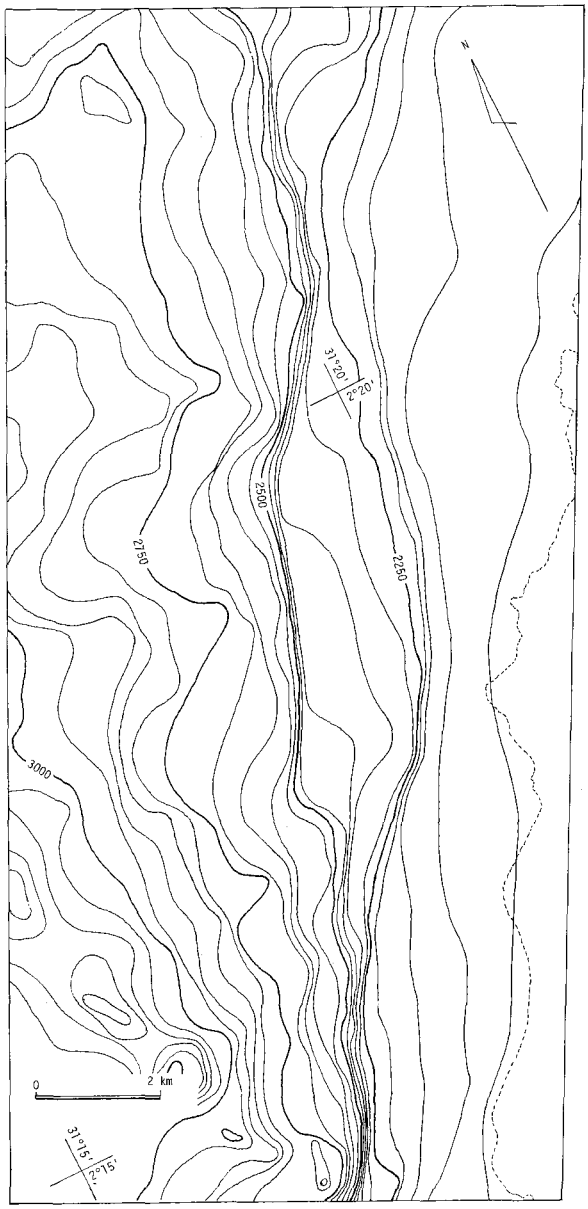

Fig. 6 Simplified topographic map of an area in Fig. 5 (contours: 50 feet intervals). Contour lines are smoothed out by burying valleys more than 1 km in width on topographic maps (scale; 1:50000).

variation along the scarps, the total throws of both faults appear to be approximately constant, about 300 feet. A strip bounded by the two faults overlapping tilts northeastwards, steeply in the south and gently in the north. These phenomena strongly attest the model shown in Fig. 3-a.

Lake Tanganyika as well as Lake Malawi is longitudinally elongated in shape and its medial part is somewhat crooked (Yairi and Mizutani, 1969). This feature can be regarded as en echelon arrangement of two graben structures overlapping each other. The bathymetric charts of these lakes are very suggestive of the tilting of the rift floor itself; below the lake level, deep strips are found along either side of the rift floor rather than along the central trough axis. These deep strips as well as steep slopes along the rift walls are also arranged en echelon and overlap each other. All these phenomena may be attributed to the throw variation of faults bounding the grabens arranged en echelon (cf. Fig. 3-b).

Acknowledgements—We wish to thank Mr.M. Adachi of Nagoya University for helpful discussions and for critical reading of the manuscript.

References

C LOOS, H. (1936): *Einführung in die Geologie.* Berlin, Gebrüder Bornträger, 503pp.

MACDONALD, R. (1969): *The Atlas of Uganda (2nd ed.),* Dept. of Lands and Surveys, Entebe.

YAIRI, K. and MIZUTANI, S. (1969): Fault system of the Lake Tanganyika Rift at the Kigoma area. western Tanzania. *Jour. Earth Sci., Nagoya Univ.,* **17,** 71-96.

YAIRI, K. (1974): En echelon pattern of the East African Rift System. *J. Afri. Studies,* **14,** 21-46(in Japanese with English abstract).

YAIRI, K. (1975): Geometry and mechanics of en echelon faulting with applications to the East African Rift System. *1st Prelim. Rep. Afr. Studies, Nagoya Univ.,* 29-38.

(Appendix)

Summit Level in Western Uganda

Yoshiziro KATO

Department of Geology, College of General Education, Nagoya University

A summit level map in western Uganda is shown in pages 50 and 51 to compare the degree of dessection of the erosion surfaces. This map is based on 2 km coordination of several geomorphic maps published by Lands and Surveys Department, Uganda.

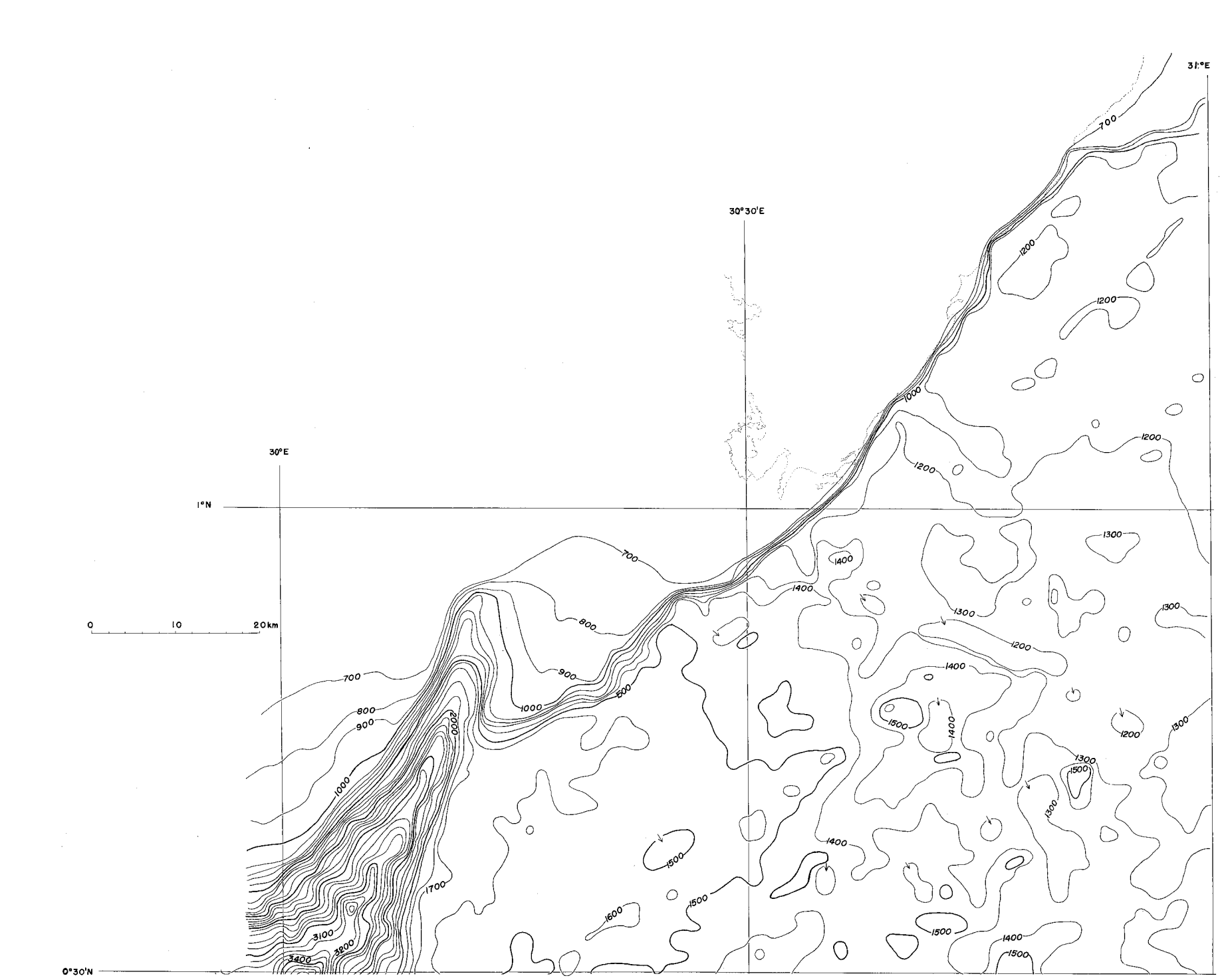
31°E
30°30'E
30°E
1°N
0°30'N
0
10
20km
700
800
900
1000
1100
1200
1300
1400
1500
1600
1700
2000
3100
3200
3400

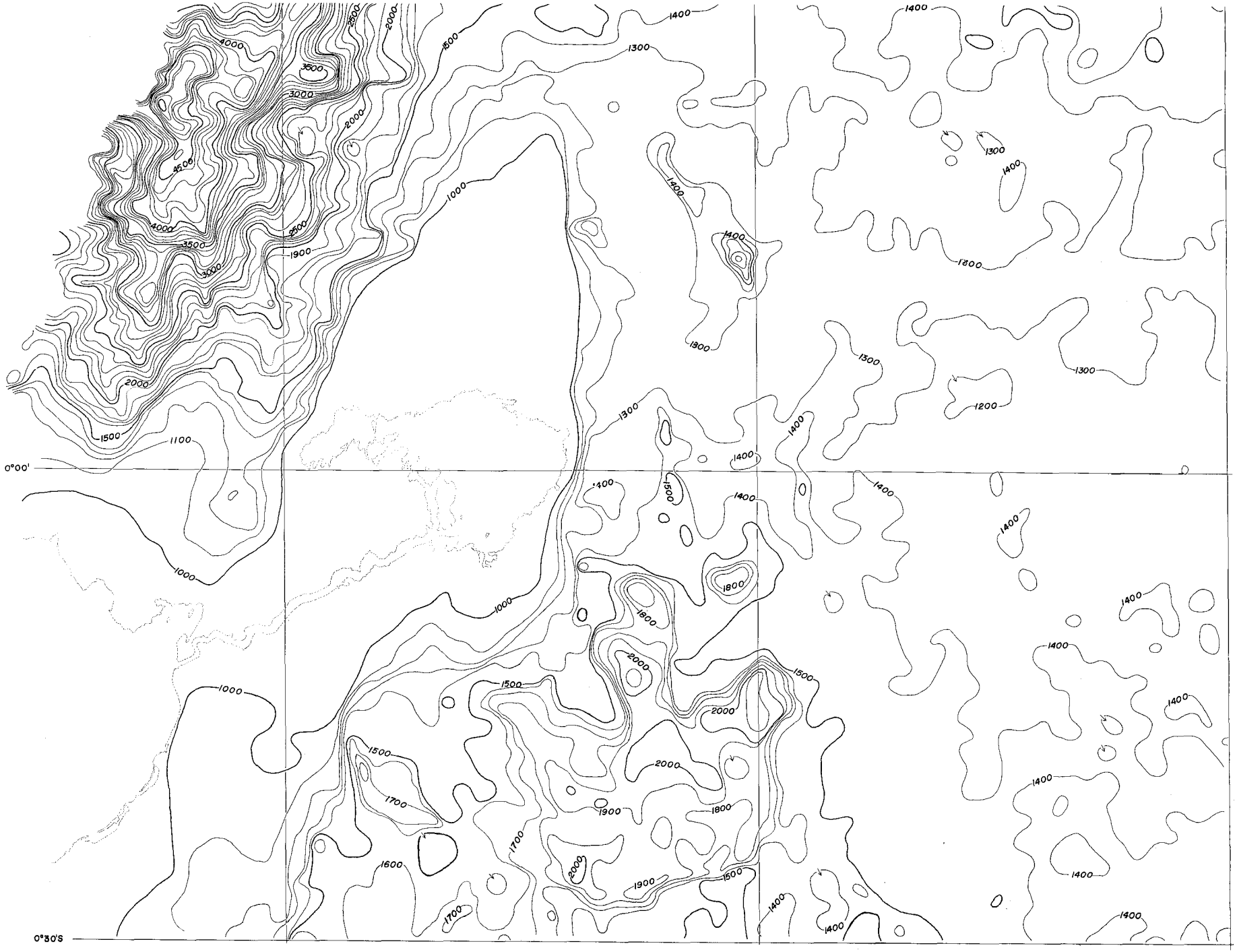
0°00'
0°30'S
4000
3500
3000
2500
2000
1900
1800
1700
1600
1500
1400
1300
1200
1100
1000

An Occurrence of Staurolite from the Kioo Pegmatite, Machakos District, Kenya

Kunihiko MIYAKAWA* and Kanenori SUWA**

* Department of Earth Sciences, Nagoya Institute of Technology
** Department of Earth Sciences, Faculty of Science, Nagoya University

Introduction

Staurolite usually appears in pelitic rocks of appropriate composition which have suffered medium- to high-grade regional metamorphism. Only in rather exceptional cases, however, it occurs in rocks of magmatic origin. One of such rare cases was found in a certain variety of pegmatite on a hill called Kioo which lies about 13 km north of Sultan Hamud in the southern Machakos area. Another interesting variety of the Kioo pegmatite is a kyanite-bearing pegmatite (Temperley, 1953; Baker, 1954), which was discovered by P.H.Cull, a resident of Sultan Hamud, in 1947 and became famous for its large crystals of kyanite. The occurrence of staurolite in pegmatite is of particular interest. In the present paper, both a brief description and a tentative interpretation of the pegmatite can be given from field and petrographic observations although laboratory work has not yet been finished.

General geology

The southern Machakos area is occupied mainly by volcanic rocks of Cenozoic age and metamorphic rocks of the so-called Basement System of Precambrian age (Baker, 1954). The former represents the vulcanism associated with the East African Rift movement. The latter constitutes part of the Mozambique belt of Kenya (Holmes, 1951).

The metamorphic rocks consist mainly of pelitic and psammitic gneisses and schists with subordinate basic and calcareous rocks. Granitoid gneiss also occurs, especially in the core part of the dome structure. Muscovite, biotite and almandine are the common metamorphic minerals in the pelitic and psammitic rocks. Staurolite and/or kyanite are contained in some aluminous metasediments. Sillimanite, andalusite and cordierite are not found in the main part of the area. The metamorphic grade is considered to be largely of the amphibolite facies.

Staurolite from the Kioo pegmatite

The Kioo pegmatite is primarily characterized by containing kyanite in a relatively large amount and was first marked as a kyanite concentration from an economic standpoint. The pegmatite is a few meters thick and occurs in the shape of irregularly cross-cutting vein. The surrounding micaceous gneisses altered to form rocks vermiculitized in variable degree at the contact. Kyanite pegmatite principally comprises quartz and kyanite. It grades partly into a staurolite-quartz mass which may be called staurolite pegmatite. The staurolite pegmatite consists of quartz and staurolite with accessories of altered biotite, garnet, ilmenite and hematite. Secondary chlorite is present in a minor amount. Kyanite is practically absent. Even though it is present, it is a trace

1st Prelim. Rep. Afr. Studies., Nagoya Univ. 52-54, 1975.

constituent only in the margin of the staurolite-concentrated part. Sodic plagioclase is also rarely present. Staurolite is contained up to about 40% by volume.

Staurolite forms anhedral grains of irregular shape. It is generally 2 to 10 mm in size and may reach 5 cm in size. The colour is black with the naked eye. The fracture is uneven, sometimes sub-conchoidal. Criss-cross twins are not found. Most grains of staurolite show poikilitic structure enclosing quartz but in these grains quartz inclusions are much smaller in amount than in those of ordinary metamorphic staurolite. Some grains are free from quartz inclusions. The pleochroism is as follows : X = very pale yellow, Y = pale brown yellow and Z = yellow brown, $X<Y\ll Z$ in thin section, and X = pale yellow, Y = yellow brown and Z = deep brown with a red tint in thick section. The refractive indices are $\alpha = 1.743$, $\beta = 1.749$, $\gamma = 1.759$ and optical angle is (+) $2V = 76°$. The X-ray powder diffraction data are given in Table 1. Ilmenite and hematite are intergrown with each other.

Table 1 X-ray powder diffraction data for staurolite from the Kioo pegmatite. (Co-Kα radiation)

$2\theta(°)$	I/I_0	d(Å)	hkl	$2\theta(°)$	I/I_0	d(Å)	hkl
12.30	12	8.349	020	60.30	4	1.781	440
14.40	17	7.137	110	60.56	5	1.774	172
24.83	40	4.160	040	61.54	6	1.748	281
26.24	4	3.940	200	62.89	5	1.715	191
29.09	34	3.562	220	64.55	3	1.675	082
32.07	4	3.238	201	64.90	11	1.667	223
33.93	9	3.066	150	65.04	9	1.664	0·10·0
34.51	57	3.016	221	67.22	6	1.616	402
36.42	8	2.862	240	67.67	37	1.606	153
36.82	11	2.832	002	70.94	24	1.541	461
37.64	84	2.773	060	71.81	8	1.525	313
38.76	83	2.696	151	72.19	19	1.518	192
40.33	8	2.595	310	72.35	27	1.515	530
41.02	24	2.553	241	72.54	21	1.512	511
43.73	100	2.402	132	74.47	6	1.478	2·10·1
44.28	52	2.373	330	76.03	10	1.452	173
44.57	37	2.359	311	77.17	4	1.434	0·10·2
45.80	8	2.299	202	78.38	10	1.416	004
46.45	10	2.268	170	79.67	51	1.396	462
50.13	40	2.111	171	80.41	16	1.386	0·12·0
53.70	80	1.980	062	89.00	5	1.276	3·11·1
54.02	33	1.970	400	90.41	4	1.260	064

Origin of the staurolite-bearing pegmatite

The staurolite of the Kioo pegmatite differs from ordinary metamorphic staurolite in having much smaller amounts of quartz inclusions and in being pleochroic from very pale yellow to brown with a red tint. Minute prisms of zircon and intergrowths of ilmenite with hematite are sometimes enclosed in the staurolite of the pegmatite. Essentially they have the same character as the other grains of zircon and ilmenite which are lying in the quartz matrix. This appears to support that the staurolite of the Kioo pegmatite is not xenocrystic in origin. Its occurrence resembles that of staurolite in kyanite pegmatite from Shepherd mine, Masons Mountain, North Carolina, which was described by Heinrich (1950).

Kyanite-bearing schists occur from many places, including the southern Machakos area, in the Mozambique belt of the southern part of Kenya. Staurolite schists with or without kyanite also occur in the area. Because of the regional distribution of such aluminous metasediments, it is probable that granitic pegmatite magma assimilated aluminous country rocks at depth. The resultant magma contains an excess of alumina over alkalies. The magma from which feldspar is separating will relatively increase in alumina and silica. In the late pegmatitic to early hydrothermal stages, kyanite crystallizes together with quartz. If available iron is present, the separation of staurolite from residual solution precedes that of kyanite to a certain extent. Whether staurolite crystallizes in addition to kyanite or not appears to depend on chemical rather than physical factors. The crystallization took place at the end of regional metamorphism. Rare occurrence of staurolite pegmatite would indicate that the formation of the pegmatitic magma of a particular chemical composition by assimilation is caused only under rather limited pressure-temperature conditions during regional metamorphism.

Acknowledgements—We greatly acknowledge the assistance given by the Mines and Geological Department of Kenya during our stay in Kenya. We wish to thank Dr. J. Walsh for his kindness and encouragement. Thanks are also extended to Mr. S.A. Dodhia for co-operation with field work. The field work was made possible by the Grant-in-Aid for Overseas Scientific Researches from the Ministry of Education, Japan, to which we express our thanks.

References

BAKER, B.H. (1954): Geology of the southern Machakos district. *Geol. Surv. Kenya, Rept.* **15.**

HEINRICH, E.Wm. (1950): Paragenesis of the rhodolite deposit, Masons Mountain, North Carolina. *Am. Mineral.*, **35**, 764-771.

HOLMES, A. (1951): The sequence of Precambrian orogenic belts in south and central Africa. *Intern. Geol. Congr. 18th, London, 1948, Rept.* **14**, 254-269.

TEMPERLEY, B.N. (1953): Kyanite in Kenya. *Geol. Surv. Kenya, Mem.* **1.**

Plagioclases in Anorthosites

Kanenori SUWA

Department of Earth Sciences, Faculty of Science, Nagoya University

Introduction

Up to now it is the commonly accepted idea that there are only two varieties of anorthosites–the stratiform Bushveld and the massive Adirondack types. Recently the third type anorthosite, a layered calcic anorthosite found in some high-grade basement terrains, was proposed by Windley(1970). Anorthosites in this third group are mostly the oldest plutonic rocks in the crust with any decipherable mode of origin, having been formed more than 3,000 m. y. ago and possibly as old as 3,500 m. y., and they are extremely similar chemically to the lunar anorthosites. These three groups of terrestrial anorthosites are shown in Table 1. Petrographical characters of plagioclases in these three groups of anorthosites are now under study by the present author.

Table 1. Three groups of terrestrial anorthosites, and lunar anorthosite

Group I.	Bytownite Anorthosite occurring as layers within stratified basic sheets and lopoliths. Age: Precambrian–Tertiary. Examples: Bushveld and Stillwater Complexes.
Group II.	Andesine or Labradorite Anorthosite occurring as large independent intrusions in Precambrian terranes. Age: 1,100–1,400 m. y. Examples: Scandinavia, Eastern North America(the Adirondacks and Quebec).
Group III.	Calcic Anorthosite occurring as stratiform igneous cumulate in the oldest parts of the Archean craton. An 85 - 100. Age: 3,500 m. y. ± Examples: Greenland, Scotland, Rhodesia, Madagascar, India.
Lunar Anorthosite:	An 96 - 98, Age: 3,600 - 4,000 m. y.

Group I Anorthosite(Bushveld Complex)

As a typical example of Group I anorthosite, the author has investigated plagioclase grains in the Bushveld Complex, which was intruded into Transvaal system at 1,950 m. y. ago.

At Dwars River Bridge, anorthosite belonging to the upper part of Critical Zone occurs as alternation of anorthosite(plagioclase adcumulate) layer and chromite(chromite-plagioclase heteradcumulate) layer. Principal mineral of the adcumulate layer is bytownite of An 75 and that of the heteradcumulate layer is bytownite of An 70-75 and chromite. In both layers all the grains of plagioclases, so far observed, are twinned according to the Carlsbad law, the combination of albite law and albite-Carlsbad law, the combination of albite law and pericline law, and the combination of Carlsbad law and pericline law. This twinning pattern of the plagioclases clearly indicates the igneous origin of the Complex. Zonal structure is found frequently in the plagioclase grains. In the adcumulate layer, all the grains of plagioclases are developed with their longer axes in parallel to the cumulate plane. And in the heteradcumulate layer plagioclase grains are developed with their longer axes in perpendicular to the

1st Prelim. Rep. Afr. Studies., Nagoya Univ. 55-59, 1975.

cumulate plane.

At Magnet Height, anorthosite belonging to the Upper Zone is found to occur. Principal mineral of the anorthosite(plagioclase adcumulate) is labradorite of An55. The twinning pattern, zonal structure and the petrofabric pattern of the plagioclases are similar to those of plagioclases of the Critical Zone. Distorted twinning lamellae are found in the plagioclases of the Upper Zone. Photomicrographs of the Group 1 anorthosites are shown in Figs. 1 and 2.

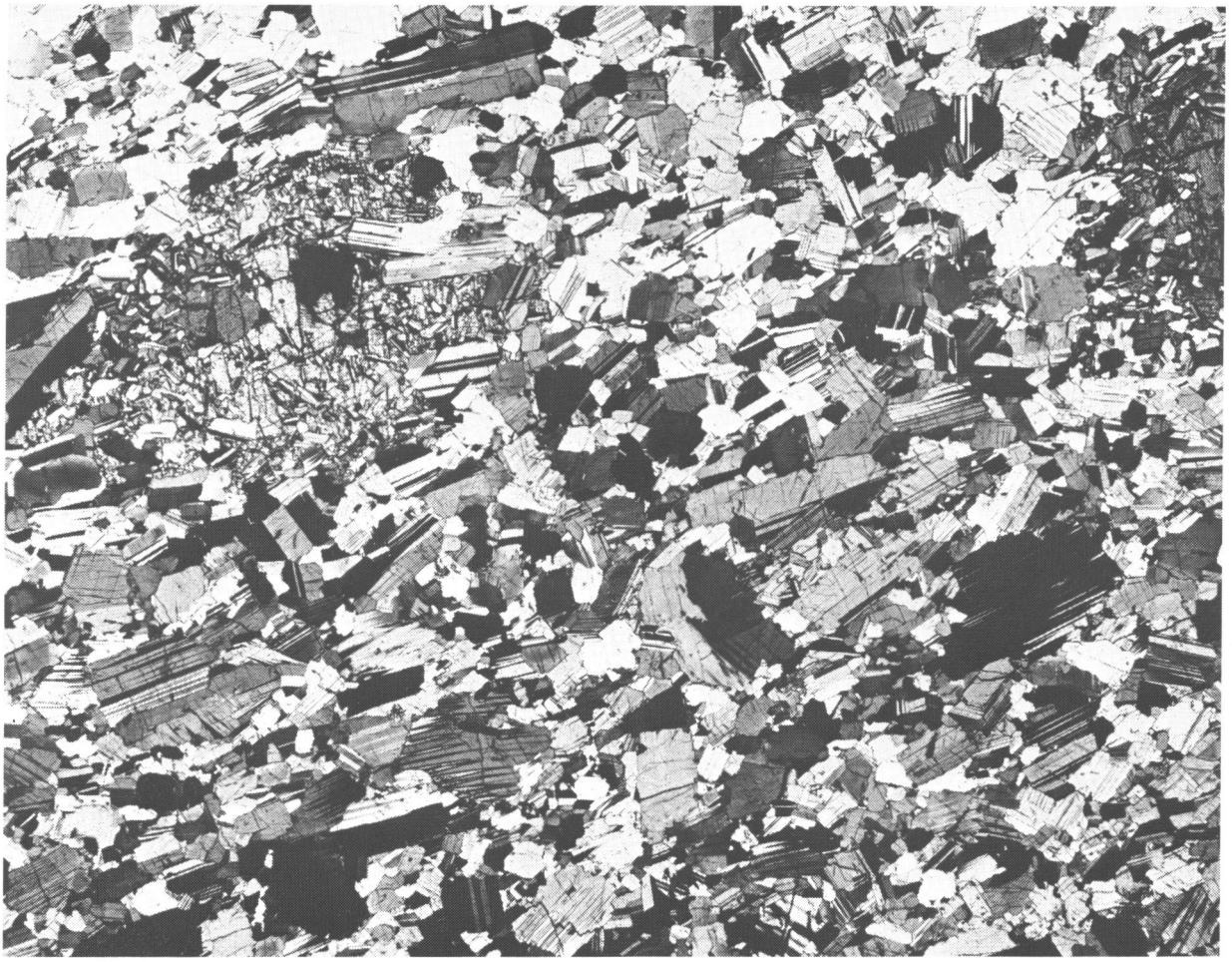

Fig. 1

Pyroxene bearing plagioclase adcumulate(Specimen No. KS-70030820). Dwars River Bridge, Bushveld Complex(Upper part of the Critical Zone). Nicols crossed. X11.

Fig. 2

Alternation of plagioclase adcumulate(upper half) and chromite-plagioclase heteradcumulate(lower half) (Specimen No. KS-70030818a). Dwars River Bridge, Bushveld Complex(Upper part of the Critical Zone). Nicols crossed. ×12.

Group Ⅱ Anorthosite(Quebec)

As a typical example of Group Ⅱ anorthosite, the author has investigated plagioclase grains in the Quebec anorthosite.

Group Ⅱ anorthosites share a number of characteristic features: (a) The anorthosite bodies are limited to Precambrian terranes, (b) They take the form of large intrusions with domed roofs and may reach batholithic proportions, (c) The principal constituent mineral is plagioclase ranging from An35 to An60. Hypersthene and augite, less commonly accompanied by olivine, make up less than 10 per cent, (d) Group Ⅱ anorthosites are distinguished from the Group I anorthosites by their greater homogeneity of composition and very coarse-grained texture. There are combined textural and chemical evidences that post-emplacement deformation and metamorphism have occurred in many of the Group Ⅱ anorthosites.

Anorthosite at La Tuque, Quebec Province shows beautiful equigranular aggregates of plagioclase grains indicating the recrystallization during emplacement of the anorthosite. The chemical compositions of the plagioclases by means of EPMA are An54.5-55.0 Ab43.5 Or 1.5 and are considered to be homogeneous in composition on neighbouring twinning lamellae from the low value of the "homogeneity index" (Boyd et al., 1968). For labradorite, homogeneity indices for Ca, Na and K are 1.5, 1.1 and 1.1, respectively. When "homogeneity index" is less than 3, it can be said the material concerned is homogeneous. The angular separations in X-ray diffraction patterns are: $2\theta(220) - 2\theta(1\bar{3}1) = 1.28°$, $2\theta(1\bar{3}1) - 2\theta(131) = 1.80°$, $2\theta(131) + 2\theta(220) - 4\theta(1\bar{3}1) = 0.525°$. Refractive indices are $\alpha_D = 1.551 \pm 0.001$, $\beta_D = 1.558 \pm 0.001$, $\gamma_D = 1.563 \pm 0.001$. These X-ray and optical data indicate that the labradorites are of "low-temperature form" (Suwa et al., 1974). All the grains of plagioclases, so far observed, are polysynthetically twinned, exclusively according to the albite law or the pericline law or the two laws in combination. None is twinned after other laws. This twinning pattern of the plagioclases of Group II anorthosites clearly differs from that of plagioclases of Group I anorthosite. As to the frequency of the composition planes in the twinning, (010) is predominant over the rhombic section, their frequency percentages being 68 and 32 respectively. The frequency percentage of the composition plane(010) is about the same with that in the granulite from east Antarctica(Suwa, 1966) and in the charnockite from India. It appears that the frequency percentage of the composition plane(010) in twinned plagioclases decreases with increase in the temperature of metamorphism(Suwa, 1966). Photomicrographs of the Group II anorthosites are shown in Fig. 3.

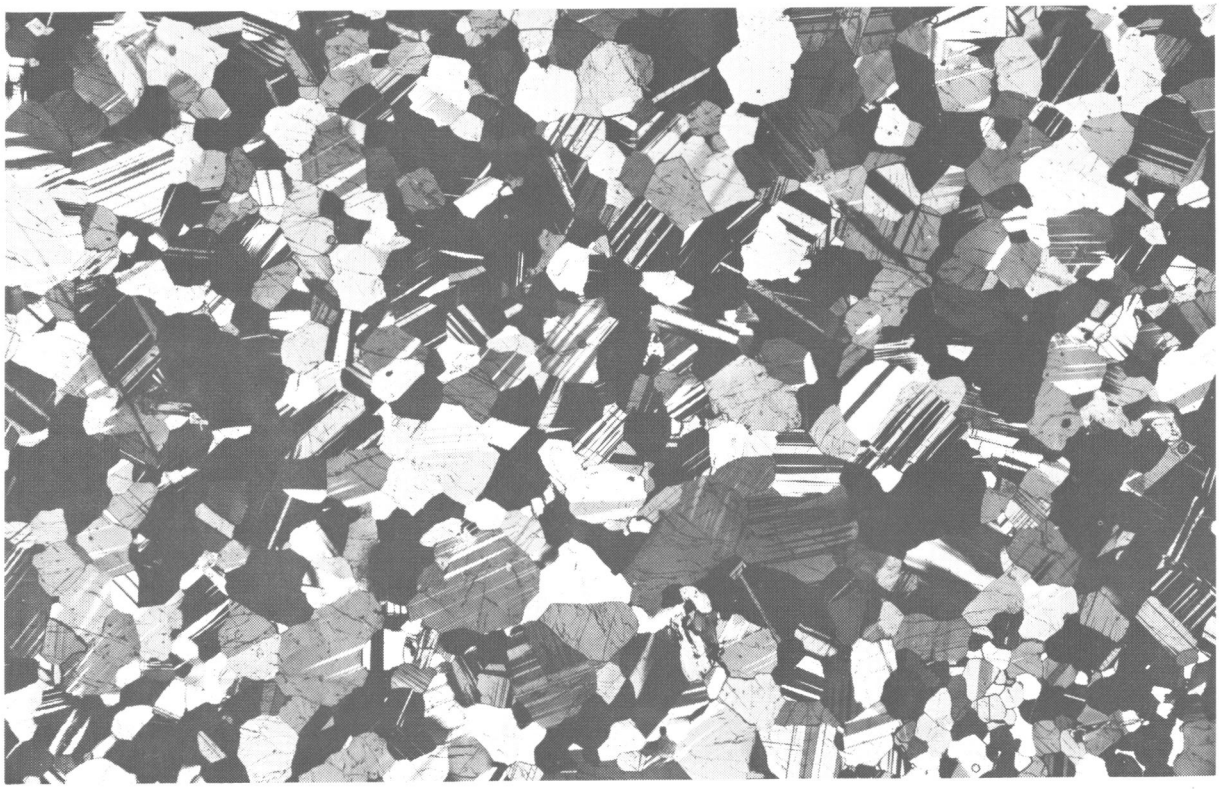

Fig. 3
Anorthosite(Specimen No. KS-72081705). La Tuque, Quebec Province, Canada. Nicols crossed. X12.

Most plagioclase crystals of Adirondack anorthosite are twinned according to a single law although a sizable proportion have more than one law. Of the twins in the groundmass plagioclase, 74 percent are albite law and 23 percent are pericline law. The other 3 percent are Manebach, Ala B, Ala A, albite-Ala B and Carlsbad laws. In some samples both megacrysts and groundmass are twinned according to the albite and pericline laws. Carlsbad and albite-Carlsbad twin laws predominate over albite and pericline twin laws in the megacrysts from other samples (Onyeagocha and Seifert, 1971).

Group Ⅲ Anorthosite

Group Ⅲ anorthosites are fine-grained, white granular rocks which include true anorthosites, gabbroic anorthosites and anorthositic gabbros. Where best preserved (e. g., Fiskenaesset of West Greenland, Sittampundi of southern India, Messina of Rhodesia) Group Ⅲ anorthosites form extensive layered stratiform sheets with major units of anorthosite, amphibolite, peridotite and pyroxenite occurring as conformable layers in granitic gneisses. These early Archaen Group Ⅲ anorthosites have suffered the orogenic effects of one or more periods of regional metamorphism and deformation, with the result that they now occur as recrystallized tectonic pods and slices. The rocks themselves are remarkably well preserved, however, probably because an original plagioclase-orthopyroxene-clinopyroxene igneous assemblage was recrystallized isochemically into a similar metamorphic assemblage.

Petrographical characters of plagioclases in Group Ⅲ anorthosites are considered to be originally similar to those of plagioclases in Group Ⅰ anorthosites, but at present those of plagioclases in Group Ⅲ anorthosites are rather similar to those of plagioclases in Group Ⅱ anorthosites as a result of regional metamorphism and recrystallization.

References

BOYD, F.R., FINGER, L.W., and CHAYES, F.(1969): Computer reduction of electron-probe data. *Carnegie Inst. Year Book,* **67,** 210 - 215.

ONYEAGOCHA, A.C. and SEIFERT, K.E.(1971): Optical properties of Adirondack anorthosite plagioclases. *Am. Mineral.* **56,** 1199 - 1207.

SUWA, K.(1966): On plagioclases in metamorphic rocks from Lützow-Holmbukta area, East Antarctica. *Proc. Japan Acad.,* **42,** 1175 - 1180.

SUWA, K., MIZUTANI, S., and TSUZUKI, Y.(1974): Proposed optical method of determining the twinning laws of plagioclase. *Mem. Geol. Soc. Japan,* No.11, 167 - 250.

WINDLEY, B.F.(1970): Anorthosites in the early crust of the earth and on the moon. *Nature,* **226,** 333 - 335.

Reverse Pleochroism of Phlogopites in Kimberlites and Their Related Rocks from South Africa

Kanenori SUWA* and Ken-ichiro AOKI**

* Department of Earth Sciences, Faculty of Science, Nagoya University
** Institute of Mineralogy, Petrology and Economic Geology, Tohoku University

Abstract

Phlogopites in kimberlites and their related rocks (e. g., mica nodule in kimberlite) in Kimberley and Pretoria districts show frequently reverse pleochroism, namely X = pale yellow to yellow, orange and brown and Y = Z = colourless to very pale yellow, and X > Y = Z. Phlogopite with reverse pleochroism is also found to occur in carbonatite from Palabora mine and in synthetic phlogopite.

These phlogopites with reverse pleochroism are characterized by the deficiency of Si and Al in the tetrahedral site and the entrance of Fe^{3+}, Ti, Cr and other cations in the tetrahedral site. If it is assumed that the tetrahedral site is filled by 8 atoms of Si, Al, Fe^{3+}, Ti and Cr, phlogopite having more than 0.30 in Fe^{3+} + Ti + Cr atoms and more than 0.90 in Fe^{3+} / Fe^{3+} + Ti + Cr ratio shows reverse pleochroism.

Introduction

In 1961, the senior author synthesized Mn^{g}-phlogopite exhibiting dark green colour in naked eye with his collaborators (Daimon et al., 1961). This synthetic Mn^{g}-phlogopite shows reverse pleochroism, X = pale yellow, Y = Z = colourless with X > Y = Z and its chemical formula is $K_{1.92}Mg_{6.16}[Si_{6.60}Al_{0.76}Mn_{0.57}]O_{20.07}F_{3.93}$. From the above data, the senior author has considered that reverse pleochroism may be due to the deficiency of Si and Al in the tetrahedral site and the entrance of Mn in the same site.

The occurrence of mica with reverse pleochroism has been observed in kimberlites, alnöites and phlogopite-bearing carbonatites (Wagner, 1914; Singewald and Milton, 1930; von Eckermann, 1948; Watson, 1955; Bobrievic et al., 1959; Hogarth, 1964; Kuharenko et al., 1965; Tatsumi, 1965; Boettcher, 1967; Watson, 1967; Suwa et al., 1969; Kapustin, 1971; Nash, 1972). Especially, Hogarth(1964) and Kuharenko, et al., (1965) have attributed the reverse pleochroism of some micas to the presence of Fe^{3+} in tetrahedral sites.

In this paper, the present authors would describe the phlogopites with reverse pleochroism in kimberlites and their related rocks from Kimberley and Pretoria districts, South Africa. The phlogopites with reverse pleochroism are certainly characterized by the deficiency of Si and Al in the tetrahedral site. Phlogopites having deficient Si and Al in the tetrahedral site, however, are not always reverse in their pleochroism. A quantitative consideration on reverse pleochroism is one of the purposes of this paper.

In kimberlites from South Africa, many types of phlogopite are sometimes found to occur simultaneously in a same specimen, i. e. , there are phlogopite with normal pleochroism, phlogopite with reverse pleoch-

1st Prelim. Rep. Afr. Studies., Nagoya Univ. 60-64, 1975.

roism, intergrowth of both phlogopites and zoned phlogopites with both pleochroisms in a same specimen. In this paper, some results of qualitative analysis with EPMA are also described.

In conclusion, the problem why phlogopites with reverse pleochroism occur selectively in kimberlites and carbonatites and their related rocks is discussed and the problem why no biotite with reverse pleochroism occur is also considered.

Phlogopites in kimberlites from Kimberley and Pretoria districts

Phlogopites in kimberlites from Kimberley district (Frank Smith, Bellsbank, Newlands and Koffyfontein mines) and Pretoria district (Premier mine) are observed and examined.

In kimberlites from Frank Smith, Bellsbank and Newlands mines, many types of phlogopite are found to occur simultaneously in a same specimen. In kimberlite from Koffyfontein mine and black kimberlite from Premier mine, almost all phlogopites show reverse pleochroism.

When we compare typical normal phlogopite with typical reverse phlogopite in the kimberlite from Frank Smith mine, three elements of Ti, Cr and Al are more enriched in normal phlogopite and three elements of Fe, Si and Mg are more enriched in reverse phlogopite, and the ratios of Fe/Ti, Fe/Al and Fe/Cr are lower in normal phlogopite and these ratios are higher in reverse phlogopite.

Phlogopites in peridotite and eclogite nodules in kimberlites from Kimberley district and Lesotho

Phlogopites in peridotite and eclogite nodules in kimberlites from Kimberley district (Bultfontein Floors, Roberts Victor, Bellsbank and Ebenhoezen mines) and Lesotho are observed and examined.

In peridotite nodules from Bultfontein Floors mine and Lesotho, almost all phlogopites show normal pleochroism. Extraordinarily in one peridotite nodule, which is harzburgite consisting of olivine, orthopyroxene, potassic richterite, phlogopite and ilmenite, from Bultfontein Floors mine, all phlogopites show reverse pleochroism.

In eclogite nodules from Roberts Victor and Bellsbank mines, all phlogopites show normal pleochroism.

Of considerable interest is the fact that the phlogopites with reverse pleochroism selectively occur only in potassic richterite bearing harzburgite nodule and the phlogopites with normal pleochroism commonly occur in common peridotite nodules without potassic richterite and eclogite nodules.

Phlogopites in mica nodules in kimberlites from Kimberley district

Mica nodules from the Dutoitspan and Wesselton mines, Kimberley district can be divided into two groups, diopside-phlogopite nodules and potassic richterite-phlogopite nodules. The latter was discovered by the junior author (Aoki, 1974) and is characterized by the presence of abundant potassic richterite and large size of the crystals.

The phlogopites show a rather wide range in composition. It is noteworthy that the

phlogopites are characterized by low Al and Mn, high Fe^{3+} and Mg, and wide ranges of Ti and Cr. There are no conspicuous differences between the phlogopites of diopside-phlogopite nodules and potassic richterite-phlogopite nodules.

The ideal formula of the phlogopite end-member can be expressed as $K_2Mg_6(Si_6Al_2)O_{20}(OH)_4$. If it is assumed that the tetrahedral site is always filled completely by 6 atoms of Si and 2 atoms of Al, in all cases, Si is close to 6. However, Al occupies only about three fourths to four fifths of the tetrahedral site and the deficiency is made up of Fe^{3+} and/or Ti and/or Cr. The numbers of Fe^{3+} + Ti + Cr in the tetrahedral site range from 0.226 to 0.458, and the numbers of Fe^{3+} in the same site range from 0.149 to 0.418.

Phlogopites with reverse pleochroism are more than 0.300 in Fe^{3+} + Ti + Cr (0.342 and 0.458) and are more than 0.90 in Fe^{3+}/Fe^{3+} + Ti + Cr ratio (0.91 and 1.00).

Phlogopites with normal pleochroism are variable in Fe^{3+} + Ti + Cr (0.226 and 0.415) and are less than 0.70 in Fe^{3+}/Fe^{3+} + Ti + Cr ratio (0.69 and 0.36).

As a result, it can tentatively be concluded that phlogopite having more than 0.30 in Fe^{3+} + Ti + Cr atoms in the tetrahedral site and more than 0.90 in Fe^{3+}/Fe^{3+} + Ti + Cr ratio in the same site shows reverse pleochroism.

When we consider the analytical results of eight phlogopites from the carbonatites, apatite-forsterite-magnetite ore and olivinite reported by Kuharenko et al.(1965) and Kapustin (1971), our tentative conclusion is also confirmed. In the case of titaniferous phlogopite in leucite lamproite, Si and Al atoms in the tetrahedral site amounts 7.852 (Prider, 1939), so we cannot expect reverse pleochroism.

Phlogopites in Palabora carbonatite

Phlogopites in carbonatite and its related rocks show reverse pleochroism.

In one specimen (TT-63100316) of phoscorite (apatite-magnetite-olivine rock) from Foskor's Quarry, fine banded structure is observed and there are at least three bands : carbonate-apatite-phlogopite band, phlogopite-chondrodite-serpentine band and phlogopite - magnetite - serpentine - forsterite band. All phlogopites of these three bands show reverse pleochroism, namely X = red brown and Y = Z = pale orange to pale brown, and X > Y = Z.

In one specimen (TT-63100323) of apatite-phlogopite carbonatite, zoned phlogopites are found to occur. In the core part of zoned phlogopites, X = colourless or very pale orange and Y = Z = very pale green, and X = Y = Z ; and in the marginal part of zoned phlogopites, X = deep red brown and Y = Z = pale brown to yellow brown, and X > Y = Z.

Phlogopites with reverse pleochroism

The reason why phlogopites with reverse pleochroism occur selectively in kimberlites, carbonatites and their related rocks is considered to be chemical compositions of these rocks.

Kimberlite is an undersaturated ultra-basic rock. For a rock of such basicity, it contains unusually high amounts of K_2O, Al_2O_3, TiO_2, CaO, CO_2, P_2O_5, H_2O and SO_3. Compared with other ultrabasic rocks it has a low Mg/Fe ratio, but unusually

high K/Na(3.4–7.4) and Fe^{3+}/Fe^{2+}(7.5) ratios. The Al_2O_3 content is 4.4 per cent for basaltic kimberlite and 4.9 per cent for micaceous kimberlite and the contents are much lower than those of basic rocks (Dawson, 1967). From such chemical environment phlogopite, being poor in Al and rich in Fe^{3+} in the tetrahedral site, can be crystallized.

Carbonatite contains unusually high amounts of CaO, MgO and CO_2 and unusually low amounts of SiO_2, TiO_2, Al_2O_3, Fe_2O_3, FeO, Na_2O and K_2O. For example, the chemical compositions of carbonatites from Fen area are SiO_2 (0.89–3.36%), TiO_2 (–0.30%), Al_2O_3 (0.66–2.01%), Fe_2O_3 (0.06–6.13%), FeO (2.06–6.23%), MgO (2.25–16.88%), CaO (30.24–48.72%), Na_2O (0.02–0.26%), K_2O (0.11–0.50%) and CO_2 (32.80–42.88%) (Barth and Ramberg, 1966). From such chemical environment phlogopite, being poor in Al and rich in Fe^{3+} in the tetrahedral site, can also be crystallized.

Pleochroism of biotites

No biotite with reverse pleochroism is reported yet. Actually biotites always show normal pleochroism.

Usually Al_2O_3 content is high (11.8–22.8%) in biotite and its tetrahedral site is filled by Si and Al atoms. A part of Al atoms is also situated in octahedral site. This is the reason why no biotite with reverse pleochroism is found.

Deer (1937) reported one biotite, whose tetrahedral site does not be filled by Si and Al atoms. However, Si and Al atoms in the tetrahedral site amounts 7.950, so we cannot expect reverse pleochroism. Of considerable interest is the fact that the biotite shows unusual pleochroism, X = medium yellow and Y = Z = medium yellow-brown and actually $X \leqq Y = Z$.

Acknowledegments – The present authors wish to thank Professors Seitaro Tsuboi and Tatsuo Tatsumi of the University of Tokyo and Professor Yoshimasu Kuroda of Shinshû University for their kind suggestion and encouragement. Especially, Professor Tatsumi kindly sent his samples collected at Palabora to the senior author.

References

AOKI, K. (1974): Phlogopites and potassic richterites from mica nodules in South African kimberlites. *Contrib. Mineral. Petrol.*, **48**, 1 - 7.

BARTH, T.F.W. and RAMBERG, I.B. (1966): The Fen circular complex, in Tuttle, O.F. and Gittins, J. ed., *Carbonatites.* Interscience Publishers, 225 - 257.

BOBRIEVIC, A.P., BONDARENKO, M.N., GNEVUSHEV, M.A., KRASOV, L.M. and YURKEVICH, R.K. (1959): *The diamond deposits of Yakutia* (in Russian). Gosud. Naulno-teh. Izd., Moscow.

BOETTCHER, A.L. (1967): The Rainy Creek alkaline ultramafic igneous rock complex near Libby, Montana. I. Ultramafic rocks and fenites. *Jour. Geol.*, **75**, 526 - 553.

DAIMON, N., SUWA, K. and YAMAMOTO, K. (1961): The synthesis of Mn9-mica(in Japanese with English abstract). *Jour. Indust. Chem. Japan*, **64**, 1906 - 1908.

DAWSON, J.B. (1967): Geochemistry and origin of kimberlite, in Wyllie, P.J. ed., *Ultramafic and related rocks.* New York, John Wiley and Sons, 269 - 278.

DEER, W.A. (1937): The composition and paragenesis of the biotites of the Carsphairn igneous complex. *Mineral. Mag.*, **24**, 495 - 502.

HOGARTH, D. (1964): Normal and reverse pleochroism in biotite. *Canadian Mineral.*, **8,** 136.

KAPUSTIN, YuL. (1971): *Mineralogy of carbonatite* (in Russian). Izdatelstvo "Nauka", Moscow.

KUHARENKO, A.A., ORLOVA, M.P., BULAH, A.G., BAGDASAROV, E.A., RIMSKAYA-KORSAKOVA, O.T., NEFEDOV, E.I., ILINSKII, G.A., SERGEEV, A.S., ADAKUMOVA, N.B. (1965): *Caledonian ultrabasic-alkaline rock complex and carbonatite in Kola peninsula and northern Karelia* (in Russian). Izd-vo "Nedra", Moscow.

NASH, W.P. (1972): Mineralogy and petrology of the Iron Hill carbonatite complex, Colorado. *Geol. Soc. Am. Bull.*, **83,** 1361 - 1382.

PRIDER, R.T. (1939): Some minerals from the leucite-rich rocks of the West Kimberley area, Western Australia. *Mineral. Mag.*, **25,** 373 - 387.

SINGEWALD, J.T. and MILTON, C. (1930): An alnöite pipe, its contact phenomena and ore deposition near Avon, Missouri. *Jour. Geol.*, **38,** 54 - 66.

SUWA, K., OSAKI, S., OANA, S., SHIIDA, I., and MIYAKAWA, K. (1969): Isotope geochemistry and petrology of the Mbeya carbonatite, south-western Tanzania, East Africa. *Jour. Earth. Sci., Nagoya Univ.* **17,** 125 - 168.

TATSUMI, T. (1965): Mineral deposits associated with carbonatites and alkaline complexes (in Japanese). *Chigaku-Zasshi (Jour. Geogr. Tokyo)*, **74,** 13 - 33.

VON ECKERMANN, H. (1948): The alkaline district of Alnö Island. *Sveriges Geol. Undersökelse Ser.* Ca. **36.**

WAGNER, P.A. (1914): *The diamond fields of southern Africa.* Transvaal Leader, Johannesburg.

WATSON, K.D. (1955): Kimberlite at Bachelor Lake, *Quebec. Am. Mineral.*, **40,** 565-579.

WATSON, K.D. (1967): Kimberlite of eastern North America, in Wyllie, P.J., ed., *Ultramafic and related rocks.* New York, John Wiley and Sons, 312 - 323.

Petrology of Peridotite Nodules from Ndonyuo Olnchoro, Samburu District, Central Kenya
(Abstract, 1975)

Kanenori SUWA*, Yasuhisa YUSA* and Nobutaka KISHIDA**

* Department of Earth Sciences, Faculty of Science, Nagoya University

** Africa Natural Resources Development Company, P.O.Box 28035, Nairobi, Kenya

Geology

Sodic alkaline volcanic rocks were extruded repeatedly in enormous volumes from Miocene time onward in Kenya, eastern Uganda and northern Tanzania.

Ndonyuo Olnchoro and Sasani in central Kenya(37°46′E, 1°24′N) are Recent scoria cones composed of olivine melanephelinite agglutinates and lava, in which many ejected blocks of ultramafic nodules are enclosed. These nodules are generally fresh, grass-green coloured peridotite and sometimes reach 30 cm but are more usually 5 to 20 cm across.

Similar nodules have been reported from the Gregory Rift Valley and flanking volcanic areas in Pleistocene-Recent volcanics from several localities as shown in Fig.1.

Petrography and Petrochemistry

The peridotite nodules are divided into two groups. Harzburgite and lherzolite belong to the first group and comprise 60-70% and 25-35% of the peridotite nodules respectively. Harzburgite is composed of magnesian olivine (55-85%), orthopyroxene(15-40%), chromian spinel (2-10%) and clinopyroxene (trace). Lherzolite is composed of magnesian olivine (80%), orthopyroxene (15-20%), chromian spinel(2%) and clinopyroxene(2-3%).

The second group of ultramafic nodules comprises only websterite consisting of orthopyroxene(80%), clinopyroxene(15-20%) and small amounts of chromian spinel(3%). No olivine occurs in the websterite. The second group makes up less than 5% of the nodule population.

The Mg0/ΣFe0 ratios(7.63-6.13) of the first group of nodules from Ndonyuo Olnchoro and the ratios(6.97-5.49) of nodules from Lashaine, northern Tanzania (Dawson et al., 1970) fall within the limit of variation(Mg0/ΣFe0 = 7.65-5.36) of nodules from kimberlite and are higher than the ratios(6.57-2.28) of most lherzolite nodules from basalts(Kuno and Aoki, 1970).

Continental peridotites such as those of Ndonyuo Olnchoro and Lashaine and those from kimberlite show a tendency to have higher Mg0/ΣFe0 ratios than found in oceanic lherzolites suggesting that they are more enriched in the higher melting-point components(magnesian olivine and orthopyroxene, etc.). This might imply that the continental upper mantle has been more depleted in the material that formed the crust.

The variation trends of some oxides in websterite-pyroxenite nodules, including the websterite nodule from Ndonyuo Olnchoro, are distinctly different from those in lherzolite nodules(Kuno and Aoki, 1970).

These two types of nodules are of different origin.

Mineralogy

Twenty olivines, twenty two orthopyroxenes, three clinopyroxenes and eighteen spi-

1st Prelim. Rep. Afr. Studies., Nagoya Univ. 65-69, 1975.

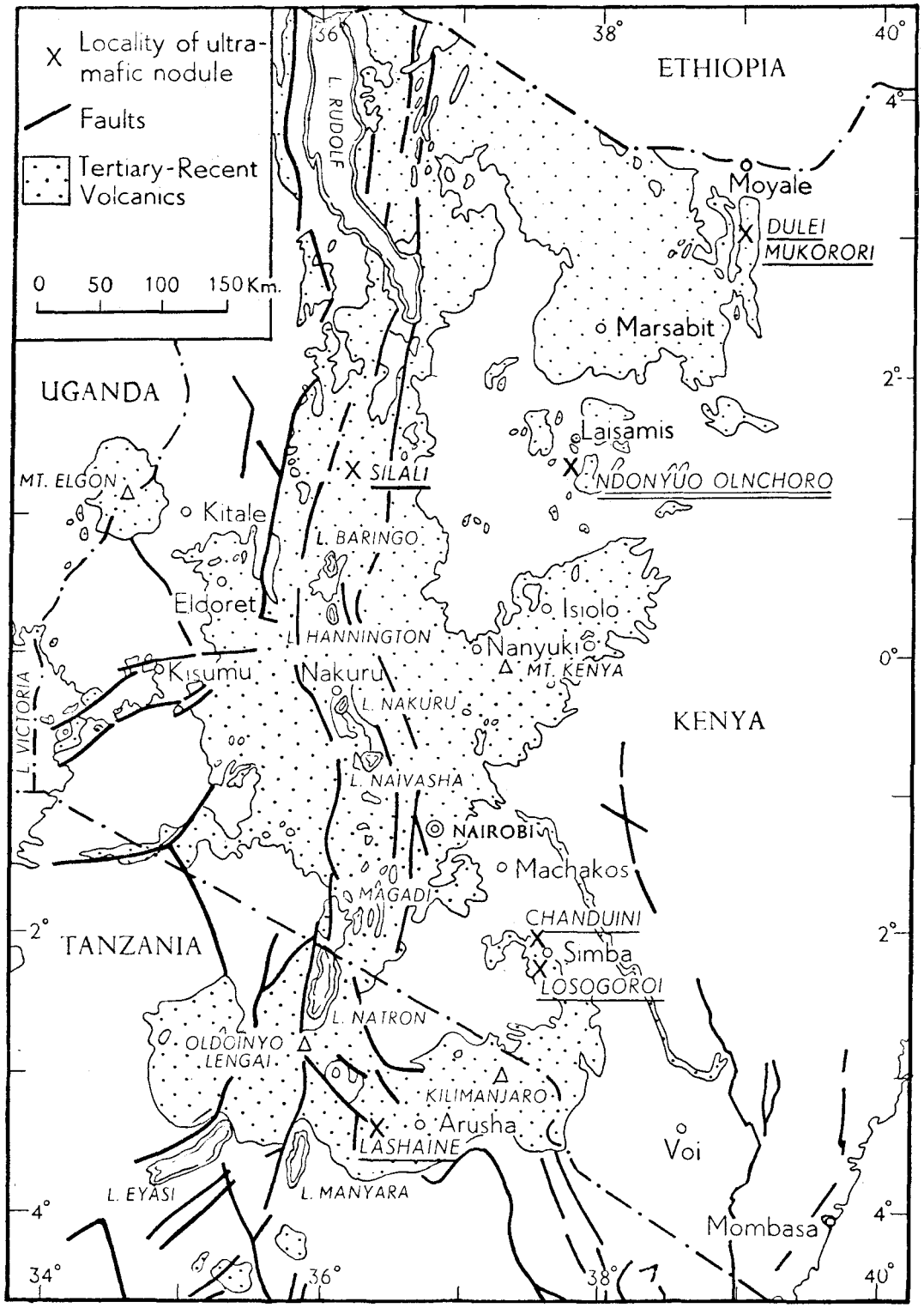

Fig. 1 Localities of ultramafic nodules in the Gregory Rift Valley.

nels from the harzburgite and lherzolite nodules; and seven orthopyroxenes, three clinopyroxenes and four spinels from the websterite nodules were analysed with EPMA.

Olivines from harzburgite and lherzolite nodules are homogeneous(Fo 92.8-92.0) from rock to rock, grain to grain, and within grains. This composition range falls within the range of olivine composition(Fo 93-87) in garnet lherzolite nodules from South African kimberlite(Chen, 1971).

The ratios of $Mg:Fe^{2+}:Ca$ of orthopyroxenes from harzburgite and lherzolite nodules vary only slightly(91.9:7.2:0.9-94.6:4.6:0.8) from rock to rock, grain to grain, and within single grains. The composition range of orthopyroxene falls within the range of orthopyroxene composition(En 88-96) of garnet lherzolite nodules in kimberlite (Chen, 1971). The ratios of $Mg:Fe^{2+}:Ca$ of orthopyroxenes from the websterite nodule are homogeneous(89.6:9.6:0.8) from grain to grain and within single grains.

The ratios of $Mg:Fe^{2+}:Ca$ of clinopyroxenes from lherzolite nodules are 55.5:4.0:40.5, and those of clinopyroxenes from the websterite nodule are 49.1:2.7:48.3. Al_2O_3 contents of clinopyroxenes are 1.8-3.0 wt.% for lherzolite nodules and 3.2-3.4 wt.% for the websterite nodule.

Chromian spinel occurs as reddish-brown rounded individual grains; as exsolved crystals in orthopyroxene; and as symplectitic constituents with orthopyroxene. The chemical compositions of chromian spinel are variable from rock to rock, but are homogeneous from grain to grain in the same rock.

Discussion

The temperature and pressure of formation obtained by plotting the clinopyroxene compositions on the grid drawn up by O'Hara (1967) are 1200-1350°C/36-38 Kbar for the lherzolites.

No garnet is found, however, in the peridotite nodules from Ndonyuo Olnchoro. Symplectites of chromian spinels and orthopyroxene occur as small grains, where chromian spinels occur as irregular and vermicular forms in host orthopyroxene crystals. The volume ratio of chromian spinel and orthopyroxene is 1:3 or 1:4. These symplectites are thought to be derived from the original garnet according to the reaction: forsterite + pyrope → 4 enstatite + spinel.

From the present compositions of forsterite, enstatite, and chromian spinel in harzburgite, the composition of original garnet is inferred to be pyrope molecule 59%, knorringite molecule 31%, almandine molecule 9% and andradite molecule 1%. Of considerable interest is the fact that the garnet composition inferred is very similar to a Ca-poor chrome pyrope from the Yakutia kimberlites(Sobolev et al., 1973).

The limited compositional range and uniformly highly magnesian character of olivine and orthopyroxene in harzburgite and lherzolite nodules suggest that these rocks are not cumulates. Such characteristics would be expected from rocks which formed as a refractory residue during partial melting of primitive mantle material.

It is concluded that after formation of garnet peridotite, the garnet peridotite was transported upward into a lower pressure regime, presumably by mantle convection. At lower pressures, presumably 15-20 Kbar, the reactions: (1) forsterite + garnet → orthopyroxene + spinel and (2) Al- and Cr-rich orthopyroxene → orthopyroxene + chromian spinel occurred simultaneously.

The websterite from Ndonyuo Olnchoro is inferred as having formed at 1090°C/16 Kbar from the grid by O'Hara(1967). It was produced by crystallization from an alkaline magma in relatively deep levels of the continental crust.

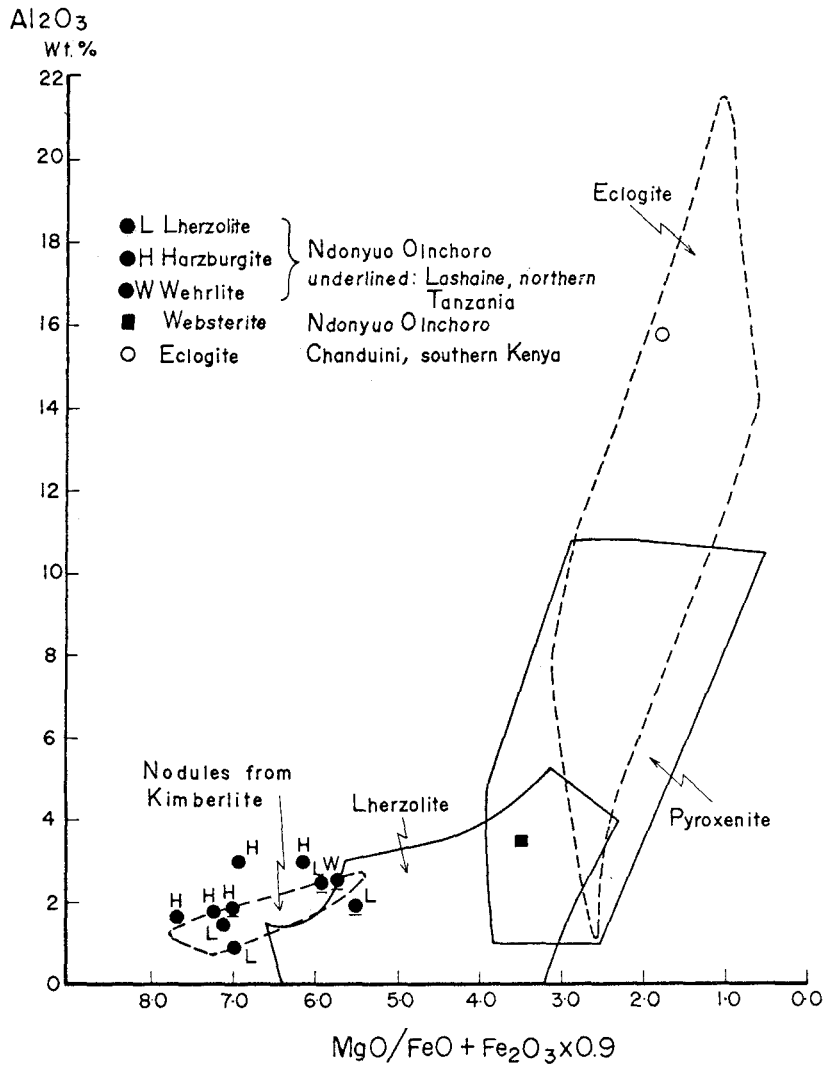

Fig. 2

Compositions of peridotite nodules from Ndonyuo Olnchoro in central Kenya, Chanduini in southern Kenya(SAGGERSON, 1968) and Lashaine in northern Tanzania(DAWSON et al., 1970 and 1973). Demarcated areas of nodules from kimberlite, lherzolite nodules, pyroxenite nodules and eclogite nodules are based on the data from KUNO and AOKI (1970).

Both groups of nodules were transported to the surface when olivine melanephelinite was erupted.

Acknowledgements—Many facilities for field work were made available by Dr.John Walsh and Mr.S.Dodhia of Kenya Mines and Geological Department, to whom the authors express their deep gratitude.

References

CHEN, J.C. (1971): Petrology and chemistry of garnet lherzolite nodules in kimberlite from South Africa. *Amer. Mineral.* **56,** 2098 - 2110.

DAWSON, J.B., POWELL, D.G. and REID, A.M. (1970): Ultrabasic xenoliths and lava from the Lashaine volcano, Northern Tanzania. *J. Petrol.* **11,** 519 - 548.

DAWSON, J.B. and SMITH, J.V. (1973): Alkalic pyroxenite xenoliths from the Lashaine volcano, Northern Tanzania. *J. Petrol.***14,** 113 - 131.

KUNO, H. and AOKI, K. (1970): Chemistry of ultramafic nodules and their bearing on the origin of basaltic magmas. *Phys. Earth Planet. Interiors* **3,** 273 - 301.

O'HARA, M.J. (1967): Mineral paragenesis in ultrabasic rocks. *In:Ultramafic and Related Rocks*(editor P.J. WYLLIE), 393 - 403. J.Wiley & Sons, New York.

SAGGERSON, E.P. (1968): Eclogite nodules associated with alkaline olivine basalts, Kenya. *Geol. Rundsch.* **57,** 890 - 903.

SOBOLEV, N.V., LAVRENTYEV, Yu. G., POKHILENKO, N.P. and USOVA, L.V. (1973): Chrome-rich garnets from the kimberlites of Yakutia and their parageneses. *Contr. Mineral. Petrol.* **40,** 39 - 52.

Fuchsite from Kibingi, Kenya

Heinosuke SHIOZAKI

Department of Geology, College of General Education, Nagoya University

A brief visit had been made to the Kibingi (or Kibini) Limestone Quarry, about 10 miles southwest of Sultan Hamud, Kenya, then an occurrence of bluish green mica in crystalline limestones was found. By means of X-ray fluorecence analysis some contents of chromium are detected. Optical properties such as refractive indices, optic axial angle, color and pleochroism have also supported it to be a a chrome mica, fuchsite.

Searles(1954) reported some occurrences of colored muscovite and sheet mica from pegmatites in this Kibingi area, where the red one is called"ruby" and the green is"green". The occurrences of sheet mica had been a small scale production.

The fuchsite from Kibingi is found as a constituent mineral of crystalline limestone in Precambrian gneisses belonging to the Mozambique belt. The Kibingi limestones are characteristically poor in dolomitic components(Searles, 1954). The limestones, presenting thick lens-shaped bodies, are bounded in pelitic and quartzo-feldspathic gneisses. They are homogeneous and massive and their interior structure is not clear, but some folding structures are seen in some impure parts. Such impure bands are composed of calcite, fuchsite, muscovite, graphite, pyrrhotite, rutile, prehnite, apatite, quartz, microcline, and plagioclase.

Generally the fuchsite takes place as a part of colorless muscovite, while in certain cases it occurs as single crystal. Contact features of the fuchsite and muscovite exhibit sometimes gradual change and sometimes clear boundary, whichever they are simultaneously extinct under crossed nicols. Along the clear border lines between the green fuchsite and colorless muscovite, Becke's lines are recognized. The refractive indices of the fuchsite are higher than those of muscovite.

Optical properties of the fuchsite and the muscovite from Kibingi are as follows,

fuchsite from Kibingi

β	1.598
γ	1.605
2Vx	35°

muscovite from Kibingi

β	1.592
γ	1.599
2Vx	41°

Excepting the pleochroism, the optical properties of the fuchsite from Kibingi are similar to those of fuchsite from Acworth reported by Clifford(1957). The pleochroism of the Kibingi fuchsite agrees with that described by Whitemore et al.(1946).

X = greenish blue
Y = yellowish light green
Z = bluish green

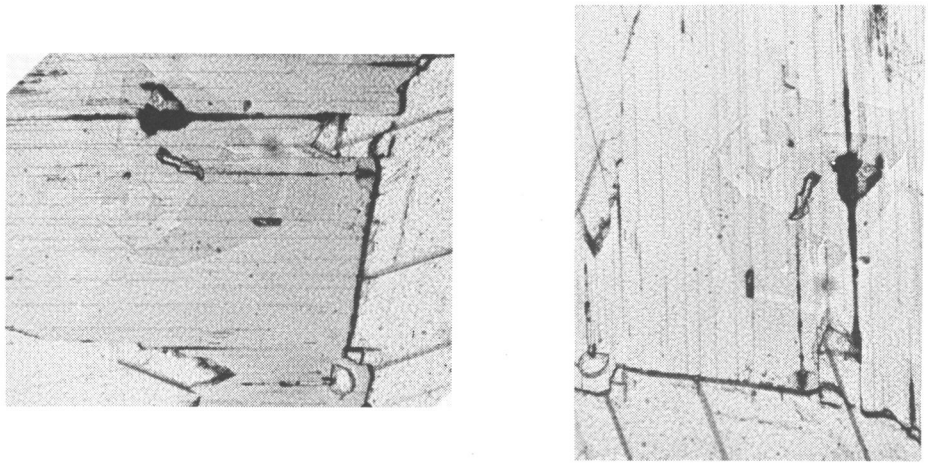

Fig. 1 Photomicrographs of Kibingi fuchsite showing distinctive pleochroism (X100).

A: ⊥ cleavage
greenishblue
Right side is calcite.

B: // cleavage
yellowish light green
Bottom side is calcite.

References

CLIFFORD, T.N. (1957): Fuchsite from a Silurian(?) quartz conglomerate, Acworth township, New Hampshire. *Am. Mineral.* **42,** 566 - 568.

SEARLE, D.L. (1954): Geology of the Sultan Hamud area. *Geol. Surv. Kenya Rept.* **29.**

WHITEMORE, D.R.E., L.G.BERRY and J.E.HAWLEY (1946): Chrome micas. *Am. Mineral.* **31,** 1 - 21.

Preliminary Geochronological Study on Metamorphic Rocks from Taita Hills, Southern Kenya

Ken SHIBATA
Geological Survey of Japan

Introduction

This report presents preliminary Rb-Sr and K-Ar age results on metamorphic rocks of the Mozambique Belt from Taita Hills in southern Kenya.

Taita Hills are situated to the west of Voi and between the East and West Tsavo National Parks. They rise rather abruptly out of the plain, and are quite hilly with the general height of 1000 ~ 2000 m above sea-level. Geologically this region is composed almost entirely of metamorphic rocks of the Mozambique Belt. The metamorphic rocks consist predominantly of hornblende-biotite gneiss, and are well foliated with the strike of EW ~ N50°E and the dip of 10 ~ 20°N. No isotopic ages have been reported so far from Taita Hills.

Samples

The rock samples used for isotopic age study were collected from an abandoned quarry (38°22.5'E, 3°28'S) at the roadside, approximately 3.5 km north of Mwatate along the road leading to Wundanyi. The rocks from this quarry are fresh in appearance and petrographically, and are composed of various types of gneisses. The analyzed samples (S80701A ~ G, Table 1) are tentatively grouped into three: psammitic gneiss (A, C, F), pyroxene-hornblende gneiss (B, D, G), and gneiss characterized by scapolite (E). The former two are thought to be derived from feldspathic arenite and basic igneous rock respectively. The metamorphic grade of these rocks is estimated to be the amphibolite facies.

Seven samples (S80701A ~ G) were analyzed by the Rb-Sr whole-rock method, and further the K-Ar analyses were done on minerals separated from a single rock (S80701C). The analytical method is essentially the same as that described in Shibata and Adachi (1974). The analyses of the Eimer and Amend Sr standard gave an average value of 0.70809 ± 0.00025 (1σ) for the $^{87}Sr/^{86}Sr$ ratio. The constants used for age calculations are $\lambda_\beta{}^{87}Rb = 1.47 \times 10^{-11}$/y, $\lambda_\beta{}^{40}K = 4.72 \times 10^{-10}$/y, $\lambda_\epsilon{}^{40}K = 0.584 \times 10^{-10}$/y, $^{40}K/K = 0.0119$ atom %.

Results

The Rb-Sr analytical data for whole-rock samples of metamorphic rocks from Taita Hills are given in Table 1, and the K-Ar analytical data and ages for minerals from sample S80701C are given in Table 2.

Rb concentrations and $^{87}Rb/^{86}Sr$ ratios of the whole-rock samples are relatively low, but there are significant differences in $^{87}Sr/^{86}Sr$ ratio owing to a rather old age of the rocks. The Rb-Sr analytical data are plotted in Fig. 1. They do not yield a well-defined isochron. Excluding A, F, and G, four points define an isochron of 827 ± 55 m.y. with an initial $^{87}Sr/^{86}Sr$ ratio of 0.7047 ± 0.0006. The points for A, F, G are slightly

1st Prelim. Rep. Afr. Studies., Nagoya Univ. 72-75, 1975.

Table 1 Rb-Sr whole-rock analytical data for metamorphic rocks from Taita Hills, southern Kenya

Sample No.	Rock type	Rb (ppm)	Sr (ppm)	$^{87}Rb/^{86}Sr$	$^{87}Sr/^{86}Sr$
S80701 A	Garnet-muscovite bearing biotite-plagioclase-quartz-microcline gneiss	122.6	286.1	1.241	0.7172
B	Biotite-clinopyroxene-orthoclase bearing quartz-hornblende-plagioclase gneiss	13.3	331.1	0.1160	0.7063
C	Garnet-biotite-hornblende-orthoclase-plagioclase-quartz gneiss	45.8	147.2	0.9011	0.7153
D	Clinopyroxene-hornblende-quartz-plagioclase gneiss	5.54	228.4	0.0703	0.7056
E	Biotite-microcline-plagioclase-sphene-quartz-scapolite-hornblende-garnet gneiss	73.8	170.7	1.251	0.7204
F	Microcline-garnet-biotite-quartz-plagioclase gneiss	60.4	370.9	0.4719	0.7082
G	Sphene-opaque-clinopyroxene-hornblende-quartz-microcline-plagioclase gneiss	46.3	187.7	0.7138	0.7158

Table 2 K-Ar ages of a gneiss from Taita Hills, southern Kenya

Sample No. and rock type	Mineral	K_2O (%)	^{40}Ar rad (10^{-6} cc STP/g)	Atmospheric ^{40}Ar (%)	Age (m.y.)
S80701C Garnet-biotite-hornblende-orthoclase-plagioclase-quartz gneiss	biotite	8.62	163	2.2	498 ± 15
	hornblende	1.59	31.5	9.9	519 ± 16

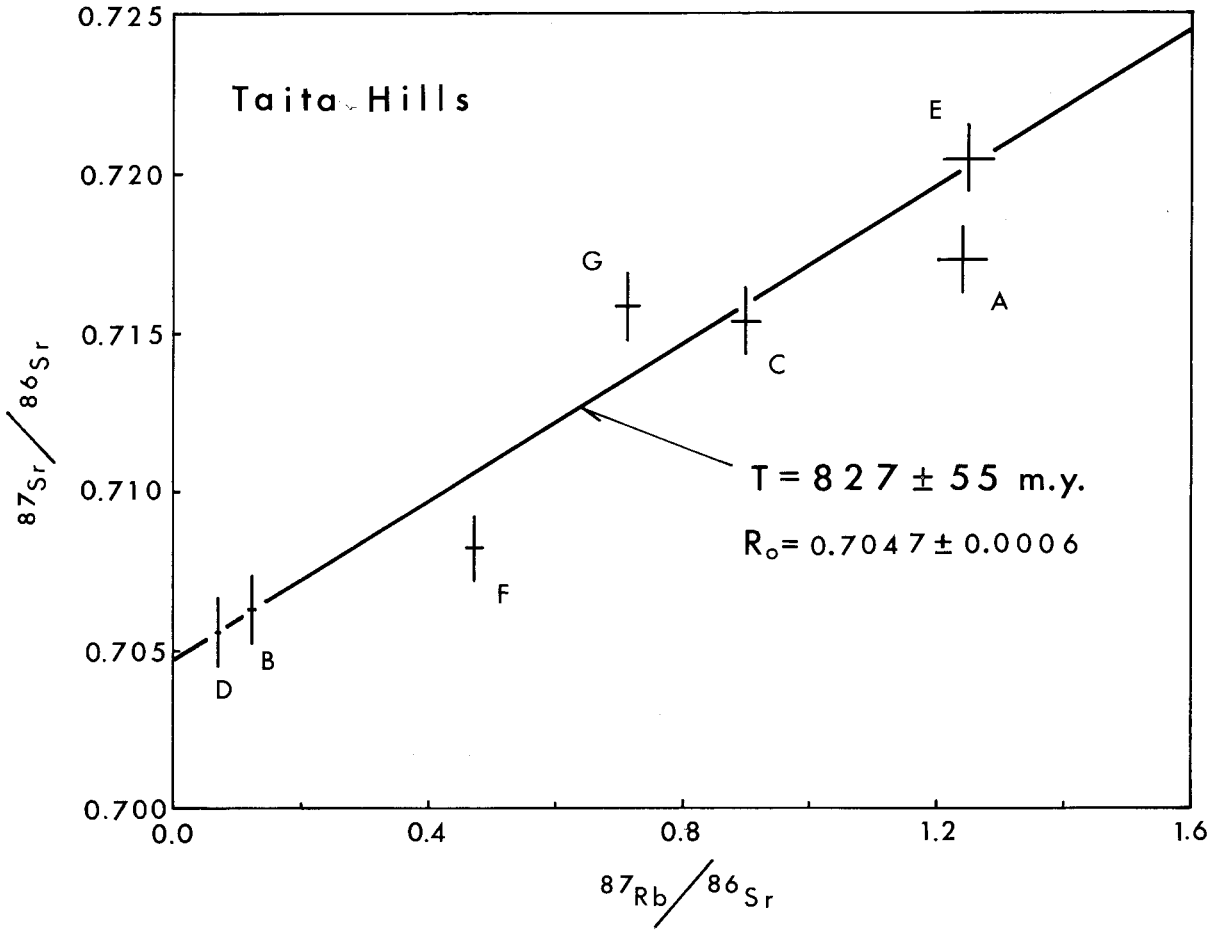

Fig. 1 Rb-Sr whole-rock plot for metamorphic rocks from Taita Hills, southern Kenya.

but significantly off the isochron. This is probably caused by a later event that is indicated by the K-Ar mineral ages (Table 2). The Rb-Sr whole-rock systems of these rocks may have been opened at that time. Samples A, F, and G contain microcline with grating texture, while microcline in other samples does not show such a texture (K. Suwa, personal communication), and this might be related with the disturbance of the isochron, although the reason is not known at present.

The Rb-Sr whole-rock age of 827 m.y. may either indicate the time of high-grade metamorphism or that of primary emplacement and sedimentation for the metamorphic rocks. It is difficult to decide which is more probable. However, the low initial $^{87}Sr/^{86}Sr$ ratio of 0.7047 excludes a possibility that the rocks originated from much older crustal material. Cahen and Snelling (1966) considered that the Mozambique orogeny occurred between 1100 and 650 m.y., and that many dates of 450 ~ 650 m.y. obtained on minerals from rocks in the Mozambique Belt reflect the uplift and cooling ages. On the contrary, Clifford

(1968) interpreted that the 450 ~ 580 m.y. dates represent the main phase of the Mozambique orogeny, and named it the Damaran episode. Although the writer has no preference of these two opinions, the whole-rock age result obtained in this study does indicate that the metamorphic rocks of the Mozambique Belt in Taita Hills had a considerably long history before the 500 m.y. event.

The age of 827 m.y. can be compared with the Rb-Sr whole-rock ages of approximately 900 and 700 m.y. for granulites from the Pare Mountains and Loibor Serrit in Tanzania, respectively (Spooner et al., 1970). Both localities are situated within the Mozambique Belt, and especially the locality of the Pare Mountains is only 90 km apart from the present site of sampling in Taita Hills. The Rb-Sr data of Spooner et al. (1970) also do not define a unique isochron, and probably there occurred some disturbance in the Rb-Sr whole-rock systems in a later time, yet the similar whole-rock ages obtained on metamorphic rocks from different localities in the Mozambique Belt give an important clue in interpreting the history of the Mozambique orogeny.

The K-Ar ages of biotite and hornblende saparated from sample S80701C are 498 and 519 m.y. respectively (Table 2), and both are similar to each other. The whole-rock system of this rock has been closed with respect to Rb and Sr since 827 m.y. ago, therefore it is evident that these mineral ages indicate the time of a later thermal event that rejuvenated the K-Ar system of minerals at about 500 m.y. ago. The similar ages obtained by both biotite and hornblende indicate that the 500 m.y. event must have been rather simple thermally. These ages are also within the much discussed ages of 450 ~ 650 m.y. for the Mozambique Belt (Cahen and Snelling, 1966; Clifford, 1968). In the vicinity of Taita Hills, K-Ar ages of 575 m.y. from the Pare district, and of 475 and 490 m.y. from the Lushoto district in Tanzania were reported (Snelling, 1964, 1966); all were determined on biotite from the Usagaran gneisses within the Mozambique Belt. All these ages are similar to those from Taita Hills, suggesting that the whole region has been involved in a similar thermal event.

Acknowledgements — The writer wishes to thank Dr. K. Suwa of Nagoya University for valuable information on petrography of the analyzed samples.

References

CAHEN, L. and SNELLING, N.J. (1966): *The Geochronology of Equatorial Africa.* 195pp, North-Holland.

CLIFFORD, T.N. (1968): Radiometric dating and the pre-Silurian geology of Africa. *In Radiometric Dating for Geologists* (ed. Hamilton, E.I. and Farquhar, R.M.), 299-416, Interscience.

SHIBATA, K. and ADACHI, M. (1974): Rb-Sr whloe-rock ages of Precambrian metamorphic rocks in the Kamiaso conglomerate from central Japan. *Earth Planet. Sci. Letters,* **21,** 277-287.

SNELLING, N.J. (1964): Age determination unit. *Ann. Rep. Overseas Geol. Surv.* 1963, 30-40.

SNELLING, N.J. (1966): Age determination unit. *Ann. Rep. Overseas Geol. Surv.* 1965, 44-57.

SPOONER, C.M., HEPWORTH, J.V. and FAIRBAIRN, H.W. (1970): Whole-rock Rb-Sr isotopic investigation of some East African granulites. *Geol. Mag.,* **107,** 511-521.

Potassium-Argon Age Determinations on the Tanzanian Igneous and Metamorphic Rocks

Yoshio UEDA*, Isao MATSUZAWA** and Kanenori SUWA***

* Institute of Mineralogy, Petrology and Economic Geology, Tohoku University
** Emeritus Professor of Nagoya University
*** Department of Earth Sciences, Faculty of Science, Nagoya University

Introduction

Many igneous and metamorphic rocks were collected from the northern, western, central and southern Tanzania by the members of the scientific expedition to Africa in 1968,organized by the Association for African Studies of Nagoya University. Among them, about twenty samples have been selected for K-Ar analysis.

Previous geochronological studies on Tanzanian rocks were carried out by Cahen and Snelling (1966), Spooner et al. (1970) and Wendt et al. (1972) and others. Cahen and Snelling's study (1966) was most comprehensive and laborious. Spooner et al. (1970) performed preliminarily Rb-Sr whole-rock isotopic analyses of granulites from Tanganyika craton (Msagali) and Katangan belt (Pare Mountains and Loibor Serrit). Wendt et al. (1972) performed in detail Rb-Sr whole-rock isotopic analyses and Rb-Sr and K-Ar mica isotopic analyses of Dodoman granites and gneisses and of Usagaran granites and gneisses.

By the present authors' study, several new informations on Tanganyika craton, Ubendian belt and Katangan (Mozambiquian) belt have been obtained.

Tanganyika craton

Pegmatite (Nos. 1 and 2), gneiss (No. 4) adamellites (Nos. 5, 6, 10 and 11) and gneissose tonalite (No. 9) have been selected for K-Ar analysis from the Tanganyika craton.

Nos. 1 and 2 : Locality is the Kimberlite Pit at Mwadui, northern Tanzania. Mother rock is muscovite-albite-quartz-microcline pegmatite, which cuts non-foliated granite with clean-cut boundary. Nyanzian schist is intruded by the non-foliated granite. The latter granite is sometimes interwoven with the small pegmatite body. The muscovite occurs as a large crystalline "books" and microcline also occurs as a large euhedral crystal reaching 20 cm.

No. 4 : Locality is two miles north from Uvinza village, western Tanzania. Mother rock is biotite-microcline-oligoclase-quartz gneiss, which occurs as alternation with amphibolite and runs NW (N50° to 60°W) with a northeasterly dip of 70°.

Nos. 5 and 6 : Locality is Imagi Mountain of southern Dodoma, central Tanzania. Mother rock is nebulitic muscovite-biotite adamellite running N60°W with a vertical dip.

No. 9 : Locality is three miles north from Rungwa village, central Tanzania. Mother rock is gneissose hornblende-biotite tonalite running N60°W with a vertical dip. Between Itigi town and Rungwa village, Dodoman granites and gneisses occur continuously.

1st Prelim. Rep. Afr. Studies., Nagoya Univ.76-80 , 1975.

Nos. 10 and 11 : Locality is 66 miles north from Chunya town, southern Tanzania. Mother rock is hornblende-biotite adamellite having petrographically igneous feature.

As a result of K-Ar dating, it may be concluded that :

(1) Nyanzian schist near Mwadui is considered to be older than 3150 m.y.

(2) It is significant fact that large argon loses from microcline (Compare Nos. 1 and 2, and Nos. 10 and 11).

(3) Metamorphic rocks around Uvinza have been so far considered to belong to Ubendian, but the rocks are considered as a member of the Tanganyika craton.

(4) Metamorphic and plutonic rocks in the Tanganyika craton represent 2200 - 2750 m.y.

Ubendian belt

Gneiss (No. 8), amphibolite (No. 15) and tonalite (No. 16) have been selected for K-Ar analysis from the Ubendian belt.

No. 8 : Locality is 46 miles east from Iringa town, central Tanzania. Mother rock is plagioclase-quartz-hornblende-biotite gneiss running NEE (N50° to 80°E) with a southeasterly dip from 40° to 90°.

No. 15 : Locality is Mulomboji river bridge, 25 miles east from Chimala village, southern Tanzania. Mother rock is plagioclase amphibolite running N0° to 10°E with a easterly dip of 60°.

No. 16 : Locality is 19 miles east from Chimala village, southern Tanzania. Mother rock is altered biotite tonalite.

As a result of K-Ar dating, it may be concluded that :

(1) Ubendian metamorphic rock near Iringa represents 1900 m.y.

(2) Ubendian metamorphic and plutonic rocks near Chimala represent 1500 - 1700 m.y. and are slightly younger than that near Iringa.

(3) Metamorphic and plutonic rocks at Mbeya Peak, Chimala, Ihanda and Tunduma in southern Tanzania have been so far considered to belong to Ubendian, but these rocks are considered to belong to Kantagan (Mozambiquian).

Katangan (Mozambiquian) belt

Pegmatite (No. 7), schists (Nos. 12, 13 and 14), plutonic rocks (Nos. 17, 20, 21 and 22) have been selected for K-Ar analysis from the Katangan belt.

No. 7 : Locality is Mautia Hill, 90 Km east from Dodoma city, central Tanzania. Mother rock is muscovite pegmatite intruding concordantly kyanite-muscovite quartzite running E - W with a vertical dip. Mautia Hill is famous as a type locality of yoderite.

No. 12 : Locality is the point of 2705 m above sea level, 350 m NE from the top of Mbeya Peak (2826.1 m above sea level), southern Tanzania. Mother rock is biotite-muscovite-oligoclase-microcline-quartz schist running NNW with a northeasterly dip of 60°.

Nos. 13 and 14 : Locality is the top of Mbeya Peak, southern Tanzania. Mother rock is oligoclase-tourmaline bearing biotite-staurolite-kyanite-almandine-muscovite-quartz schist running same trend with No. 12.

No. 17 : Locality is Chimala river, southern Tanzania. Mother rock is coarse-grained allanite bearing hornblende granite.

Nos. 20 and 21 : Locality is Ihanda, 70 Km S60°W from Mbeya town, southern Tanzania. Mother rock is clinopyroxene-amphibole-biotite syenite.

No. 22 : Locality is eastern Tunduma, boundary between Tanzania and Zambia.

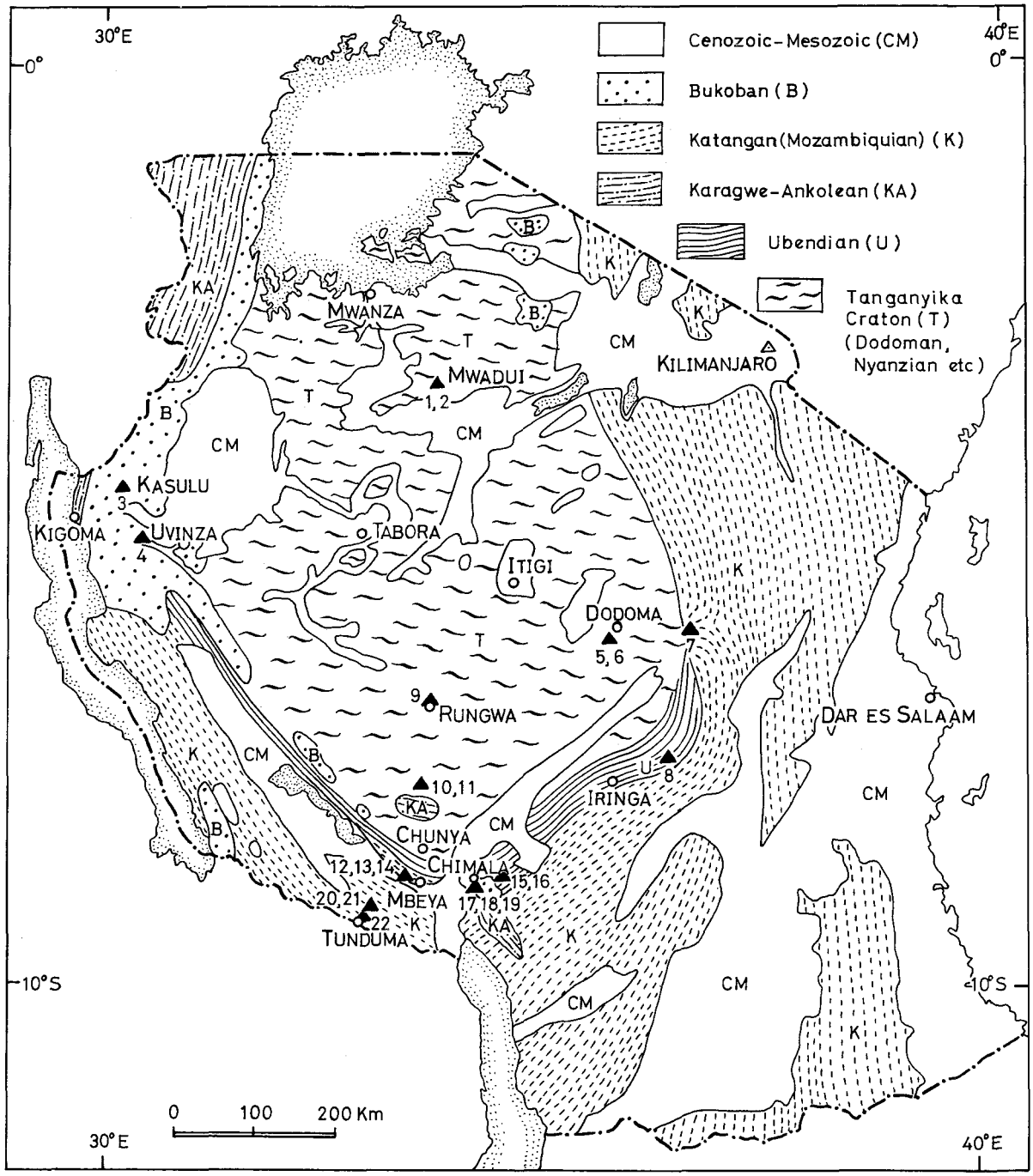

Fig. 1 Outlined Geological map of Tanzania.
Numbers refer to the age determinations listed in Table 1.

Table 1 Potassium-argon analytical data

Location No.	Locality	Sample No.	Material analysed and rock type	%K	$^{40}Ar^{R}/^{40}K$	Air contamination %	Age m. y.
1	Mwadui	3-680810-31	muscovite; pegmatite	8.73	0.476025	0.26	3150
2	Mwadui	2-68081001	microcline; pegmatite	11.77	0.196997	0.72	1930
3	Kasulu	2-68090201	W. R.; basalt	1.37	0.037782	3.62	560
4	Uvinza	2-68083002	biotite; gneiss	6.05	0.276451	0.08	2370
5	Imagi Mt.	2-68082501	biotite; adamellite	7.66	0.333192	0.43	2630
6	Imagi Mt.	2-68082501	biotite; adamellite	7.66	0.324862	0.02	2590
7	Mautia Hill	2-68082405	muscovite; pegmatite	8.30	0.046617	9.38	670
8	Iringa	2-68101105	biotite and hornblende; gneiss	1.41	0.196159	2.47	1930
9	Rungwa	2-68092801	biotite; gneissose tonalite	5.55	0.361792	1.86	2740
10	Rungwa	2-68093001	biotite; adamellite	4.27	0.249262	1.49	2230
11	Rungwa	2-68093001	microcline; adamellite	6.68	0.118168	1.68	1380
12	Mbeya Peak	2-68100402	musovite; schist	5.55	0.027914	3.39	430
13	Mbeya Peak	2-68092204	muscovite; schist	5.24	0.042365	1.31	610
14	Mbeya Peak	2-68092204	muscovite; schist	5.24	0.041001	2.22	600
15	Chimala	2-68100301	hornblende; amphibolite	0.75	0.137700	2.17	1530
16	Chimala	2-68100310	altered plagioclase; tonalite	1.24	0.155489	2.40	1660
17	Chimala	468092905	K-feldspar; granite	6.43	0.073069	0.52	960
18	Chimala	468092902	W. R.; altered rock	2.43	0.070027	5.17	730
19	Chimala	468092901	W. R.; altered rock	2.16	0.006383	21.08	120
20	Ihanda	2-68092507	biotite; syenite	4.46	0.052582	1.81	740
21	Ihanda	2-68092507	biotite; syenite	4.46	0.051215	14.95	720
22	Tunduma	2-68092406	W. R.; recrystallized mylonitic granodiorite	2.82	0.050427	2.03	710

Analyst : Y. Ueda
$\lambda\beta = 4.72 \times 10^{-10}\ yr^{-1}$
$\lambda e = 0.584 \times 10^{-10}\ yr^{-1}$

$^{40}Ar^{R}$: radiogenic Ar 40
W.R. : whole rock

Mother rock is recrystallized hypersthene-diopside-biotite mylonitic granodiorite.

As a result of K-Ar dating, it may be concluded that :

(1) Metamorphic and plutonic rocks at Mautia Hill, Mbeya Peak, Chimala, Ihanda and Tunduma represent mainly 600 - 750 m.y. and these ages are considered to correspond to Katangan cycle. There is the possibility of polymetamorphism, namely these rocks may be produced at the period of Ubendian cycle and are polymetamorphosed at the period of Katangan cycle.

(2) Southeastern marginal area along Lake Tanganyika has been so far considered to be composed of Ubendian rocks, but the area may be occupied by the polymetamorphosed Katangan rocks.

Bukoban system

The Bukoban system of western Tanzania includes a varied assortment of rock types including conglomerates, sandstones, quartzites, greywackes, shales, dolomitic limestones and basalts. They have suffered slight folding and are virtually unmetamorphosed. Gagwe basalt (No. 3) from Malagarasi river near Kasulu town, western Tanzania has been selected for K-Ar analysis from the Bukoban system.

A result of K-Ar dating is conformable with geological situation and previous works.

Acknowledgements – The present authors would like to express their sincere appreciation to Professors Isao Shiida, Kunihiko Miyakawa and Shinjiro Mizutani for their laborious collaboration in the field survey during July – November in 1968.

References

CAHEN, L., and SNELLING, N.J. (1966): *The geochronology of equatorial Africa.* North Holland Publ. Comp. Amsterdam, 195pp.

SPOONER, C.M., HEPWORTH, J.V., and FAIRBAIRN, H.W. (1970): Whole-rock Rb-Sr isotopic investigation of East African granulites. *Geol. Mag.,* **107,** 511-521.

WENDT, I., BESANG, C., HARRE, W., KREUZEN, H., LENZ, H., and MÜLLER, P. (1972): Age determinations of granitic intrusions and metamorphic events in the early Precambrian of Tanzania. *24th Intern. Geol. Cong.,* Sect. **1,** 295-314.

Isotope Geochemistry and Petrology of African Carbonatites

(Abstract, 1975)

Kanenori SUWA*, Shinya OANA*, Hideki WADA* and Susumu OSAKI**

* Department of Earth Sciences, Faculty of Science, Nagoya University

** Department of Chemistry, Faculty of Science, Kyushu University

Introduction

Many carbonatite bodies have been emplaced in the African continent since the Precambrian period, particularly during the Mesozoic and Cenozoic eras, and current exposures represent a range in depth of consolidation.

The carbonatite bodies examined are the Palabora, Spitskop and Premier Mine carbonatites of Precambrian age, the Mbeya carbonatite of Mesozoic age, the Homa Mountain cabonatite of Tertiary age and Recent eruptions of the Oldoinyo Lengai carbonatite.

Palabora carbonatite(South Africa)

The carbonatite occurs in the centre of the Palabora Igneous Complex. The two principal types of carbonatite are an older banded sövite and a younger transgressive sövite. The banding of the older carbonatite is due mainly to parallel magnetite-rich layers. The main younger sövite forms a well-defined but irregular shaped intrusion in the central part of the pipe.

The field of oxygen and carbon isotopic ratios of the Palabora carbonatite, especially the older carbonatite, coincides with that of primary igneous carbonatites such as Oka box.

Spitskop carbonatite(South Africa)

The Spitskop alkaline complex is composed mainly of ijolite intruded by two foyaite ring-dyke and by a central plug of carbonatite. The carbonatite measures approximately 1 mile across and has a more or less vertical concentric structure from centre to margin.

Spitskop carbonatite shows a slight deviation in oxygen and carbon isotopic ratios from primary igneous carbonatites such as in the Oka box. The Spitskop carbonatite is regarded as a pipe-like body whose composition was modified after emplacement by circulating fluids in several stages marked by progressive enrichment in magnesium and iron.

Premier Mine carbonatite(South Africa)

The Premier Mine carbonatite is located within the Premier kimberlite pipe near Pretoria. Eight kimberlite types have been distinguished according to the predominant matrix colour. It would appear that these different types have intruded in at least three distinct phases corresponding to the brown, grey and black varieties.

The main carbonatite is intruded into kimberlite, forming a set of radial dykes. Carbonatized varieties of black kimberlite, named "Pale Piebald" and "Dark Piebald", occur in the kimberlite surrounding the carbonatite dykes. It is apparent that the carbonatized nature of "Pale Piebald" and "Dark Piebald" must be due to carbonate solutions which occupied the channels now filled by the carbonatite dykes. Meteoric water may also have played its part in the replacement processes. Premier Mine carbonatite shows a significant enrichment in ^{18}O and is isotopically similar to the primary hydrothermal calcite at Providencia, Mexico(Rye, 1966).

Mbeya carbonatite(Tanzania)

Carbon and especially oxygen isotopic

compositions show a considerable range in the Mbeya carbonatite(Suwa et al., 1969). Calcite and dolomite samples from unaltered carbonatites lie in a small field in $\delta^{18}O$ and low in $\delta^{13}C$. This field coincides with that of primary igneous carbonatites. Carbonates coexisting with abundant metal oxides become enriched in ^{18}O and lie in the field low in $\delta^{13}C$. Enrichment of ^{18}O in calcite and dolomite samples is due to interaction with atmospheric oxygen and meteoric water during eruption. The fractionation factors of oxygen and carbon isotopes between the coexisting calcites and dolomites in the primary Mbeya carbonatites suggest that the carbonates crystallized at temperatures from 800°C to 380°C and > 700°C to 380°C, respectively.

Homa Mountain carbonatite(Kenya)

The multi-centred carbonatitic complex of Homa Mountain consists of a central cone-sheet complex intruded into a dome area of country rock. Earlier events include intrusion of a body of ijolite and later events include at least five stages of carbonatite intrusion and also numerous carbonatitic breccias (Clarke, 1968). Five main divisions are, in order of intrusion, C1, C2, C3, C4 and C5.

Heavy oxygen isotope values are noted for the Homa Mountain carbonatite samples excluding the unaltered sövite(C1) as shown in Fig. 1, and probably the values are due to interaction with atmospheric oxygen and meteoric water during eruption.

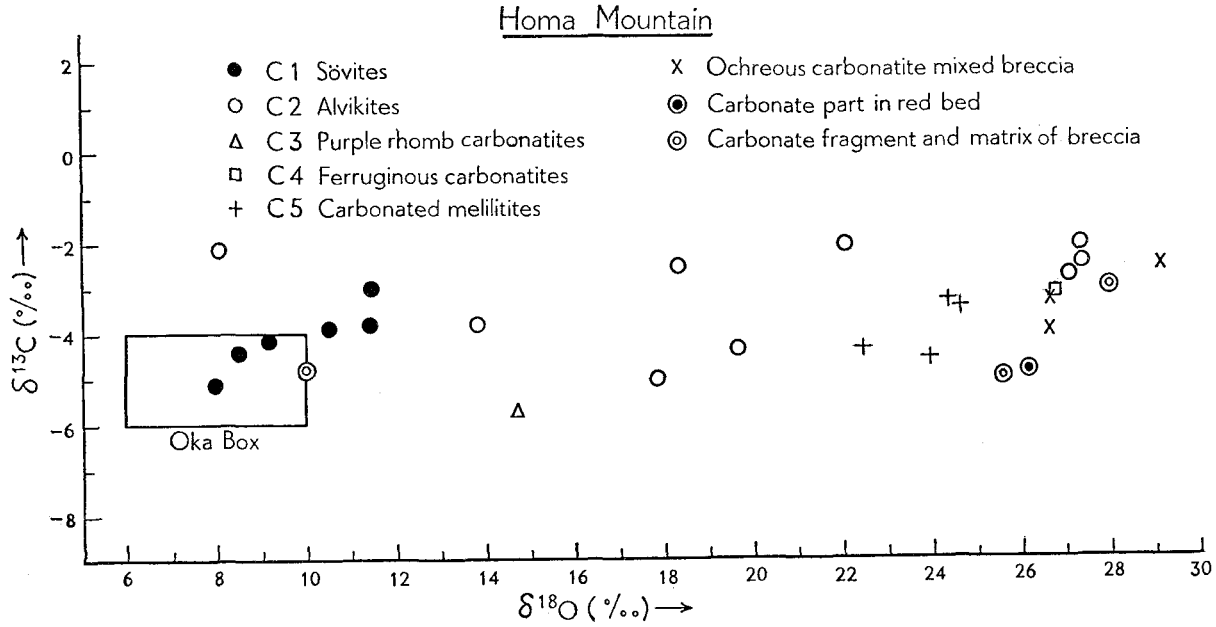

Fig. 1 The oxygen and carbon isotope ratios of carbonates in Homa Mountain carbonatite, western Kenya.

Oldoinyo Lengai carbonatite(Tanzania) and Lake Magadi trona(Kenya)

In 1960 and 1961, soda-rich and essentially silica-free lava was extruded from the vent of the northern crater as pahoehoe and aa (Dawson, 1962).

Sodium carbonate lava is deliquescent and readily alters in air. The lower value of $\delta^{13}C$ in the sodium carbonate lava is due to the evolution of CO_2 gas during vulcanicity, fractionating heavy carbon into the gas phase and concentrating lighter carbon in the sodium carbonate.

In Fig. 2 the isotopic data of the trona samples from the bore-holes B, C and D in Lake Magadi are also plotted. The high $\delta^{18}O$ and $\delta^{13}C$ values for trona seem to invalidate Milton's hypothesis that the "natro-carbonatite" lavas of the nearby volcano Oldoinyo Lengai are trona mobilized and mixed with alkaline lavas of the volcano.

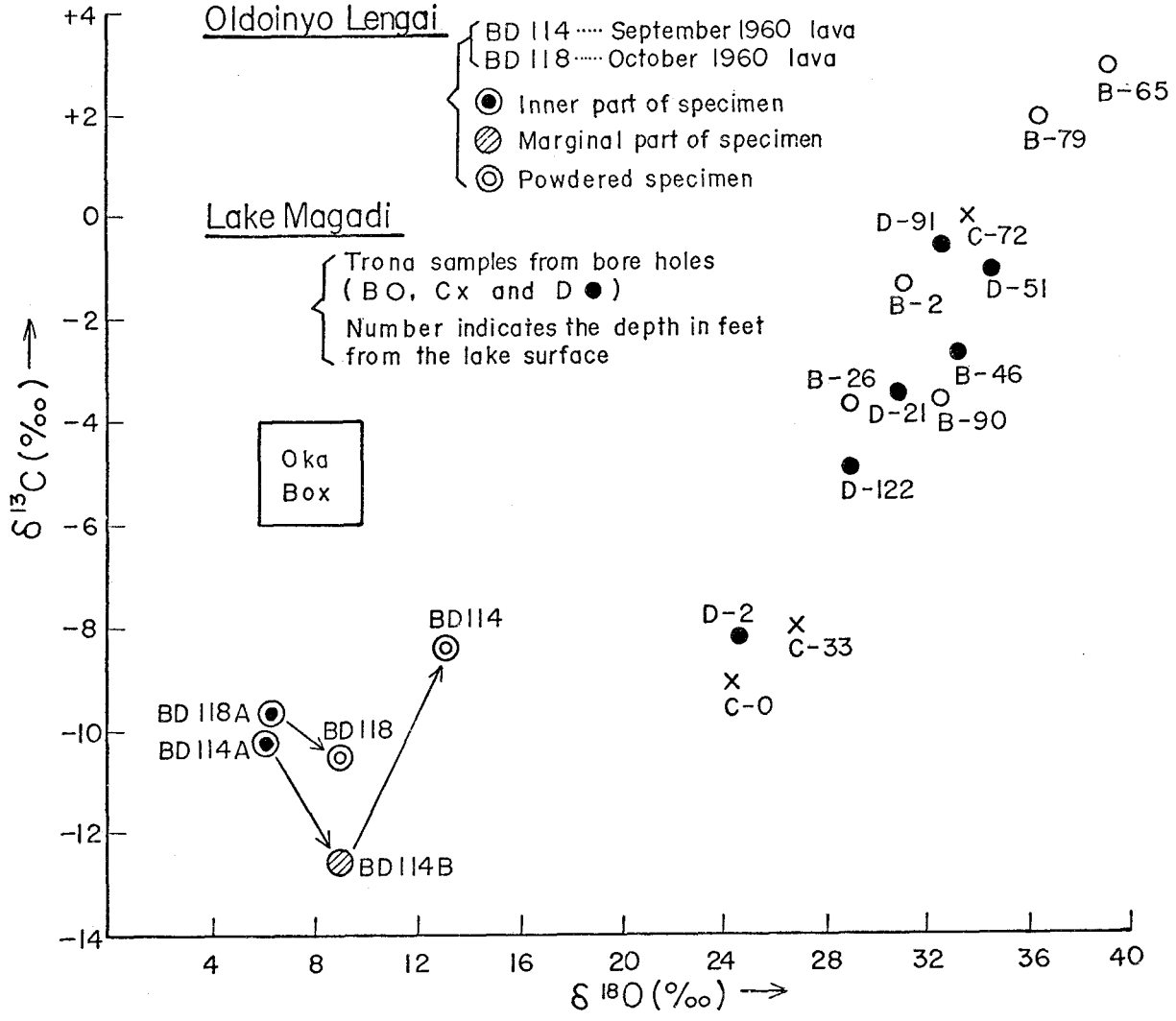

Fig. 2

The oxygen and carbon isotope ratios of carbonates in Oldoinyo Lengai carbonatite, northern Tanzania and those ratios of tronas in Lake Magadi, southern Kenya.

Conclusion

A classification of carbonatites based on the associated rock-types bears some relationship to a genetic classification. The carbonatites examined are divided into the following three associations.

A. Volcanic association
   Carbonatite - tuff - volcanic breccia-alkali carbonate: Oldoinyo Lengai.
B. Volcanic-Subvolcanic association
   (a) Carbonatite - breccia : Mbeya
   (b) Carbonatite - volcanic rocks - ijolite -nepheline syenite:Homa Mountain.
C. Subvolcanic association
   (a) Carbonatite - foyaite - ijolite : Spitskop.
   (b) Carbonatite-phoscorite-pyroxenite : Palabora.

Carbonatite complexes of subvolcanic association show a restricted carbon and oxygen isotopic composition range, and those of volcanic and volcanic-subvolcanic associations show considerably wider variations as a result of interaction with atmospheric oxygen and meteoric water during eruption.

Acknowledgements—The present authors would like to express their sincere appreciation to Drs. John Walsh and Martin C.G.Clarke of Kenya Mines and Geological Department; to Dr.J.B.Dawson of the University of St.Andrews; to Professor W.J.Verwoerd of the University of Stellenbosch, for their advice and encouragement.

References

CLARKE, M.C.G. (1968): The geology of the Southern part of Homa Mountain carbonatitic complex, Western Kenya, with particular reference to the petrology of the alkaline silicate, metasomatic and melilite bearing suites. *A thesis presented for the degree of Doctor of Philosophy in the University of Leicester, Manuscript,* 1 - 291.

DAWSON, J.B. (1962): Sodium carbonate lavas from Oldoinyo Lengai, Tanganyika. *Nature* **195,** 1075 - 1076.

RYE, R.O. (1966): The carbon, hydrogen, and oxygen isotopic composition of the hydrothermal fluids responsible for the lead-zinc deposits at Providencia, Zacatecas, Mexico. *Econ. Geol.* **61,** 1399 - 1427.

SUWA, K., OSAKI, S., OANA, S., SHIIDA, I. and MIYAKAWA, K. (1969): Isotope geochemistry and petrology of the Mbeya carbonatite, south-western Tanzania, East Africa. *J. Earth Sci. Nagoya Univ.* **17,** 125 - 168.

List of publications on African geology

1963 * SUWA, K., Geological excursion of north-east Africa. *Monthly Africa,* **3,** Nos.5-10.
* SUWA, K., Geology of Ethiopia. *Nagoya Jour. Geol.,* **18,** 13-25.

1964 * SUWA, K., Geological excursion of north-east Africa. *Monthly Africa,* **4,** Nos.1 and 3.
* SUWA, K., African Rift Valley. *World Geography,* **13,** 320-322.

1965 * SUWA, K., Geology of Egypt and Sudan. *Nagoya Jour. Geol.,* **20-21,** 34-48.

1966 MATSUZAWA, I., A study on the formation of the African Rift Valley. *Jour. Earth Sci., Nagoya Univ.,* **14,** 89-115.
MIZUTANI, S. and SUWA, K., Orthoquartzitic sand from the Libyan desert, Egypt. *ibid,* 137-149.
SUWA, K., Maximum microcline in Aswan granitic rocks, Egypt. *ibid,* 116-136.
** SUWA, K. and UEMURA, T., Geology of the African Rift Valley and the Olduvai Gorge. *Jour. Afr. Studies,* **3,** 18-48.
* SUWA, K., Precambrian of Africa (I). *Earth Science (Chikyu Kagaku),* **84,** 39-48.

1967 ** MATSUZAWA, I., Some considerations on the formaiton of the African Rift Valley. *Jour. Afr. Studies,* **4,** 1-24.
* SUWA, K., Precambrian of Africa (II). *Earth Science (Chikyu Kagaku),* **21,** 32-44.

1968 ** SUWA, K., Precambrian of African Continent—geology and mineral resources. *Jour. Afr. Studies,* **6,** 25-51.

1969 AOKI, H., Gravity measurements of Rift Valleys in Tanzania. *Jour. Earth Sci., Nagoya Univ.,* **17** (special volume), 169-188.
MATSUZAWA, I., Nagoya University African Rift Valley Expedition(NUARVE) in 1968. *ibid,* 1-10.
MATSUZAWA, I., Formation of the African great rift system. *ibid,* 11-70.
MIYAKAWA, K., SUWA, K., and SHIIDA, I., Metamorphic rocks of the North Pare Mountains, Tanzania. *ibid,* 97-106.
MIZUTANI, S. and YAIRI, K., Tectonic sketch of the Mbeya area, southern Tanzania. *ibid,* 107-124.
SUWA, K., OSAKI, S., OANA, S., SHIIDA, I., and MIYAKAWA, K., Isotope geochemistry and petrology of the Mbeya carbonatite, south-western Tanzania, East Africa. *ibid,* 125-168.
YAIRI, K. and MIZUTANI, S., Fault system of the Tanganyika Rift at the Kigoma area, western Tanzania. *ibid,* 71-96.

1970 * SUWA, K., Six months of geological studies in Africa during 1969-1970. *Gakujutsu-geppo(Monthly Rept. Sci. Research),* **23,** 46-55.

1971 * MATSUZAWA, I., On Africa. *Jour. Afr. Studies,* **11,** 1-8.
* MIYAKAWA, K., Recent trends of African studies in Japan—geology. *ibid,* 9-15.
* SUWA, K., Field studies in Africa—geological researches. *ibid,* 49-58.
* SUWA, K., Earth scientific characteristics of African Rift Valley. *World Geography Seminor,* **5,** 73-91. Daimyodo Pub. Co.

1972 * SUWA, K., African Rift Valley and volcanism. *Geography,* **17,** 7-14.
* SUWA, K. and YAIRI, K., African Rift Valley Research Expedition(2nd). *Gakujutsu-geppo(Monthly Rept. Sci. Research).,* **25,** 548-554.

1973 SUWA, K., OANA, S., WADA, H., and OSAKI, S., Isotope geochemistry and petrology of the African carbonatites. *1 st International Kimberlite Conference, extended abstract,* 297-300.
SUWA, K., YUSA, Y., and KISHIDA, N., Petrology of peridotite nodules from Ndonyuo Olnchoro, Samburu district, central Kenya. *ibid,* 301-304.

1974 ** ADACHI, M., The Mesozoic group near Mombasa, Kenya. *Jour. Afr. Studies,* **14,** 14-20.
* SHIOZAKI, H., Mineral resources of Africa (I). *Nagoya Jour. Geol.,* **30,** 2-10.
** SHIOZAKI, H., Mineral resources and mining affairs of East Africa. *Jour. Afr. Studies,* **14,** 73-81.
** YAIRI, K., En echelon pattern of the East African Rift System. *Jour. Afr. Studies,* **14,** 21-46.
1975 SUWA, K., OANA, S., WADA, H., and OSAKI, S., Isotope geochemistry and petrology of African carbonatites. *Phys. Chem. Earth,* **9,** 735-746(Pergamon Press).
SUWA, K., YUSA, Y., and KISHIDA, N., Petrology of peridotite nodules from Ndonyuo Olnchoro, Samburu district, central Kenya. *ibid,* 273-286(Pergamon Press).

* In Japanese
** In Japanese with English abstract